RUHR-UNIVERSITÄT BOCHUM

SFB 837
Interaction Modeling in Mechanized Tunneling

Elham Mahmoudi

Probabilistic analysis of a rock salt cavern with application to energy storage systems

Bochum 2017

Heft 63

Schriftenreihe des Lehrstuhls für
Grundbau, Boden- und Felsmechanik

Herausgeber: Tom Schanz

ISSN 2190-3255

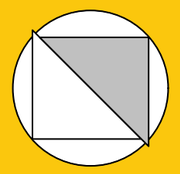

Elham Mahmoudi Probabilistic analysis of a rock salt cavern

63

ISSN 2190-3255

Ruhr-Universität Bochum
Schriftenreihe Grundbau, Boden- und Felsmechanik
Heft 63

Herausgeber:
Prof. Dr. -Ing. habil. Tom Schanz
Ruhr-Universität Bochum
Fakultät für Bau- und Umweltingenieurwissenschaften
Lehrstuhl für Grundbau, Boden- und Felsmechanik
44801 Bochum
Telefon: 0234/ 3226135
Telefax: 0234/ 3214236
Internet: www.gbf.ruhr-uni-bochum.de

ISSN 2190-3255

Probabilistic analysis of a rock salt cavern with application to energy storage systems

Dissertation

as a requirement of the degree of
Doktor-Ingenieur (Dr.-Ing.)

at the Faculty of
Civil and Environmental Engineering
Ruhr-Universität Bochum

submitted by
Elham Mahmoudi

Reviewers

Prof. Dr.-Ing. habil. Tom Schanz
Prof. Dr.-Ing. Markus König
Prof. Dr. rer. nat. Tom Lahmer

Bochum, Nov 2017

Vorwort des Herausgebers

Die vorliegende Promotion von Frau Mahmoudi wurde im Rahmen des Projekts ANGUS+ (gefördert durch die Bundesregierung im Programm GEOTECHLOGIEN II) angefertigt. In diesem großen Forschungsverbundvorhaben ging es u.a. um die Untersuchung der Möglichkeit der Speicherung von erneuerbarer Energie in Form von Druckluft in unterirdischen Hohlräumen, im Speziellen um die Nutzung von Salzkavernen. Salzkavernen werden bereits heute zur Energiespeicherung, u.a. von Erdgas oder Erdöl benutzt. In diesem Zusammenhang spricht man von saisonalen Speichern, da ihre Beschickung bzw. Entnahme im mehreren Monate Zyklus erfolgt. Hingegen handelt es sich bei der Nutzung als Speicher für erneuerbare Energie um eine mehrtägige Betriebsabfolge. Die Bemessung von Kavernen unter derartigen Szenarien ist weitestgehend Neuland und die tatsächlichen Praktiken, auf Grund der etablierten Strukturen zwischen Betreibern, Aufsichtsbehörde und Experten, für Außenstehende nicht auf den ersten Blick durchschaubar. Die Konzepte zur probabilistischen Analyse sind z.B. im Konstruktiven Ingenieurbau sehr gut etabliert, wo hingegen ihre Anwendung auf die spezifischen Fragen der Geotechnik nur exemplarisch und oftmals akademisch behandelt wird. Frau Mahmoudis Arbeit leistet einen hervorragenden Beitrag zur Verbesserung dieser Situation. Ausgehend von den äußerst anspruchsvollen Konzepten der Statistik, Probabilistik und der Kontinuumsmechanik gelingt es Frau Mahmoudi schlussendlich Aussagen bezüglich der Zuverlässigkeit von Salzkavernen in Abhängigkeit derer Betriebsparameter zu erzielen. Derartige praxisrelevante Ergebnisse in vergleichbarere Art sind dem Gutachter nicht bekannt.

Salzkavernen sind allein wegen ihren Abmessungen und dem damit verbundenen Volumen der Hohlräume Bauwerke, die einer eingehenden Analyse bedürfen. Daneben ist Steinsalz als Wirtsgestein in seinem thermischen und mechanischen Verhalten äußerst komplex. Bezüglich der „Baugrundschichtung“ ist festzustellen, das Steinsalz äußerst heterogen auftritt und die Konstitutiveigenschaften deutlich von seiner Diagenese geprägt sind. Aus diesen Gründen haben deterministische Analysen nur einen geringen Wert. Statistische Konzepte zur Erfassung der Variabilität einzelner Parameter als auch zur Abbildung der räumlichen Variabilität sind unbedingt erforderlich. Diese computerbasierten

Konzepte der Zuverlässigkeitsanalyse sind numerisch sehr aufwendig und erfordern unterstützende Konzepte wie etwa Ersatzmodelle und „subset modelling“-Ansätze. Genau diesen (existierenden) statistischen Werkzeugen widmet sich das erste Kapitel der Dissertation. Neben den genannten Methoden werden die globale Sensitivitätsanalyse und die Methode der Zufallsfelder eingeführt. Kapitel 2 widmet sich der Abbildung des thermisch-mechanisch gekoppelten Konstitutivverhaltens von Steinsalz. Es werden drei gut etablierte unterschiedlich komplexe Modelle eingeführt und in die verwendete FE-Software erfolgreich implementiert. Zusätzlich wird die quantitative Beschreibung der Dilatanzgrenze diskutiert, die bei der späteren Herleitung und Überprüfung der Stabilitätskriterien eine entscheidende Rolle spielt. Kapitel 3 ist ein erstes Kernstück der Arbeit von Frau Mahmoudi. Detailliert und sehr gut nachvollziehbar wird das verwendete allgemeine Konzept zur Systemanalyse nun auf den Fall der Salzkaverne angewendet. Dabei steht die Diskussion des Initialzustands im Vordergrund. Dieser wird durch zwei Komponenten beeinflusst, den geostatischen Spannungszustand und die darauf folgenden Spannungsumlagerungen zufolge des schrittweisen Auffahrens der Kaverne. Durch detaillierte Simulationen, die sowohl den zeitlichen Verlauf als auch die prozessspezifischen Parameter des sogenannten „solution-mining“ abbilden, kann Frau Mahmoudi eindrücklich zeigen, dass diese Vorgänge nur einen geringen Einfluss auf den Primärspannungszustand vor dem eigentlichen zyklischen Betrieb der Kaverne haben. Die für eine Zuverlässigkeitsbetrachtung notwendigen Kriterien der Gebrauchstauglichkeit und der Standsicherheit existieren für Salzkavernen unter „hoch-frequenter“ zyklische Beanspruchung bisher nicht. Frau Mahmoudi implementiert neben der Berücksichtigung der Oberflächensetzungen vier weitere neuartige Kriterien, welche die speziellen Eigenschaften von Steinsalz berücksichtigen: Dilatanz, geringe Zugfestigkeit, relavante Kriechverformungen und Schädigungspotential. Kapitel 5 beinhaltet die Ergebnisse der implementierten und durchgeführten globalen Sensitivitätsanalysen (GSA). Sehr gut verständlich, textbuchartig, wird in diese für Geotechniker komplexe Materie eingeführt. Von herausragender Bedeutung ist hier aus meiner Sicht die Erarbeitung einer Vorgehensweise zur Auswahl der angemessenen Methode zur GSA. Dabei werden sowohl der Grad der Nicht-Linearität des behandelten Randwertproblems als auch eventuell vorhandene Interaktionen zwischen unterschiedlichen Modellparametern analysiert. Sowohl zur Durchführung der GSA als auch für die im Kapitel 5 durchgeführten probabilistischen Analysen verwendet Frau Mahmoudi sogenannte Ersatzmodelle. Diese werden in ihren konzeptionellen Unterschieden, ihren Vor- und Nachteilen gegenübergestellt und bewertet. Im Rahmen der probabilistischen Berechnungen werden unterschiedliche Möglichkeit zur „Beschleunigung“ der Monte-Carlo-Simulationen implementiert. Eindrucksvoll kann die Effizienz derartiger Konzepte gezeigt werden. Besonders

für sehr geringe Versagenswahrscheinlichkeiten sind trotz Ersatzmodellen eine Vielzahl von sampling-Punkten notwendig. Durch die von Frau Mahmoudi implementierte Subset-Methode kann der Rechenaufwand signifikant reduziert werden. Bevor Kapitel 7 die Ergebnisse der Arbeit zusammenfasst und einen Ausblick gibt behandelt Kapitel 6 die Verwendung von Zufallsfeldern im Zusammenhang mit numerischen Analysen von Strukturen im Steinsalz. Eindrücklich kann gezeigt werden, wie durch die Wahl geeigneter statistischer Parameter (hier u.a. der Auto-Korrelationslänge) räumliche Verteilungen d.h. Felder der Materialparameter erzeugt werden können, die trotz nur eines Parametersatzes spatial den in Steinsalz zu beobachtenden Schichtungen ähneln. In detaillierter Art und Weise kann gezeigt werden, dass random-variables Simulationen mit homogenen Baugrund geringere Versagenswahrscheinlichkeiten liefern als die Analyse mit Zufallsfeldern. Dies unterstreicht in hervorragender Art und Weise die Notwendigkeit der Berücksichtigung von Zufallsfeldern bei der Zuverlässigkeitsanalyse.
Die Arbeit von Frau Mahmoudi bewegt sich international auf höchstem Niveau der numerischen Geomechanik. Die Arbeiten zur Zuverlässigkeitsanalyse von Speicherkavernen im Steinsalz sind international wegweisend und nach Wissen des Gutachters in ihrer Systematik und Qualität einzigartig. Neben den spezifischen Fragen der Modellbildung derartiger Kavernen bei täglicher zyklischer Beanspruchung entwickelt Frau Mahmoudi ein Konzept auf probabilistischer Grundlage zur Durchführung von Zuverlässigkeitsanalysen. Unter Berücksichtigung sowohl der stochastischen Natur der Konstitutivparameter von Steinsalz als auch unter Verwendung von Zufallsfeldern kann Frau Mahmoudi praxisrelevante Aussagen zu den signifikanten Betriebsparametern von derartigen Kavernen ableiten.

Bochum, Oktober 2017 Tom Schanz

To my beloved parents

Acknowledgement

This dissertation is the outcome of four years of my research activity at the Chair of Foundation Engineering, Soil and rock Mechanics at the Ruhr-Universität Bochum. First and foremost, I would like to dedicate this thesis to the memory of Prof. Dr.-Ing. habil. Tom Schanz, who passed away unexpectedly some weeks before my defence. I missed the chance to express my profound gratitude to Prof. Dr.-Ing. habil. Tom Schanz for all his guidance and encouragement in my defence meeting, but I am glad to proceed his last assignment for mine through to its completion. His enthusiasm, ultimate support and vast knowledge gave me the opportunity to do my research on this topic. Prof. Dr.-Ing. habil. Tom Schanz supervised this dissertation with his priceless comments and suggestions which led always to significant improvements. I certainly will miss my great mentor and his extraordinary vision and outstanding personality in my future career.

My gratitude should also be extended to Prof. Pierre Bérest at the Ecole Polytechnique for his precise advices and his continuous assistance and support. Besides his brilliant and valuable research studies which inspired me a lot, his kindness and hospitality during my research stay in his institute in Ecole Polytechnique impressed me as well.

Also, I am grateful to Prof. Dr.-Ing. König, and Prof. Dr. rer. nat. Tom Lahmer for their agreement to be reviewers of this dissertation. I would also like to specially thank Prof. Dr. Maria Datcheva for her kind support to substitute the position of Prof. Tom Schanz in the examination committee.

I would also like to express my gratitude to my colleague Dr.-Ing. Shorash Miro for his support, feedback and constructive advice. He was always ready for a discussion in the field of sensitivity analysis. I would like to thank all my fellows, colleagues and administrative staff in the Chair of Foundation Engineering, Soil and Rock Mechanics, and especially the ANGUS+ research team, Dr.-Ing. Diethard König and Achim von Blumenthal. In particular, I should thank my fellow Kavan Khaledi for all of his feedbacks, cooperation and of course friendship. We had many scientific discussions through last four years, which lead to our common publications. I am also appreciative of my colleague Raoul Hölter, for his friendly cooperation in the concept of probabilistic methods.

I would like to acknowledge the financial support from the German Academic Exchange Service (DAAD), and its friendly staff, especially Ms. Dagmar Hosseini-Razi in the section of Iran, for her remarkable kindness. In addition, I am grateful to the colleagues at the Collaborative Research Center (SFB 837) and a period of two years financial support of the German Research Foundation (DFG) through the SFB 837.

Last but not least, I sincerely thank my dear friends Farzaneh and Kaveh who accept nothing less than excellence from me. I also dedicate my dissertation to my lovely parents whose their moral and emotional support kept me always strong despite the thousands of kilometres between us. Without their helps I would not be able to accomplish my study. I also dedicate this work to my brothers Hamid and Mohammad for their very special way of being supportive, they never left my side.

Bochum, November 2017 Elham Mahmoudi

Abstract

The fluctuating nature of renewable energy sources can be managed by storing the surplus of electrical energy in an appropriate reservoir. The excess electricity available during off-peak periods of consumption may be used to compress air or electrolyse Hydrogen. Afterwards, the pressurised gas is stored in the rock salt cavities and discharged to compensate the shortage of energy when required. During this process, the rock salt surrounding the cavern undergoes different loading conditions. The validation of the short and long-term integrity and stability of rock salt cavern is a prerequisite in their design process. In order to achieve a reliable geotechnical design, the stress-strain response of rock salt under such loading condition has to be identified and predicted. To investigate the rock salt behaviour during the three phases of cavern's life i.e. solution mining, debrining process as well as cyclic operation, a deterministic study using numerical analysis is conducted.

The computational model relies primarily on the governing constitutive model for predicting the behaviour of rock salt cavity. Hence, some constitutive models are utilised to take into account different creep phases and dilatancy progress. The contributed input parameters in the constitutive model can be calibrated using the experimental measurements. However, because of the significant levels of uncertainties involved in the design procedure of such structures, a reliable design can be achieved by employing probabilistic approaches. Therefore, the numerical calculation is extended by statistical tools such as sensitivity analysis, probabilistic analysis, random field discretisation and reliability-based design to evaluate design parameters of paramount need for practice.

In the present study, sensitivity measures of different variables involved in the mechanical response of cavern are computed by three different global sensitivity methods, namely the Morris, Random balance designs and Sobol'/Saltelli methods. An interpretation of the sensitivity indices provided by different methods is presented through a comparative study. The execution time of the numerical model makes the conduction of a sensitivity analysis mostly prohibitive, because performing these analyses require hundreds of model runs. Therefore, the original finite element models are substituted by surrogate modelling techniques.

The propagation of parameter uncertainties and the failure probability against different failure criteria are evaluated by utilising a Monte Carlo-based analysis, considering key input variables. Subset simulation methodology is also performed to determine the failure probability of the system with less number of required simulation runs. This methodology is further validated through a comparison with a Monte Carlo-based probabilistic analysis. The stability of the cavern under different loading scenarios is evaluated, and finally, a reliability-based analysis approach is employed to obtain the minimum admissible internal pressure in the cavity.

In the following, the random field method is used to study the effect of spatial uncertainty of the constitutive parameters on the behaviour of the rock salt cavern. To achieve a reliable design, a probabilistic model is presented to compute the failure probability of a cavern mined in a spatially varying salt dome. Here, the no-dilatant condition around the cavity is regarded as the failure criterion. In this regard, a thermo-mechanical model of a natural gas storage in the rock salt, employing BGRa creep law, is developed. Afterwards, the most effective input variable on the model response is identified, using global sensitivity analysis. The Karhunen-Loève expansion is introduced to generate the random field. In the following, the subset simulation approach is utilised to facilitate the execution of Monte Carlo method. The findings of this part emphasise that considering spatial variability in rock properties significantly affects the reliability of a solution-mined cavity.

Zusammenfassung

Die Energiegewinnung mittels erneuerbarer Ressourcen unterliegt natürlichen Schwankungen. Ein Ausgleich intermittierender Unterschiede zwischen Energieerzeugung und Netzauslastung kann durch eine zeitweise Speicherung überschüssiger Energie in einem geeigneten Reservoir erzielt werden. Der während der Überschussphasen zur Verfügung stehende Strom kann zur Erzeugung von Druckluft oder zur Wasserstoffgewinnung per Elektrolyse genutzt werden. Das komprimierte Gas kann anschließend in Kavernen in Salzgestein gelagert werden und bei Bedarf zur Energieerzeugung wieder entnommen werden. Während dieses Prozesses erfährt das umliegende Salzgestein verschiedene Belastungsszenarien.

Die Überprüfung der kurzzeitigen sowie dauerhaften Gebrauchstauglichkeit und Stabilität der Salzkavernen ist die Grundvoraussetzung während des Entwurfsprozesses. Um eine zuverlässige geotechnische Bemessung durchzuführen, muss das spannungsabhängige Verformungsverhalten des Salzgesteins bei entsprechenden Belastungsszenarien bekannt bzw. prognostizierbar sein. Zur Untersuchung der drei Nutzungsphasen einer solchen Kaverne, der Kavernensolung, der Solentleerung und der Betriebsphase mit zyklischer Belastung, wird eine deterministische Simulation mittels einer numerischen Analyse durchgeführt.

Das Berechnungsmodell beruht maßgeblich auf dem verwendeten Stoffgesetz, das zur Voraussage des Verhaltens der Kaverne im Salzgestein genutzt wird. Dementsprechend werden geeignete Stoffgesetze verwendet, um die verschiedenen Kriechphasen und das Dilatanzverhalten zu berücksichtigen. Die zugrundeliegenden Modellparameter können mittels experimenteller Daten kalibriert werden. Da allerdings ein hohes Maßan Unsicherheiten im Bemessungsvorgang solcher Strukturen vorliegt, können probabilistische Ansätze verwendet werden, um eine zuverlässige Bemessung zu erreichen. Hierzu wird die numerische Berechnung um statistische Hilfsmittel ergänzt, wie der Sensitivitätsanalyse, probabilistischen Analyse, Diskretisierung mittels Zufallsfelder, sowie der zuverlässigkeitsbasierten Bemessung, um die Entwurfsparameter zu evaluieren, die für die Praxis von höchster Bedeutung sind.

In der vorliegenden Arbeit wurden die Sensitivitäten der für das mechanische Verhalten der Kaverne relevanten Parameter untersucht. Dazu wurde drei unterschiedliche

Methoden zur Bestimmung der globalen Sensitivität angewandt, namentlich die Morris-, die Random Balance Design- sowie die Sobol'/Saltelli-Methoden. Eine Auswertung der durch die verschiedenen Methoden ermittelten Sensitivitäten wird durch eine Vergleichsstudie vorgestellt. Die Durchführung einer Sensitivitätsanalyse wird durch den Berechnungsaufwand des numerischen Modells stark eingeschränkt, da für eine solche Analyse hunderte Modellaufrufe erforderlich sind. Daher wird das ursprüngliche Finite-Elemente Modell mittels eines Metamodells substituiert.

Die Auswirkung der Parameterunschärfe und die Versagenswahrscheinlichkeit hinsichtlich verschiedener Versagenskriterien wird unter Berücksichtigung der maßgebenden Eingangsparameter, mittels einer auf dem Monte-Carlo-Ansatz beruhenden Auswertung, untersucht. Zur Reduzierung des Rechenaufwandes, insbesondere bei der Berechnung von geringen Versagenswahrscheinlichkeiten, wird zudem eine Subset-Simulation verwendet. Auch diese Methode wurde mittels einer probabilistischen Analyse auf Monte-Carlo-Basis validiert. Die Standsicherheit der Kaverne wird für verschiedenen Belastungsszenarien untersucht, um schließlich, mittels eines zuverlässigkeitsbasierten Berechnungsansatzes, den minimal zulässigen Innendruck der Kaverne zu bestimmen.

Anschließend wird die Methode der Zufallsfelder verwendet, um den Einfluss der räumlichen Unsicherheiten der Konstitutivparameter auf das Verhalten der Salzkaverne zu untersuchen. Ein probabilistisches Modell wird vorgestellt mit dem die Versagenswahrscheinlichkeit einer in räumlich veränderlichem Salzgestein erstellten Kaverne berechnet werden kann. Als Grenzbedingung wird diesbezüglich ein nicht-dilatantes Verhalten der Kavernenumgebung angesetzt. Hierzu wird, unter Verwendung des BGRa-Kriechgesetzes, ein thermo-mechanisches Modell für die Speicherung von Erdgas in Steinsalz entwickelt. Durch Verwendung der globalen Sensitivitätsanalyse können die Parameter mit dem größten Einfluss auf die Modellantwort identifiziert werden. Die Karhunen-Loève-Erweiterung wird vorgestellt, um die Zufallsfelder zu erstellen. Anschließend wird die Subset-Simulation verwendet, um die Durchführung der Monte-Carlo-Simulation zu vereinfachen. Die Ergebnisse dieses Abschnittes unterstreichen, dass die räumliche Streuung der Felseigenschaften einen erheblichen Einfluss auf die Zuverlässigkeit solch einer durch Solung erzeugten Kaverne haben.

Contents

List of Figures

List of Tables

Nomenclature

α	MPa^{2-n}	Hardening Parameter
α_t	1/ °C	Linear thermal expansion coefficient
β	[-]	Constitutive model parameter
β_1	MPa^{-1}	Constitutive model parameter
β_i	[-]	Standardised regression coefficient
β_r	[-]	Reliability index
γ_{cr}	$\mathrm{kN/m^3}$	Density of cap rock
γ_{rs}	$\mathrm{kN/m^3}$	Density of rock salt
γ	[-]	Ultimate parameter
δ_{ij}	[-]	Kronecker delta
$\dot{\varepsilon}_{ij}$	s^{-1}	Tensor of total strain rate
$\dot{\varepsilon}_{ij}^{el}$	s^{-1}	Tensor of elastic strain rate
$\dot{\varepsilon}_{ij}^{vp}$	s^{-1}	Tensor of viscoplastic strain rate
$\dot{\varepsilon}_{ij}^{cr}$	s^{-1}	Tensor of creep strain rate
$\dot{\varepsilon}_{ij}^{th}$	s^{-1}	Tensor of thermal strain rate
η	[-]	Hardening parameter
$\overline{\eta_M^*}$	MPa s	Maxwell coefficient
θ	°	Lode's angle
λ	s^{-1}	Fluidity parameter
λ_i	[-]	Eigenvalue of the covariance function
μ	[-]	Mean value (EE index)
μ^*	[-]	An EE index
ν	[-]	Poisson ratio
ρ	[-]	Correlation coeffiecient in random field theory
σ_{ij}	MPa	Stress tensor
σ	[-]	Standard deviation
$\Phi(.)$	[-]	The standard normal cumulative distribution function

ϕ_i	[-]	Eigenfunction of the covariance function
ξ	[-]	Accumulated viscoplastic strain
ξ	[-]	Accumulated viscoplastic strain
$\xi_i(\psi_i)$	[-]	standard uncorrelated random variables
ω	[-]	Frequency of search curve in FAST method
A	[s^{-1}]	Fluidity at a reference temperature
a_1	MPa^{2-n}	Constitutive model parameter
b	[-]	Constitutive model parameter
b_i	[-]	Regression coefficient
$C_H(.,.)$	[-]	Auto-covariance function
COV_{P_F}	[-]	COV of the failure probability
DF	[-]	Indicator of dilatant behaviour
$DF_{u,p}$	[-]	Tolerable and present value of DF
E	MPa	Elastic modulus
EE_i	[-]	Elementary effect of i^{th} parameter
F	[-]	Failure event
F^{vp}	MPa^2	Yield surface
F_0^{vp}	MPa^2	Normalising factor
G_x	[-]	Performance function
$G_{s,v,l}$	[-]	Performance function against dilatancy, volume loss and admissible minimum, res.
I_1	MPa	First invariant of the deviatoric stress
J_2	MPa^2	Second invariant of the deviatoric stress
k	[-]	Number of input parameters
l	[-]	Number of intermediate levels in subset simulation approach
m_0	MPa^{-1}	Constitutive model parameter
N	[-]	Sample size
n	[-]	Transition parameter
N_f	[-]	Flow rule exponent
l_y	m	Auto-correlation distance

p	[-]	The number of levels of the grid space in Morris method
P_i	MPa	Internal pressure
P_F	[-]	Probability of failure
Q	[kJ/mol]	Activation energy
R	kJ/(mol.K)	The universal constant of perfect gas
r	[-]	Number of trajectories in Morris method
R^2	[-]	Coefficient of determination
S_i	[-]	First-order sensitivity index
S_{Ti}	[-]	total order sensitivity index
s_{ij}	MPa	$= \sigma_{ij} - I_1/3$
s_m	[-]	System realisation based on m^{th} set of input data ($m = 1, ..., Z_s$)
T	[degree]	Absolute temperature
T_i	[-]	Transformation function
V	[-]	Variance
$VL_{u,p}$	[-]	Tolerable and current volume convergence
y_j	[-]	Intermediate failure threshold
Z_s	[-]	Number of model evaluations in each intermediate level of subset simulation approach

1 Introduction

1.1 Motivation and Background

The production of electrical energy from renewable resources, like solar, wind and geothermal have observed increasing attention in recent years. A vast amount of investment has been made in many developed countries to phase out the fossil fuels/ nuclear sources and transmit to the renewable energy resources. In 2014, the share of renewable resources in gross German power production reached to more than a quarter (AGEB, 2016). A challenge in using the renewable energy resources is their intermittent production profile. Renewable sources of energy may not provide a sustainable power supply to handle the network demands. During the history of producing electrical energy, various storage facilities have been developed e.g., batteries, surface pumped-hydro power plants, thermal storage facilities and underground storage in the porous medium or deep rock cavities. This dissertation analyses the behaviour of the deep rock salt repositories. In this approach, the pressurised gas, compressed by the excess electrical energy, is stored in the caverns and released when there is a peak of energy demand in the consumption grid. The rock salt formation, which has provided cavities for the storage of hydrocarbons and nuclear waste disposal for more than three decades, is an appropriate host rock for such repositories. In general, salt cavities provide very large and secure underground either storage or disposal for materials that do not dissolve salt. The idea of storing gases and hydrocarbons in the solution mined cavities was conceived in Canada in the early 1940s (Bay, 1963). Such energy storages were basically planned to peak shaving the strong fluctuation in the seasonal demands. The first cavern in rock salt to store natural gas was excavated in Michigan, U.S. in the 1950s (Pollak, 1994). Rock salt is ideally suited for storing pressurized gas because it is almost impermeable with high compressive strength. Also, due to the particular viscoplastic features of rock salt, a large proportion of stress may be relieved by deformation instead of the brittle fracture. Furthermore, the rock salt shows healing properties, i.e., allowing any cracks that may occur in the damaged zone to seal quickly. Besides proper hydro-mechanical properties of rock salt, its solubility in

water makes the excavation process economic, rather than the other available options. The salt can be leached out from the domal structure or bedded salt strata to make the required storage volume by the solution mining. All of the mentioned reasons justified the construction of the significant percentage of gas storage caverns in rock salt or depleted salt mines around the world (see Fig. 1.1). Favourable conditions to excavate a salt cavern can be found in Europe, Asia, and Gulf Coast states, USA. Salt caverns in the U.S. can deliver up to 23% of total natural gas from underground storage on a given day (EIA, 2015). China scheduled further expansion plans in Jintan gas storage field, near to Shanghai. Jintan gas storage is designed to have 36 gas wells with a total storage capacity more than one billion cubic meters (Wu, 2012). In early 1970s France and Germany began gas storage projects in salt at Tersanne and Kiel storage fields, respectively. Nowadays, cavern storages provide more than 17% of European storage capacity, i.e. around 18 *bcm* (Hureau, 2016). The most suitable salt deposit in Europe, Zechstein (Upper Permian) is extended in the northern Germany (Gillhaus, 2007). Domal salt formations in the Zechstein stratum in Germany are nearly homogeneous, involving a high proportion of halite ($> 90\%$). They provide an ideal depth for mining a pressurised gas storage, up to $1700\,m$ with no excess of the insoluble inter-layers. These facts encouraged German industry to do enormous investments in the last three decades in the installation of natural gas storages in deep underground formations. For instance, Etzel storage site in Germany includes 29 gas caverns with a maximum storage volume of 1.8 *bcm*. Meanwhile, Germany has numerous expansion plans for increasing the share of renewable energies in the power production and different consumption sectors. For instance, a major development project is launched for the offshore wind farms in the northern regions, and the government introduced many stimulus projects for industrial and agricultural consumers to raise the renewable energy consumption (see Fig. 1.2). Therefore, underground energy storage in the rock salt caverns is a considerable opportunity.

In the context of underground storage in rock salt caverns, the surplus electrical energy can be utilised to compress air, that will be stored in underground cavities and discharged to pass a turbine generator when the electricity is further required. This concept, known as compressed air energy storage CAES, was firstly applied in the 1980s. Currently, there are two operational CAES plants worldwide. One is located in Huntorf, Germany, providing 290 MW storage capacity (Crotogino et al., 2001). This storage plant includes two mined salt caverns. Another rock salt cavity provides compressed air storage medium of about 19.6 *mcf* for an 110 MW plant in Alabama, USA (Pollak, 1994).

The excess energy also may be utilised to electrolyse water to Hydrogen and Oxygen. The Hydrogen is compressed and stored in the solution mined caverns, subsequently, to

release further and compensate the energy lack in consumption peaks. Hydrogen as a chemical storage media has a high volumetric storage density. Thereupon, it is regarded as a suitable media to store a large amount of expected surplus energy generated by the expansion plans of the renewable plants. Long term positive experiences do exist with high-pressure H_2 underground storage facilities in rock salt worldwide. Two storage plants in the U.S. (Texas) are managed by ConocoPhillips and Praxair (Leighty, 2008). Another one in Teeside, U.K. is managed by Sabic Petrochemicals (Lord et al., 2011).

However, although an underground storage plant is generally safer and more stable than similar facilities on the ground, a poorly designed or operated plant can lead to severe accidents (Bérest & Brouard, 2003). Therefore, the safety and stability of a rock salt cavity in an underground storing plant are among the most important criteria in their geomechanical design process. In order to investigate how reliable the safety of a rock salt cavity is, there should be some criterion like no-dilation. Exceeding the limit state of these criteria may cause initiation and growth of cracks in the rock salt, which leads to failure in the sealing and, consequently, the loss of the product. The other criterion can be the limitation of volume convergence that prevents excessive closure without brittle failure. A reliable design of solution mined cavities requires adequate knowledge about the behaviour of the host rock. While the standard high pressurized natural gas caverns can be emptied in 10 days and refilled in 30 days or less (Spreckels & Crotogino, 2002), a CAES may experience up to one cycle per day. Thereupon, the particular cyclic loading conditions of the renewable energy storage caverns, deduced from daily or weekly charge/withdrawal cycles should be considered. It can be achieved by an effective interaction among the experimental investigations, constitutive modelling, and the numerical analysis. The stability analysis may include data sets of laboratory results of mechanical testing, numerical modelling, and constitutive models. A conceptual approach which encompasses the concepts of experimental exploration, constitutive modelling, and forward simulations, their interdependencies and contributions in the framework of an iterative study, specific to the solution mined salt cavities is presented by the author in Mahmoudi, Khaledi, von Blumenthal, König & Schanz (2016).

A consistent picture of the rock salt characteristics may form by gathering different information sources as laboratory analyses, geotechnical in-situ measurements, and on-site observations. Nevertheless, laboratory investigations are regarded as the first step of getting aware of the governing phenomena on the rock salt behaviour. Utilising the experimental apparatuses, one can observe the physical response of rock salt under different boundary conditions. Due to the cyclic essence of the thermo-mechanical loading conditions in renewable energy concept, the rock salt around the cavern undergoes com-

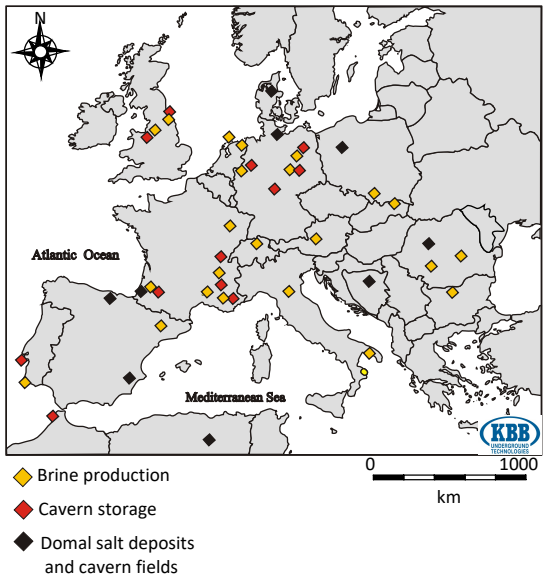

(a)

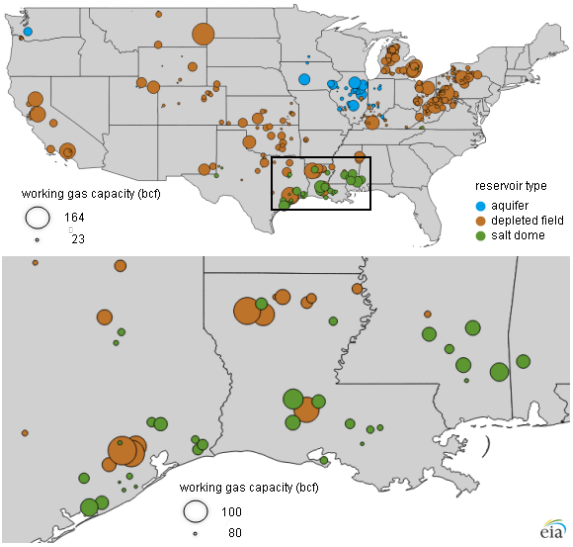

(b)

(c)

Figure 1.1: Underground salt facilities in (a) Europe (www.kbbnet.de) and (b) USA (www.eia.gov) and (c) China (www.cedigaz.org)

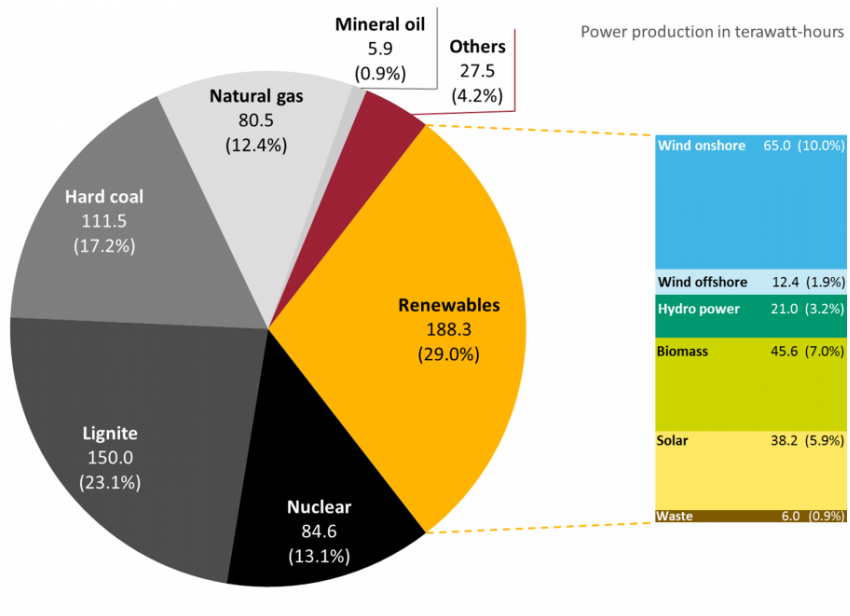

Figure 1.2: The share of different resources in the energy production in Germany (data obtained from AGEB (2016), www.cleanenergywire.org)

plicated stress conditions rather than what are conventionally applied in the geotechnical laboratory tests. Although, numerous experimental investigations were conducted on the monotonous loaded rock salt (Cristescu & Hunsche (1998) comprehensively reviewed them), the experimental evidence for describing constitutive rock salt behaviour under cyclic mechanical and thermal loading are rare in the literature. Rock salt behaviour under cyclic mechanical loading was investigated e.g. by Fuenkajorn & Phueakphum (2010), Liang et al. (2012), Guo et al. (2012) and Liu et al. (2014) for uniaxial stress condition. Thermal effects were not considered in the aforementioned experimental set-ups. Further studies, applying triaxial stress conditions and various complex stress paths on rock salt, were executed among others by Bauer et al. (2011), Düsterloh et al. (2013), Ma et al. (2013) and Roberts, Buchholz, Mellegard & Düsterloh (2015). Although no cyclic thermal loads were applied, the temperature was considered by means of isothermal conditions at different temperatures in some of these studies. The concept of an experimental setup that can apply cyclic thermo-mechanical loading is proposed in Mahmoudi, Khaledi, von Blumenthal, König & Schanz (2016). Nevertheless, the imposed loads are periodically changing during the excavation and operation phase of a storage cavity changes in temperature as well as in mechanical stress. The host rock encounters various stress states along caverns wall due to different reasons such as geometry or overburden. In this regard, a finite element simulation of a rock salt cavern, employing known constitutive laws, is conducted to estimate the accurate boundary conditions and loading paths in the experi-

mental configuration. The stress path for most critical point around the cavern obtained from simulation is simplified in a way that it takes into account the main characteristics of the loading (e.g. extension or compression, minimum and maximum loadings and temperature). The simplified stress path may be then used as a reference for experimental control parameters such as confining pressure, axial load and thermal loading. A preliminary study in this framework was conducted in von Blumenthal et al. (2016) to provide a more precise insight into stress evolution at critical points in the vicinity of a rock salt cavern.

However, the computational analysis is primarily based on the governed relations between the physical properties of the rock salt, which is usually expressed through a constitutive model. A comprehensive constitutive law for evaluating the behaviour of rock salt under long-term cyclic loading should consider the elasto-viscoplasticity features, as well as creep behaviour. Also, it has to be able to formulate and predict the dilatancy behaviour and considering thermal effects. It should be stated that based on the proposed iterative concept, the introduced sophisticated constitutive model will be calibrated further using experimental measurements. The calibrated material model is an appropriate basis for the assessment and approval of the stability of an underground repository by the computational model introduced in advance. The concept is visualised in Fig. 1.3. It also worth to mention that the proposed concept is applicable to every other investigation with the minor possibility to access to the real measurements.

Generally, the natural variability of the rock salt in the field, measurement errors, difficulties in running in-situ experiments, and lack of adequate experimental set up for conducting full-scale tests may result in significant levels of uncertainties (Einstein & Baecher, 1983). Therefore, utilising probabilistic and reliability-based analysis approaches developed in Tang et al. (1976), Wang (2011), Mollon et al. (2013) and Phoon & Ching (2014) is a necessity. Due to the fact that the uncertainties of the rock medium properties are unavoidable, a reliable design procedure can not rely merely on the deterministic approaches. Thereupon, in addition to the above-mentioned iterative process to provide an adequately accurate computational model, the stochastic analysis approaches should be utilised as well, to reach a reliable design. In this thesis, the probabilistic analyses are utilised, as substantial tools to describe the associated uncertainties and evaluate the impacts of their propagation. In this context, the constitutive parameters are represented as random variables with predefined statistical measures. The effect of the uncertainties in the input parameters on the system responses is inquired by carrying out the global sensitivity analysis. After determining the governing parameters, their relevant uncertainties are quantified and the failure probability of the system considering different failure

criteria is evaluated. The failure probability in the system is investigated using classical Monte-Carlo simulation methods and a more sophisticated methodologies as subset simulation. Also, the reliability-based design approach is conducted to determine the design parameters considering safety issues. Last but not least, as a vigorous statistical tool, random field discretization is utilised to describe the spatial variability of the excavation medium and links it to the reliability analysis concept. In this order, the Karhunen-Loève expansion has been introduced to generate the random field and the subset simulation methodology was utilised to estimate the reliability measures.

1.2 Computational model

The computational analysis of a rock salt cavity can be divided into two main categories: *i*) physical modelling (constitutive models) and *ii*) numerical simulation. Urai & Spiers (2007) defined the rock salt as a polycrystalline material consisting of grains of halite with small amount of impurities. Under the influence of the applied thermo-mechanical loads, rock salt behaves in different ways in the stress space. According to the experimental investigations conducted by several researchers, a boundary in the stress space known as dilatancy boundary separates the ductile behaviour of rock salt from the brittle response; (see Hunsche & Hampel (1999), Cristescu (1993), Günther & Salzer (2007), Schulze et al. (2001), Hampel & Schulze (2007) and Alkan et al. (2007)). When the stress state is below the dilatancy boundary, a time-dependent ductile deformation without any visible macroscopic fracture is observed. This time-dependent behaviour is highly affected by the magnitude of the applied load as well as the environmental factors like temperature. In case that the stress state exceeds the dilatancy boundary, the micro-cracking, intergranular slip as well as crystal plasticity occur (Hunsche & Hampel, 1999). Thus, the irreversible volumetric strain increases due to the opening of micro-cracks, and other relevant factors such as damage, permeability increase and long-term failure take place in this zone. To take into account the above-mentioned mechanical properties of rock salt, different constitutive models have been developed (Cristescu & Hunsche, 1998; Olivella & Gens, 2002; Hou, 2003; Minkley & Muehlbauer, 2007; Ma et al., 2012). In this thesis three well-established rock salt constitutive models are employed, namely LUBBY2, BGRa and Desai elasto-viscoplastic model. Moreover, the latter one is combined with the material model of LUBBY2 to develop an elasto-viscoplastic creep model.

In order to simulate the behaviour of a rock salt cavity under realistic imposed load conditions, numerical methods e.g., finite difference and finite elements have been widely

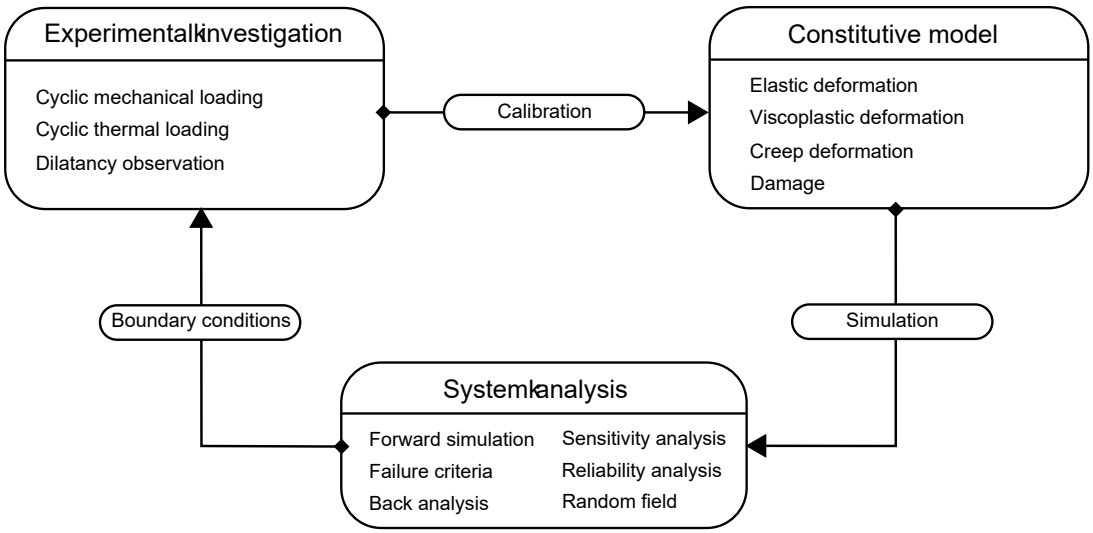

Figure 1.3: The applied iterative approach

employed in previous studies. For examples, a series of finite element analyses that simulate hypothetical natural gas storage caverns were performed and reported by DeVries et al. (2003) to illustrate the cavern responses under a wide range of conditions that are expected to exist in the Appalachian Basin, USA. Heusermann et al. (2003) performed a finite element study based on the LUBBY2 constitutive model to investigate two types of design proof, namely stability and usability. Moghadam et al. (2015) conducted a series of numerical analyses to investigate the influence of the cavern geometry and non-salt interbeds on the performance of underground storage caverns excavated in rock salt, considering an elasto-viscoplastic constitutive model. The stability of horizontal caverns mined in thin-bedded rock salt formations, considering different geometry and boundary conditions, was examined by Xing et al. (2015) using finite difference method. Wang et al. (2015) verified a time-dependent prediction model of the subsidence above storage caverns in rock salt, using a finite difference method analysis. In this thesis, different finite element simulations are carried out on to investigate various aspects in the storage cavern's response.

1.3 Non-deterministic analysis

The uncertainty in the behaviour of any system originates from the accuracies in determining the value of those parameters which provide the strength of the structure as well as the lack of certainty in the structure demands.

In general, the random characteristics of the imposed loads and boundary conditions of a structure can be reasonably estimated. In the case of utilising quality-controlled materials like steel or concrete, the associated uncertainties into the structural strength, which is mainly dominated by the material parameters, are relatively small and known as well. There is a well-established database of the features of quality-controlled materials, which can be considered as a priori knowledge to estimate the mean value of the parameters. Due to their practically uniform properties, which is warranted during the production process, performing the representative laboratory experiments on a few number of given samples can obtain the mean parameter's value of such substances. On the other hand, the strength parameters of geomaterials like rock and soil or even their type may noticeably differ even in a medium size construction site. Hence, gathering a comprehensive database of all the rock soil types around the world is mostly infeasible. In addition to that, due to the natural origin of the geomaterials, their strength parameters are dealing with an inherent randomness, and the spatial randomness is a significant source of uncertainty in such materials. Therefore, the variance of the strength parameters in geomaterials is relatively high, and running the reliability analysis is a primary requirement for every geotechnical structure.

It should be noted that among the other factors, the imposed loading conditions, i.e., minimum and maximum pressure, minimum and maximum temperature, and the allowable rate of charge and discharge the gas can be regarded as uncertain design variables. These parameters may vary due to the imperfections in the operating and monitoring instruments, unmeasured heat exchange between the stored product and host rock medium and transmission pipeline during the injection or withdrawal. Hence, the conventional deterministic analyses cannot adequately predict the realistic behaviour of the rock salt cavities, while they neglect the great extents of involving uncertainties. Accordingly, this study utilised the probabilistic analyses and design methodologies to consider the imprecision and their influence on the system output to develop a robust and stable design.

However, this study focuses on the effect of the mechanical properties of the rock salt on its response as a geological host rock. Each numerical simulation is associated with uncertainties that can be due to aleatoric (statistical) and epistemic (systematic) uncertainties (Kennedy & O'Hagan, 2001).

Hartford & Baecher (2004) presented the following taxonomy for the uncertainties:

- **Aleatory uncertainty** which represents the randomness of nature in the gained results from experimental studies. The aleatory uncertainty can not be omitted but

approximated using mathematical models. The temporal and spatial variation of geomaterial properties are examples for this class of variabilities.

- **Epistemic or knowledge uncertainty** is attributed to the lack of available knowledge or understanding about the process or the physical phenomena. The amount of this type of uncertainties may be decreased by the adequate investigations, measurements and exploration plans. In geotechnical applications the epistemic uncertainty includes (Baecher & Christian, 2005): *i*) **Parameter uncertainty**, which is due to the errors of parameter identification process. Besides measurement and calibrating errors, lack of the conducted in-situ observations and laboratory tests may cause such uncertainties. *ii*) **Model uncertainty**, it originates mainly from the lack of available knowledge or facilities to represent and simulate the real physical behaviour of the investigated problem.

Additional types of uncertainties in the field of geotechnical engineering are introduced by Baecher & Christian (2005). These are related to **operational uncertainties**, which include construction, deterioration in the condition, and maintenance uncertainties, and *decision uncertainties* considering the economic, social and timing issues. However, this dissertation does not consider these matters neither in the rock salt behaviour predictions obtained from numerical simulations nor in the probabilistic analyses. Fig. 1.4 depicts different categories of the uncertainties, which can be considered in a reliability analysis of a geotechnical problem.

In the numerical simulation of a solution-mined cavity, the epistemic uncertainties may result from the associated variability in the experimental investigation, the governed constitutive model, input factors (e.g., geometrical characteristics, thermo-mechanical properties), and the numerical approximations.

Besides the spatial variability of rock salt properties which is considered as aleatoric uncertainty, the small amount of investigated undisturbed rock salt specimens compared to the huge volume of rock salt will be affected during the construction and operation phases as well as error measurements are main origins of uncertainties. Also, the accessibility to the adequate site exploration may be restricted to a few boreholes, in this particular structure which is extended vertically downward more than the hundred meters from the ground level, compared to the common construction sites. Furthermore, the complex geometry which may be created by the solution mining is also taking into consideration as a source of uncertainty in the framework of numerical model approximation, because in the most cases of numerical simulation a simplified geometry is regarded.

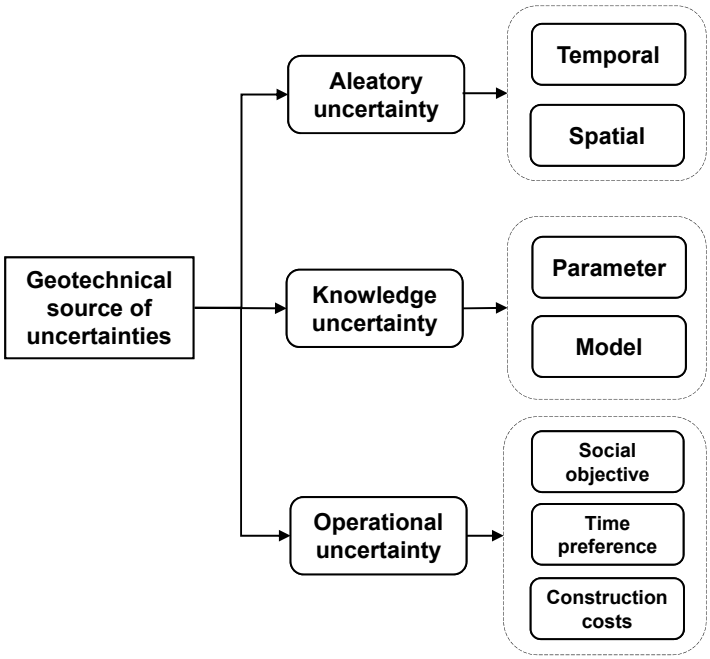

Figure 1.4: Categories of uncertainty involved in the reliability analysis of a geotechnical problem (adjusted from Hartford & Baecher (2004))

This thesis investigates the impact of the input parameters uncertainties on the failure probability of the underground rock salt storage. The input factors which are principally related to the thermo-mechanical properties of the rock salt are subject to different sources of uncertainties resulting from aleatory and epistemic sources. The uncertain material properties are customarily defined as random variables described by the expected value and standard deviation and a probability density function as well. These measures are driven by the existing data set about the mechanical properties of rock salt formation (Ratigan & Hannum, 1980; Hansen & Carter, 1983; Van Sambeek et al., 1993; Sane et al., 2008; Guo et al., 2012; Ma et al., 2013).

In the first step, the variability of the related input factors in a rock salt cavity, and their impacts on the system behaviour must be investigated. This is achieved by conducting a sensitivity analysis which determines the most effective parameters in the output variability as well as the most inefficient ones. Afterwards, the corresponding uncertainties in the most relevant input variables may reduce by utilising the parameter identification and optimisation methods. Moreover, identifying the most informative measurement arrangement to obtain input parameters in the framework of optimal experimental design can supplement the deterministic approaches. Nevertheless, some amount of uncertainties which are most related to the mechanical properties of the excavated rock salt are

inevitable, therefore using the reliability design approaches is substantial to consider the uncertainties and their probable consequences on the system output. The results of probabilistic analyses will be accurate when the knowledge about the variability amounts and measures of the input factor were precise, in such case, the reliability-based design is utilised with least cost objective constrained with a minimum reliability index requirement. Meanwhile, the variability of geotechnical parameters due to the lack of undisturbed given rock samples, in-situ measurements, laboratory investigations, and probably measurement errors is large (Phoon & Kulhawy, 1999). Thus the statistical distribution may be either overestimated or underestimated which may cause uneconomical or unsafe design, respectively. The approach of robustness in the design without eliminating the sources of uncertainty is developed to overcome this issue (Juang & Wang, 2013).

The employed supportive tools to run the mentioned analyses are introduced in the following section in brief.

1.4 Statistical Tools

1.4.1 Sensitivity analysis

A large number of input factors involved in a sophisticated computational model is a big challenge in the concept of probabilistic analyses because exploring all of the uncertain variables exponentially influences the computational effort of conducting probabilistic techniques. Utilising sensitivity analysis techniques to determine the key factors which govern the system responses, can address this issue. Afterwards, more investigation and exploration merely about the key input factors may be conducted to reduce the propagation of variability in the system output. This facilitates the probabilistic analysis since it may reduce the computational time, drastically. Moreover, sensitivity analysis determines the most irrelevant input parameters that allows one to neglect their variation (i.e., fixing) in the further analyses and reduce the corresponding computational effort, consequently. The sensitivity analysis has been widely utilised in geotechnical engineering problems (for instance, see Homma & Saltelli (1996), Schanz et al. (2006), Hamm et al. (2006), Knabe et al. (2012), Mollon et al. (2013), Long (2014) and Miro et al. (2014)).

Sensitivity analysis techniques are divided into two main categories, local and global. The derivative based local sensitivity analyses methodologies evaluate the local impacts of the input factors on the system outputs. The local term indicates that all derivatives are taken at a base point in the input space while the global approaches explore the entire

parameter space of each variable to evaluate its effects on the outputs. Using the global sensitivity approaches make the identification of interactions between the input parameters in non-linear models feasible. Nevertheless, a global sensitivity analysis usually requires much more amount of computational evaluations compared to the local methodology. The methods for sensitivity and uncertainty analysis are based on either statistical or deterministic procedures. Although, the statistical methods can be utilised by both local and global analyses methods, the local analysis mostly employs the deterministic methods (Cacuci, 2003). While a comprehensive computational model of an underground storage system, probably includes non-linearity, the global sensitivity analyses approaches are conducted in this study. In this study global sensitivity analysis is considered as the first step in probabilistic analysis dealing with its complex computational model including a multitude variables.

This thesis introduced different well-known global sensitivity analysis methodologies, namely random balance design, Sobol'/Saltelli, and elementary effect. The first two methods are classified as the variance-based techniques and the last one is considered as a screening method. The variance-based methods, as a general variance decomposition scheme, investigate and quantify how the variance of inputs contribute to the variance of the model output. The idea of the variance-based method in global sensitivity analysis was developed by Sobol' (1990). Saltelli et al. (2008) later modified it in the concept of computational burden. Elementary effect (a.k.a. one-at-a-time or Morris) method (Morris, 1991) as a screening sensitivity analysis methodology originated from the local sensitivity analysis method. In this approach, the number of required model evaluations are considerably less than what is needed in the variance-based method. Thus, when the number of input parameters is very large, this methodology may be applied, with considerably less computational burden, to identify which of input parameters can be fixed without any major effect on the important characteristic.

This dissertation presents the obtained results of conducting the three mentioned global sensitivity methods on the corresponding constitutive variables in a rock salt cavern numerical analysis.

1.4.2 Metamodel

The execution time of a comprehensive numerical model of a rock salt cavity, considering excavation and operation phases is relatively high. Conducting the sensitivity analysis and the probabilistic analyses generally requires hundreds of model evaluations which make these analyses computationally expensive or even infeasible. Numerous statistical

and probabilistic tools (regression, smoothing, statistical learning, Monte Carlo, etc.) aim at determining the model input variables which mostly contribute to an interest quantity depending on model output.

In general, a metamodel, is an analytical model that substitute the original simulation with sufficient accuracy and evaluates the behaviour of a multivariate complex system while it is computationally inexpensive and plausible. All metamodelling techniques consist of running the original but computationally expensive simulation on a set of samples and using the gained information to predict the result of conducting the simulation at other points in the parameters' space. Depending on the structure of input parameter set and system behaviour, several approximation techniques are introduced (e.g., see Lancaster & Salkauskas (1981); Powell (1987); Forrester et al. (2008); Bolzon & Buljak (2011); Buljak (2012)). In this dissertation, Proper Orthogonal Decomposition (POD) combined with Radial Basis Functions (RBF) is employed in the sensitivity analysis of a rock salt cavern to evaluate the corresponding system responses. This technique is proposed by Buljak (2010), for more details about the approach and its implementation process see Khaledi et al. (2014).

1.4.3 Reliability analysis

In order to assess the effects of uncertainties on system performance, the designer commonly use a technique that yields an approximation to the true value of the reliability index and the probability of failure (Baecher & Christian, 2005). In this regard, there are several methods, involving different computational effort, and they may provide different levels of accuracy. Among the others, the Monte Carlo simulation-based methods as crude Monte Carlo and subset simulation are employed in this thesis.

- **Monte Carlo simulation**

  In this conceptually simple approach, a large number sets of randomly generated values for the uncertain parameters are created and the corresponding system response for each set is evaluated. If the amount of imposed loads does not exceed the obtained strength value corresponding to the randomly generated set of parameter, the system is regarded as safe and vice versa. Such a comparison can be formulated through a performance function. The statistics of the resulting set of performance function's values can be presented as either the failure probability or the reliability likelihood. A large set of input samples and model evaluations are needed in the crude Monte Carlo method to obtain adequate accuracy. The increasing expectation on the reliable performance of the modern engineering systems enhances their

complexity. They are supposed to be designed in a way that their failure be a rare event, but this makes its assessment by crude Monte Carlo method computationally prohibitive. Therefore, the computational effort can be reduced significantly by employing more advanced sampling methods as Markov chains as it proposed in subset simulation.

- **Subset simulation**

  The idea behind subset simulation is quite simple and makes use of fundamental probability logic, namely, conditional probability. The probability of a rare event is equal to the probability of a not-so-rare event multiplied by the probability of the not-so-rare event happens (Au & Beck, 2001).

  In order to conduct subset simulation, a powerful simulation method called Markov Chain Monte Carlo (MCMC) is utilised. This sampling method allows the efficient generation of random samples according to an arbitrarily given probability distribution. The samples are generated as a sequence of a Markov chain. The distribution of the samples is either equal to the target distribution right from the start or otherwise converges to it as the Markov chain develops.

1.4.4 Reliability-based design

After calculating the failure probability of the system, the interested level of safety based on the reliability index (Hasofer & Lind, 1974; Haldar & Mahadevan, 2000; Phoon, 2008) can be applied to evaluate the value of the design parameters in a manner that ensure the system safety. The flow work shown in Fig. 1.5 describes the non-deterministic analysis procedure which is utilised in this thesis. The statistical analysis includes different methodologies of sensitivity and reliability analyses combined with the metamodel concept.

1.4.5 Random Field

In most engineering problems the material parameters spread over spatial extents but they are neglected commonly. The analyses mostly assign the mean value of a variable to the whole medium, while in the case of heterogeneous materials, this may lead to an unreliable design. The existing scatter in such material can be represented in the design procedure using the random field concept. Various random field generator algorithms are available in literature, (see e.g., Baecher & Christian (2005)). In the last chapter of this thesis, Karhunen-Loève expansion method is applied to generate random field realisations.

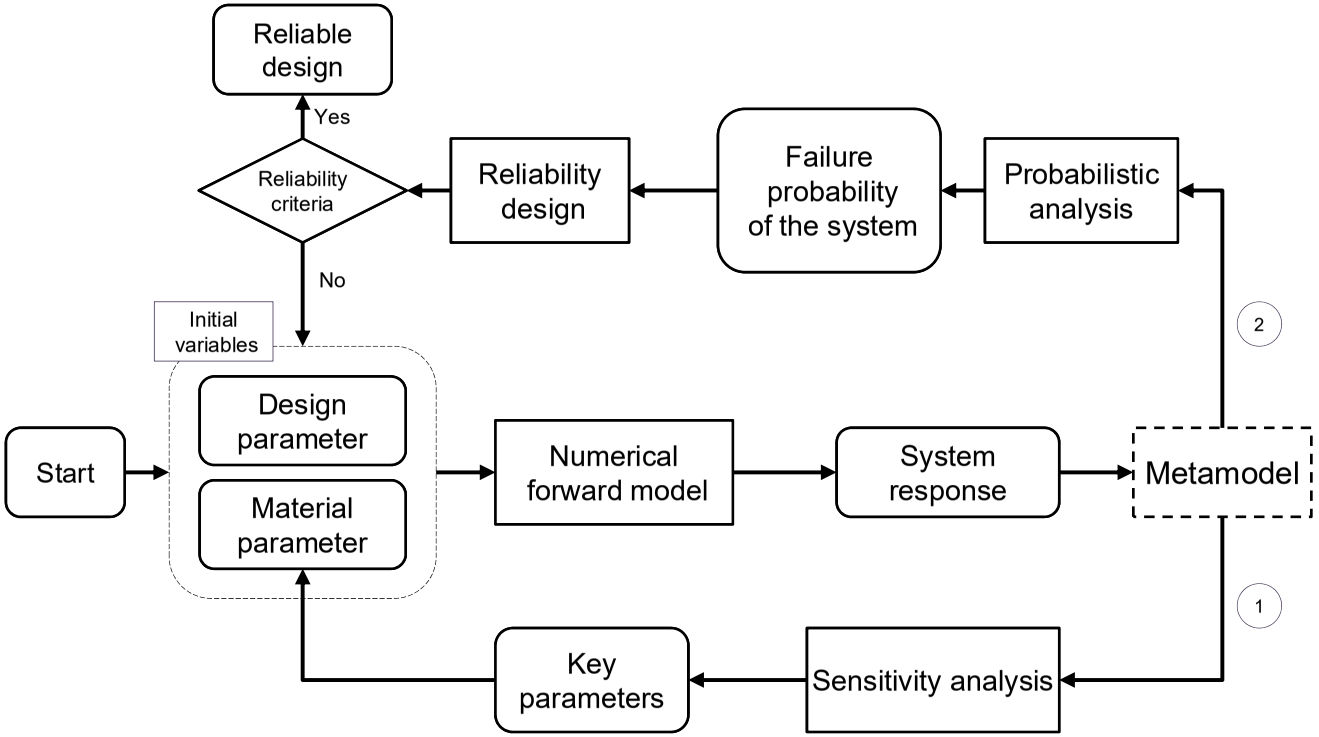

Figure 1.5: Flow chart of the proposed non-deterministic approach to achieve a reliable design

Series expansion methods as Karhunen-Loève, approximate the random field by a finite sum of products of deterministic spatial functions and random variables. Therefore, the material properties can be specified as functions of point coordinates.

The inherent randomness of natural materials like rocks and soils causes a wide extent of spatial distribution in their physical properties. Thereupon, the spatial variability and consequently the induced uncertainty must be considered in complex geomechanical problems. In this thesis, the random field method is used in a probabilistic analysis of a gas storage cavern in the rock salt. Consideration of the spatial variation of mechanical properties in this particular structure which is extended vertically downward more than a hundred meters from the ground level is substantial. In this regard, a probabilistic model is presented to compute the failure probability of a cavern mined in a spatially varying salt dome. Here, the no-dilatant region around the cavity is regarded as the failure criteria. A deterministic thermo-mechanical model of the natural gas storage in rock salt is defined using finite element method. Then, a random field model of material parameters applying Karhunen-Loève expansion is introduced with spatially varying constitutive parameters of BGRa creep law (Hunsche & Hampel, 1999). Afterwards, the finite element code is substituted with a metamodel to execute Monte Carlo stochastic finite element method. After that, the failure probability calculations are performed for different spatial variability scenarios to present the effect of the autocorrelation lengths on the safety measures of the system against dilation.

1.5 Overview of the dissertation

The structure of this dissertation is organised according to the following chapters: **Chapter 1** introduces the thesis through the motivation and background of the subject, introducing the supportive tools and providing the organisation of the content. **Chapter 2** presents a review of the existing computational models to simulate the thermo-mechanical behaviour of the rock salt. The basic features of different constitutive models, namely the elasticity, creep, and viscoplasticity of the rock salt are presented. **Chapter 3** investigated the behaviour of rock salt under particular geomechanical conditions utilising finite element simulations. In this regard, different issues as the depth of the cavern and its geometry and solution mining process are investigated. Moreover, various failure criteria for ensuring the stability and the integrity of a rock salt cavern are presented.

Chapter 4 introduces various global sensitivity analysis methodologies, namely the regression methods, different variance-based techniques, and a screening method. Moreover,

it briefly explains metamodelling methodology to substitute the computationally expensive finite element simulations in the further sensitivity and reliability analyses procedures. Three different sensitivity analysis methods are utilised to assess the relative importance of the input variables in a computational model of a typical rock salt cavity.

The objectives of **Chapter 5** are to define measures of reliability and to examine some different types of failure. The final section is devoted to the reliability-based design concept. **Chapter 6** presents a case study, where the failure probability of a cavern mined in a spatially varying salt dome is assessed. No-dilatant region around the cavity is regarded as the failure criteria. The random field model of constitutive parameters of the BGRa creep law is generated using Karhunen-Loève expansion.

2 Thermo-Mechanical Behaviour of Rock Salt

Since the mechanical properties of the rock salt govern the stress-strain response of a storage cavity, the numerical simulation of such a structure should be based on an appropriate constitutive model. During last four decades, tens of different constitutive models are introduced to simulate the thermo-mechanical behaviour of rock salt through mathematical equations. Among the others, one may mention studies of Hansen & Carter (1983); Olivella et al. (1996); Hou (2003); Hampel & Schulze (2007); Günther (2009); Ma et al. (2012) (for a brief review see Cristescu & Hunsche (1998)). In the following, three well established constitutive models in both industrial and research communities are presented and subsequently applied to study the response of the cavity.

2.1 LUBBY2

The LUBBY2 model is used to describe the time-dependent response of the rock salt around the cavern under quasi-static geological loading. To model the creep behaviour of rock salt formation, the LUBBY2 model presented by Heusermann et al. (2003) is a viscoelastic constitutive model for describing creep behaviour of rock salt. It describes transient and secondary phases of creep phenomena. Based on this model, the total strain rate is obtained by

$$\dot{\varepsilon}_{ij} = \dot{\varepsilon}^{el}_{ij} + \dot{\varepsilon}^{ve}_{ij}, \tag{2.1}$$

where, $\dot{\varepsilon}^{el}_{ij}$, $\dot{\varepsilon}^{ve}_{ij}$ are the elastic and viscoelastic parts of the total strain rate, respectively. The equation 2.2 gives the non elastic part of strain rate.

$$\dot{\varepsilon}^{ve}_{ij} = \frac{3}{2}\left[\frac{1}{\overline{\eta}_K(q)}(1 - \frac{\epsilon_{tr}}{q}\overline{G}_K(q)) + \frac{1}{\overline{\eta}_M(q)}\right] S_{ij}, \tag{2.2}$$

where, q is the deviatoric stress, and S_{ij} represents deviatoric stress tensor.

ε_{tr} shows transient creep strain and $\overline{G}_K$ is Kelvin spring modulus (stress-dependent). $\overline{\eta}_M$ and $\overline{\eta}_K$ are Maxwell viscosity modulus (stress-dependent) and Kelvin dashpot modulus (stress-dependent), respectively.

Eq. 2.3 shows the stress dependency of material's creep rate by exponential laws.

$$\begin{aligned} \overline{G}_K &= \overline{G}^*_K e^{k_1 q}, \\ \overline{\eta}_M &= \overline{\eta}^*_M e^{mq}, \\ \overline{\eta}_K &= \overline{\eta}^*_K e^{k_2 q}. \end{aligned} \tag{2.3}$$

Fig. 2.1 shows the rheological sketch of this model. The material characteristic of the dashpots and springs in this model are stress dependent. The constitutive model properties' values are usually determined from the results of some creep tests on samples taken from boreholes. Heusermann et al. (2003) presented a uniaxial multi-stage creep test at stress levels of 12, 14, and 16 MPa on a rock salt sample (see Fig. 2.2). This uniaxial test is modelled by CODE-BRIGHT using LUBBY2 model. Firstly, the parameters' value were set based on Heusermann et al. (2003) suggested values (represented in Tab. 2.2). Then the difference between results of laboratory tests and the respective outcomes, obtained from numerical simulations is minimised employing back analysis approach (Knabe et al., 2012). The material parameters' values which are presented in Tab. 2.2 are the optimised set for fitting experimental and numerical data sets utilising genetic algorithm optimisation method. Fig. 2.2 shows a comparison of experimental and numerical results in the case of strain and strain rate. Tab. 2.2 also includes parameter sets which are used by Hou (2003) for the LUBBY2 material model; these values are obtained for rock salt of the *Asse mine* in Germany. By comparing these three data sets, it seems that the identified values for parameters in this study are in good agreement with the other studies.

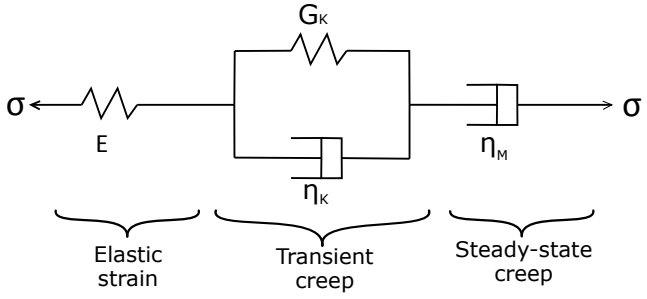

Figure 2.1: Illustration of the LUBBY2 model

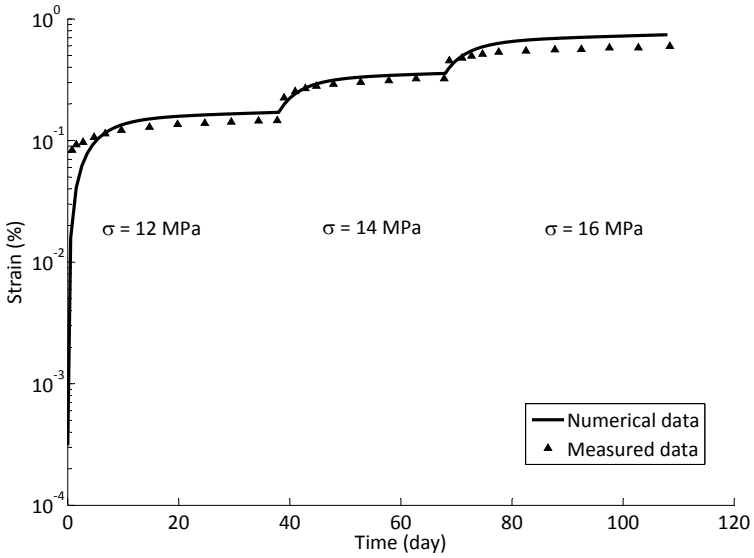

(a)

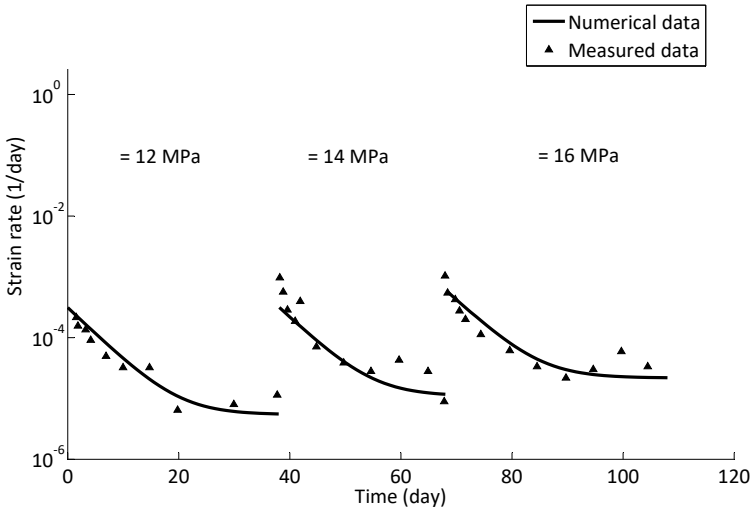

(b)

Figure 2.2: Strain (a) and strain rate (b) curve of rock salt in uniaxial compression test, (test data obtained from Heusermann et al. (2003))

Table 2.1: The LUBBY2 constitutive model parameters

Parameter	Description	Dimension	Range
$\overline{G}_K^*$	Kelvin spring coefficient	MPa	[3e5 - 6e5]
$\overline{\eta}_M^*$	Maxwell viscosity coefficient	MPa s	[0.5e12 - 2.5e12]
$\overline{\eta}_K^*$	Kelvin viscosity coefficient	MPa s	[4e9 - 9e9]

Table 2.2: The considered values for the LUBBY2 parameters in different studies

Parameter	Heusermann et al. (2003)	Hou (2003)	Current study
$\overline{G^*}$[MPa]	1.88e08	5.08e05	2.17e05
$\overline{\eta^*}_M$[MPa s]	1.04e13	1.76e12	5.18e12
$\overline{\eta^*}_K$[MPa s]	4.30e10	7.72e09	8.30e10
k_1[MPa^{-1}]	-0.254	-0.191	-0.275
k_2[MPa^{-1}]	-0.267	-0.168	-0.267
m [MPa^{-1}]	-0.327	-0.247	-0.275

2.2 BGRa

BGRa is one of the well-established creep models in the literature, it proposed by Hunsche & Hampel (1999), and has been used widely in different studies (e.g., Bräuer et al. (2011) and Müller-Hoeppe et al. (2012). In this constitutive model, the creep induced strain rate of rock salt is obtained using the following equation:

$$\dot{\varepsilon}_{ij}^{cr} = A \exp\left(\frac{-Q}{RT}\right)\left(\frac{\sigma_{ij}}{\sigma_0}\right)^u, \tag{2.4}$$

where A denotes the value of fluidity at a reference temperature; R is the universal constant of perfect gas (8.314 e03 kJ/(mol K)), and T is the absolute temperature (For more details see Hunsche & Hampel (1999)). In the present study, the induced strain rate by the temperature change is also considered as an additional strain tensor in the mechanical model. This quantity is related to the linear thermal expansion coefficient α_t and the temperature changing rate $\dot{T}$:

$$\dot{\varepsilon}_{ij}^{th} = \alpha_t \dot{T} \delta_{ij} \tag{2.5}$$

where, δ_{ij} denotes the Kronecker delta.

2.3 Elasto-viscoplastic creep model

Here, an elasto-viscoplastic creep model is proposed to describe the time-dependent behaviour of rock salt considering dilation and creep behaviour. This constitutive law is developed based on *Perzyna* viscoplastic model (Perzyna, 1966) and Maxwell model. The rheological scheme of the employed material model is demonstrated in Fig. 2.3. Based on this model, the total strain rate is obtained using the equation

$$\dot{\varepsilon}_{ij} = \dot{\varepsilon}^{el}_{ij} + \dot{\varepsilon}^{vp}_{ij} + \dot{\varepsilon}^{cr}_{ij}, \tag{2.6}$$

where $\dot{\varepsilon}^{el}_{ij}$, $\dot{\varepsilon}^{vp}_{ij}$ and $\dot{\varepsilon}^{cr}_{ij}$ are the elastic, viscoplastic and viscoelastic parts of the total strain rate, respectively. The elastic strain is obtained using the generalised Hooke's law. The viscoplastic component of strain rate is described by utilising an associated flow rule represented in Eq. 2.7, which has been developed by Desai & Zhang (1987) based on the viscoplastic model of Perzyna

$$\dot{\varepsilon}^{vp}_{ij} = \lambda \left\langle \frac{F^{vp}}{F^{vp}_0} \right\rangle^{N_f} \frac{\partial F^{vp}}{\partial \sigma_{ij}}. \tag{2.7}$$

The proposed yield surface, F^{vp}, which is equal to the potential function depends on three stress invariants, namely the first stress invariant (I_1), the second invariant of the deviatoric stress (J_2), and the Lode's angle (θ) according to the equations

$$F^{vp} = J_2 - \left(-\alpha I_1^n + \gamma I_1^2\right) \left(exp\left(\beta_1 I_1\right) - \beta cos\left(3\theta\right)\right)^b, \tag{2.8}$$

$$\theta = \frac{1}{3} cos^{-1}\left(\frac{-\sqrt{27} J_3}{2 J_2^{1.5}}\right), \quad I_1 = -\sigma_{ii}, \quad J_2 = \frac{1}{2} s_{ij} s_{ij}, \quad J_3 = det(s_{ij}). \tag{2.9}$$

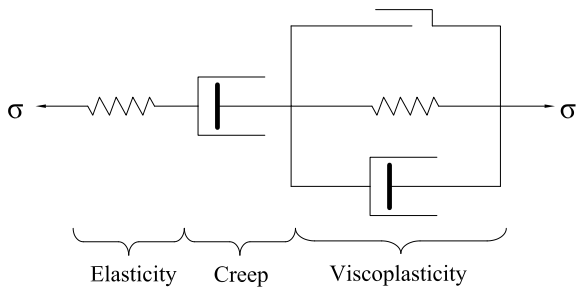

Figure 2.3: Illustration of the elasto-viscoplastic creep model

In the former equations, β, β_1 and b determine the variation of the failure boundary with respect to the change of Lode's angle θ, which varies from 60° at a triaxial compression to 0° at triaxial extension. F_0^{vp} is a normalising constant with the same dimension as F^{vp}; here the value is assumed to be equal to one. N_f and λ represent the rate-dependent behaviour of rock salt. The parameter γ is associated with the slope of the ultimate yield envelope. α is the hardening parameter which determines the size of the yield surface. This parameter is a function of the accumulated viscoplastic strain ξ, and its value decreases by increasing the viscoplastic deformation (Sane et al., 2008). The value of ξ is represented in Eq. 2.10, where a_1 and η are model parameters,

$$\alpha = \frac{a_1}{\xi^{\eta}}, \qquad \xi = \int_0^t \sqrt{\dot{\varepsilon}_{ij}^{vp} : \dot{\varepsilon}_{ij}^{vp}}\, dt. \tag{2.10}$$

The dilatancy boundary, which is defined by the beginning of the irreversible volumetric expansion, entitled as compression/dilatancy (C/D) boundary is mathematically represented by

$$J_2^{dil} = \left(1 - \frac{2}{n}\right) \gamma I_1^2 \left(exp(\beta_1 I_1) - \beta cos(3\theta)\right)^b \left\{1 + \frac{b\beta_1 I_1 exp(\beta_1 I_1)}{n(exp(\beta_1 I_1) - \beta cos(3\theta))}\right\}. \tag{2.11}$$

The C/D boundary is defined by the beginning of the volumetric expansion and is used to identify the stress state which results in dilatant behaviour. When the stress state locates above the C/D boundary, the material experiences dilatancy, i.e., an increase in permeability and development of micro-cracks that may lead to failure. Based on Eqs. 2.8 and 2.11, the dilatancy and failure boundaries are functions of Lode's angle. The dependency of the yield surfaces on Lode's angle results in different responses during triaxial compression, shear and extension loading. Therefore, for comparing the stress paths of the various regions around the cavern independently of Lode's angle, the scaled value of the second invariant of the deviatoric stress ($\sqrt{J_2^s}$) is calculated as

$$\sqrt{J_2^s} = \sqrt{J_2 \frac{J_2^{dil}(60°)}{J_2^{dil}(\theta)}}, \tag{2.12}$$

here $\sqrt{J_2^{dil}(60°)}$ indicates the distance of dilatancy boundary from the hydrostatic axis in π-plane (the plane normal to the hydrostatic axis), for compression ($\theta = 60°$), and $\sqrt{J_2^{dil}(\theta)}$ measures this distance for the current value of Lode's angle.

The third component of the strain rate in Eq. 2.1 describes the steady state creep behaviour of the rock salt

$$\dot{\varepsilon}_{ij}^{cr} = \frac{3}{2}[\frac{1}{\overline{\eta}_M}]s_{ij}, \tag{2.13}$$

where $\overline{\eta}_M$ is the viscosity of Maxwell dashpot (stress-dependent). The stress dependency of this parameter is described exponentially by

$$\overline{\eta}_M = \overline{\eta}_M^* e^{-m_0(\sqrt{3J_2})}, \tag{2.14}$$

where, $\overline{\eta}_M^*$ and m_0 are material parameters. Commonly, the value of the constitutive model properties is determined from the results of experimental tests on samples taken from boreholes. Here, triaxial test data reported by Desai & Zhang (1987) is simulated based on the proposed constitutive law in order to calibrate the constitutive model. This experiment was carried out to define the stress-strain relation under triaxial compression loading at a confining pressure equal to $\sigma_3 = 3.45$ MPa. The tested rock salt specimen in this experiment was collected from the *Salado* rock salt formation in New Mexico, USA. Fig. 2.4 illustrates the comparison between the observed and the predicted behaviour based on the numerical model in the stress-strain space. An extensive investigation in order to determine the material parameters of the viscoplastic component of the constitutive model is previously presented in Khaledi, Mahmoudi, Datcheva & Schanz (2016*b*). It should be stated that the value of $\overline{\eta}_M^*$ is adopted from Hou (2003). The constitutive parameters utilised to provide the numerical results are presented in Tab. 2.3.

2.4 Compression/Dilation boundary

Shear stress or deviatoric stress which can be induced by different internal pressures and in-situ stress of rock around the cavities results in creep deformation. If the pressure in the cavern is too small, the deviatoric stresses in the surrounding salt can lead to dilation in the rock salt. Salt dilation causes developing of micro-cracks, and volume increases. Irreversible volume increasing is the sign of exceeding no dilation criteria. C/D boundary defined by the beginning of volumetric expansion under compressive load, are used to identify states of stress which result in dilatant behaviour.

Over the years many equations have been developed for the description of no dilatation criteria; for instance, BGR (Hunsche et al., 2003) criterion which has been established

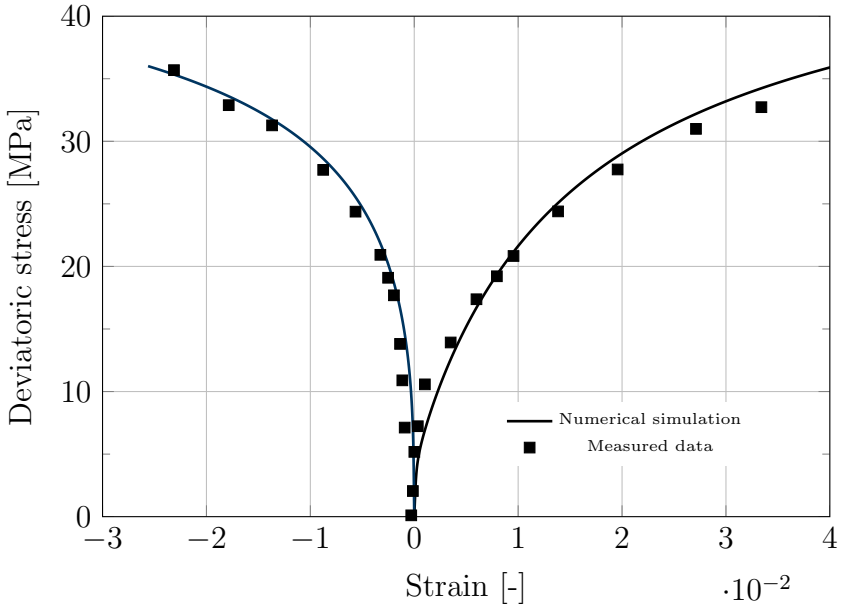

Figure 2.4: Triaxial compression test under confining pressure $\sigma_3 = 3.45\,\mathrm{MPa}$ (test data from Desai & Zhang (1987))

based on experimental studies is presented in Eq. 2.15.

$$\sqrt{J_2} = \frac{b_D}{\sqrt{2}} \left(\frac{I_1}{3} \right)^{c_D}, \tag{2.15}$$

where $b_D = 2.61248$ and $c_D = 0.78093$. Also, Eq. 2.16 represents Cristescu C/D line (Cristescu & Hunsche, 1998) for describing the rock salt behaviour based on some true triaxial experiments.

$$\sqrt{J_2} = \sqrt{\frac{3}{2}} \left(f_1 \left(\frac{I_1}{3} \right)^2 + f_2 \left(\frac{I_1}{3} \right) \right). \tag{2.16}$$

DeVries et al. (2003) and Desai & Zhang (1987) presented their boundaries by Eq. 2.17 and 2.19, respectively.

$$J_2 = \frac{(2-n)\gamma I_1}{(m\beta_1 exp(\beta_1 I_1))F_s - \frac{n}{I_1 F_s}}, \tag{2.17}$$

here the parameter of F_s is

$$F_s = (exp(\beta_1 I_1) - \beta sin(-3\theta))^m, \tag{2.18}$$

Table 2.3: The description of material parameters

	Parameter	Dimension	Value
Elastic parameter	E	MPa	2200
	ν	[-]	0.27
Viscoplastic parameters	n	[-]	3
	N_f	[-]	3
	β	[-]	0.995
	β_1	MPa^{-1}	4.8e-3
	b	[-]	-0.5
	λ	s^{-1}	0.58e-11
	a_1	$\mathrm{MPa}^{(2-\mathrm{n})}$	0.4e-4
	γ	[-]	0.095
	η	[-]	0.8
Creep parameters	$\overline{\eta}^*_M$	MPa s	1.75e12
	m_0	MPa^{-1}	0.275

where, γ, β, β_1, n, k and m are the constant parameters. θ is Lode's angle, varies from $+30°$ at triaxial compression to $-30°$ at triaxial extension.

$$\sqrt{J_2} = \frac{D_1 I_1^n + T_0}{\sqrt{3}cos(\theta) - D_2 sin(\theta)}, \tag{2.19}$$

where, $D_1 = 0.773$, $D_2 = 0.524$, $n = 0.693$, $T_0 = 1.95$ and θ is Lode's angle.

DeVries and Desai both presented non-linear compression/dilatancy boundaries considering the effect of intermediate stress (Lode's angle) on the dilation limit. C/D boundary suggested by Desai is introduced in Sec. 2.3. Hence they provide different dilatancy boundaries for various zones around the cavern. A comparison of the four C/D boundaries or criteria is expressed in Fig. 2.5 in the invariant stress plane. Since below these lines, rock salt experiences no dilatancy, they named as no dilation criterion. As Fig. 2.5 shows various constitutive models based on different empirical investigations or rheological models define slightly different C/D boundaries. It should be pointed out that based on many experimental data in a wide domain around of C/D boundary, carried out by Cristescu & Hunsche (1998), the irreversible volumetric strains have a negligible variation. They investigated the width of the domain where ϵ_v has a slight variation in the neighbourhood of the C/D boundary for rock salt. See Fig. 2.6, where the x signs demonstrate the domain of the volumetric strain variation is smaller than the maximum reached on the boundary. Hence it could be concluded that C/D boundary can be assumed as a domain not a single line. Within this thesis, Desai C/D boundary is considered as no dilatation criteria.

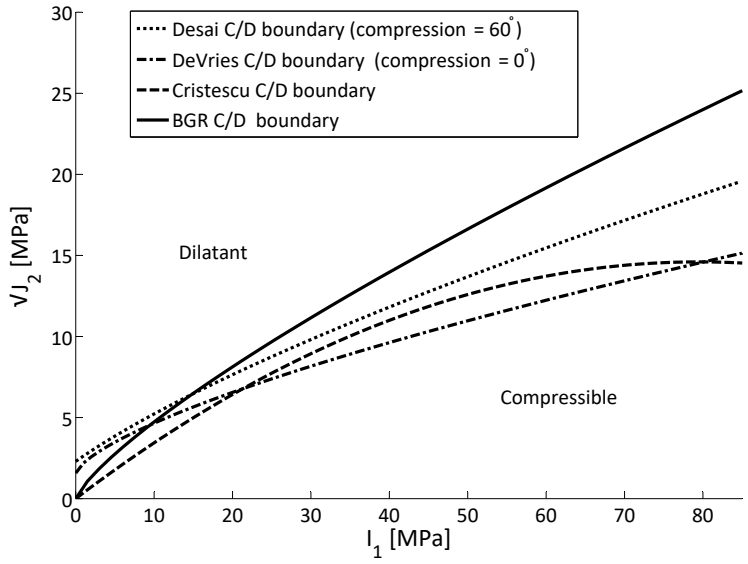

Figure 2.5: Various Compression/Dilatancy boundaries

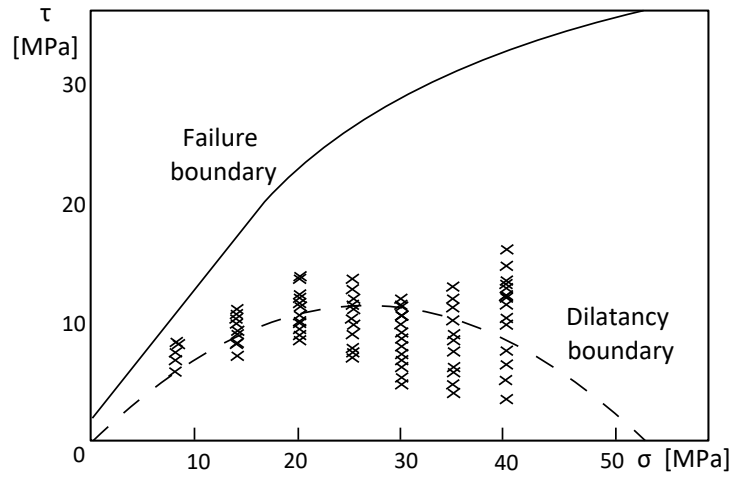

Figure 2.6: Width of the domain of the irreversible volumetric strain (after Cristescu & Hunsche (1998))

3 Numerical Simulation

3.1 Introduction

In this chapter, the finite element simulation of a typical rock salt cavern is developed, involving different aspects of excavation and operational phases of a typical rock salt cavity. The real shape of a cavity cannot be precisely defined before the completion of the excavation phase. Although, the designer may define the key features of the geometry as the height, diameter and the required volume, the final shape of the mined cavity can only be determined using sonar measurements. Also, cavern's depth is usually dictated by the elevation and thickness of the bedded salt deposits or the depth of salt dome below the surface. Within this chapter, an independent investigation is presented to consider some different scenarios for the location of the casing shoe (see Sec. 3.3).

3.2 Geometry

A real cavern is usually irregular in shape and contains sediments in the bottom, see Fig. 3.1 and Fig. 3.2, where some real cases are shown. Fig. 3.1 represents the sonar measurements which have been conducted during different phases of the solution mining procedure in the cavern TE02 located in the natural gas cavern field of Terssane, the Valence salt basin France. Different coloured lines determine the cavern's boundary in different phases of the solution mining process. However, in the most cases of numerical simulation, a simplified geometry is assumed (Pudewills, 2007; Nazary et al., 2013; Wang et al., 2013). In this dissertation also the irregularities in the wall of the cavern are neglected, and as a synthetic case study, the shape of the cavity after excavation is idealised by a rounded roof cylinder. A cylinder models the body of the cavern with a height of 233 m, and a diameter of 75 m. A 15 m flat area in the roof and the bottom are considered and the corners are assumed to be circular with a 30 m radius. Fig. 3.3 shows the geometry and boundary conditions of this cavity in details. This cavern provides around 985,000 m^3 volume storage. In-situ and laboratory experimental tests show that

the initial stress state in rock salt formations is isotropic (Heusermann et al., 2002; Bräuer et al., 2011). The rock salt is an evaporated material and shows slow trends to dissipate shear stresses over times of several hundred years. Hence its initial stress state should be different rather than the other rock types. Some measurements on the initial stress state of rock salt formation have been carried out by BGR Institute on the Gorleben salt dome, located in the north of Germany. Their observation shows that the primary stress state increases linearly with depth with the application of density of $2\,\mathrm{t/m^3}$. Therefore, the initial stress value in all directions is assumed to be equal and in proportion to the depth. Therefore, in the numerical model at far enough distance from the cavern hydrostatic stress state should exist, as well. Also, during the excavation and operation phases, at far enough distance of the cavern, isotropic stress condition exists. This situation is considered in the simulation by applying a lateral load increasing linearly with depth ($p_h = p_v + z\gamma_{rs}$) on the outer edge of the rock salt column. The vertical displacement of the model is restrained at the bottom of the rock column. The non-saline material above the rock salt formation, i.e. cap rock with a specific weight of $\gamma_{cr} = 21\,\mathrm{kN/m^3}$ is simulated as a uniform load at the top of the rock salt column.

The temperature of surrounding host rock changes during the injection and withdrawal cycles. The fluctuation of temperature imposes thermal expansion and contraction on the rock salt around the cavern, which causes additional stresses. The rate of creep deformation is also influenced by the temperature of rock mass that may affect the rate of cavern closure, subsequently (Bérest et al., 2007). Moreover, the influence of fast cooling and induced thermal contraction on the minimum principal stresses should be examined within a thermo-mechanical analysis (Khaledi, Mahmoudi, Datcheva & Schanz, 2016*a*; Khaledi, Mahmoudi, König & Schanz, 2016). However, as the main focus of this thesis is proposing a probabilistic approach to face with such complex application dealing with a significant amount of uncertainties, and in the sake of simplicity, the thermal interactions are neglected and the numerical simulation is done at constant ambient temperature T=298 K. GID software models the salt cavern with the above mentioned simplified geometry. GID is used as the pre-processor and post-processor of the Code–Bright finite element solver (Olivella et al., 1996).

3.3 Depth of location

The typical geological profile that cavern could be excavated in is shown in Fig. 3.3a. The rock mass is idealised by dividing into two homogeneous layers, rock salt and overburden.

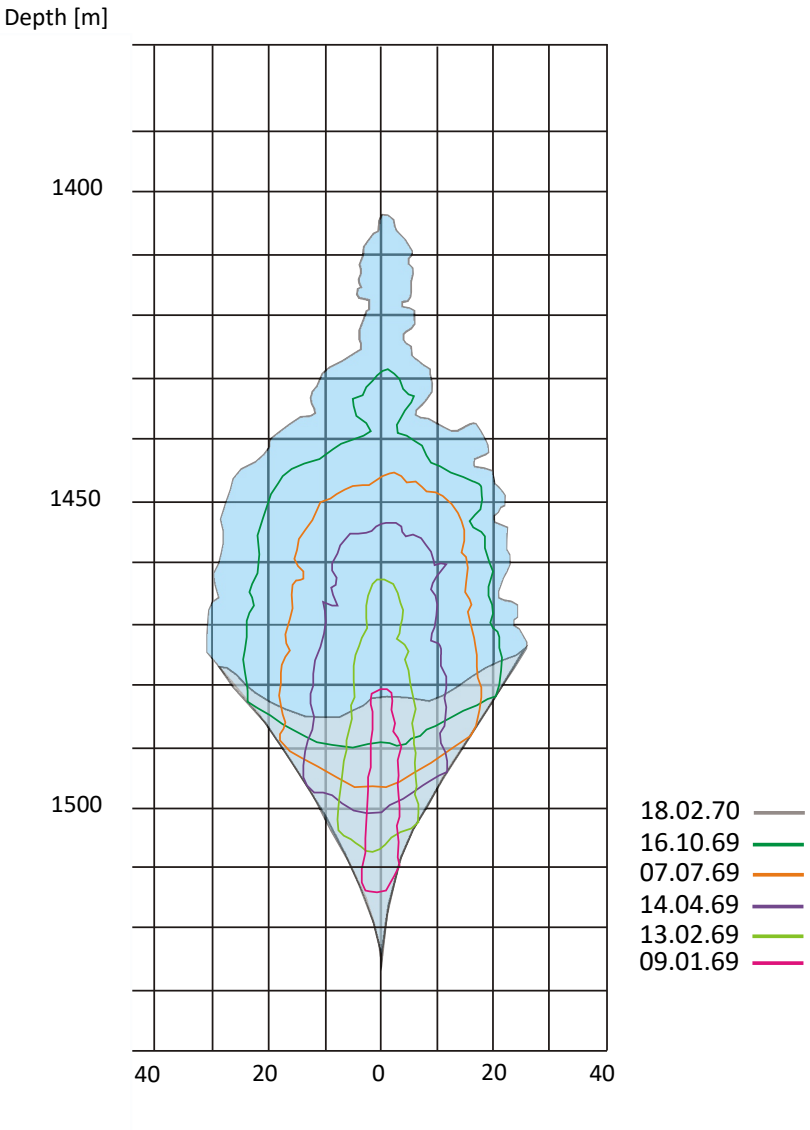

Figure 3.1: Sonar measurements from cavern Te2 at cavern field Tersanne, France (after Boucly (1982))

Cavern's depth is usually dictated by the elevation and thickness of the bedded salt deposits or the depth of salt dome below the surface that can be solution mined. Thereupon, there are different cavities around the world mined in different depth. Fig. 3.2 shows various excavated rock salt cavities around the world, whose their depth of locations may differ from 150 m to 1700 m.

Within this section, three different depths for the location of cavern's casing shoe (i.e. the bottom of the casing string, close to the top of cavern's roof) are assumed 560 m, 800 m and 1250 m. These three depths are referred to hereafter as shallow, mid and deep caverns, respectively. Same geometry as presented previously in Sec. 3.2 for three caverns is considered. In this work, a column of domal rock salt, which is shown in Fig. 3.3, with a length of 800 m and radius of 300 m, is considered. By taking advantage of the rotational symmetry, the model is transformed into an axisymmetrical numerical model. The finite element mesh is composed of 1137 quadrilateral elements (see Fig. 3.4). To simplify the simulation procedure, excavation process is neglected, and it is assumed that cavern is immediately excavated, but a geostatic analysis was performed in a time step before loading to establish the initial stress state in the rock salt before excavation. Other material parameters of rock salt based on LUBBY2 constitutive model are represented in Tab. 2.2 which have been calculated from an uniaxial creep tests on salt rock samples from a salt mine located in the north of Germany (Heusermann et al., 2003).

Scaled deformed shape of rock salt formation for mid deep cavern, casing shoe at depth of 800 m is shown by Fig. 3.5 in comparison with the undeformed shape. It clearly shows that deformations due to creep behaviour have more value at the bottom half of the cavern and in the floor of the cavern close to cavern axis as well. This observation corresponds with more deviatoric stress at these areas which based on Eq. 2.2 has a major effect on creep strain value. In the sake of determining the minimum operating pressure value, the state of stress around the cavity is compared with Desai C/D boundary. The stress-state of two nodes around the cavern one at the mid height of cavern and one at the floor of the cavity (i.e. Point A and B in Fig. 3.3, respectively) are monitored. These points experience different intermediate stresses.

As explained in Sec. 2.4, when the stress state locates above the C/D boundary, the material experiences dilatancy, an increase in permeability, development of micro cracks and creep failure. Thereupon, those internal pressure which leads the stress paths in all regions locating below C/D line (i.e. compressible zone) could be considered as safe scenarios. Based on Eq. 2.17 the dilatancy and failure boundaries are functions of Lode's angle, then for comparing the stress paths of different region around the cavern independent of Lode's angle, the second invariant of deviatoric stress is scaled using the Eq.2.12 formulation.

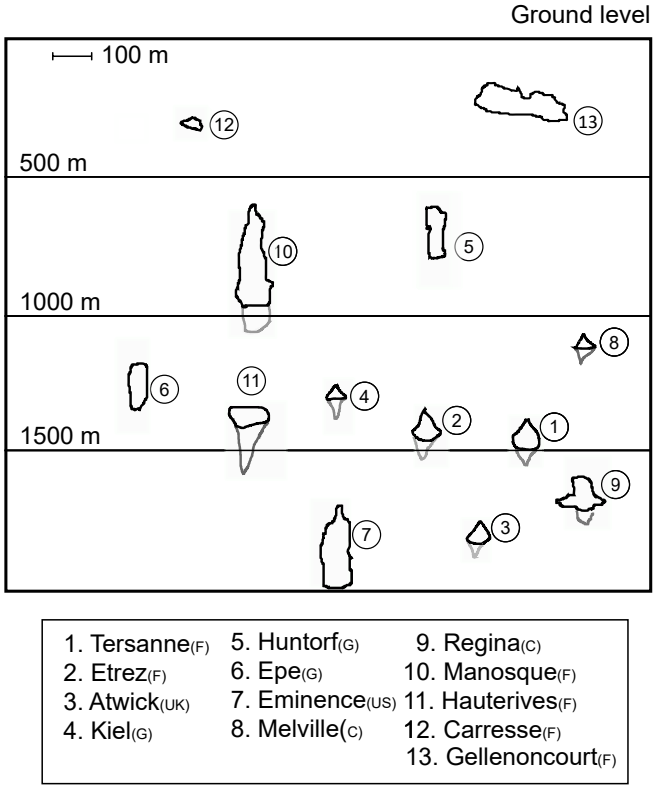

Figure 3.2: Solution-mined caverns around the world and their excavation depths (adjusted from Bérest & Brouard (2003), Berést, Brouard, Hertz, Lheur, Hévin, d. Laguérie & Hardy (2013))

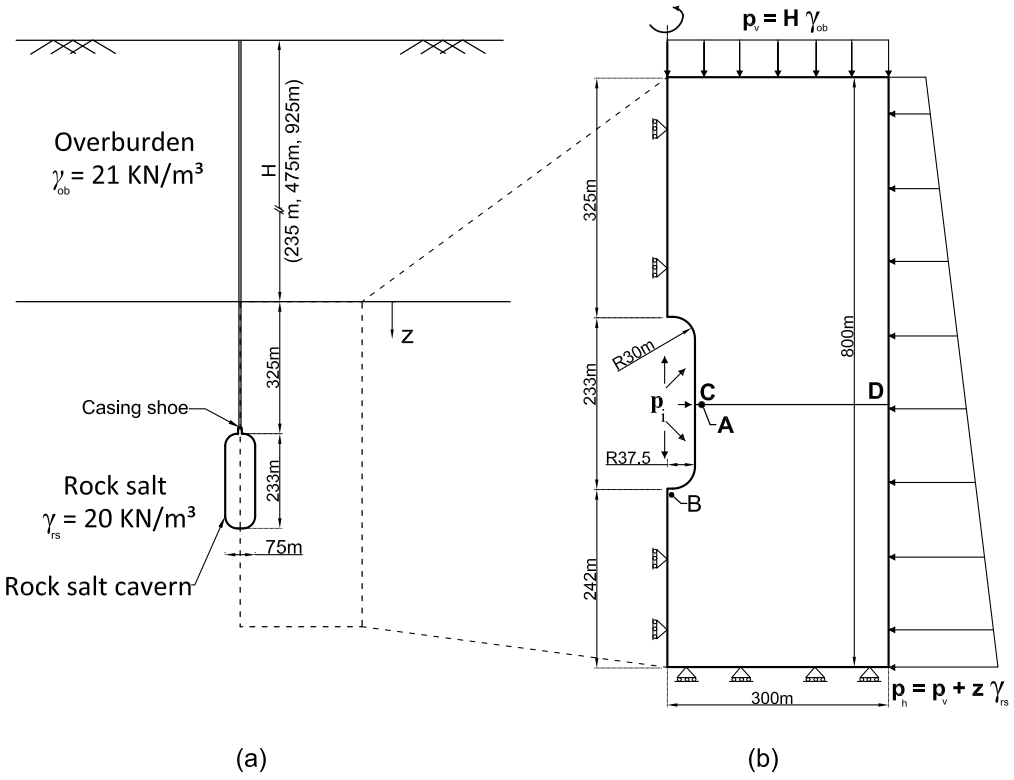

Figure 3.3: Geometry and boundary condition of the salt cavern model

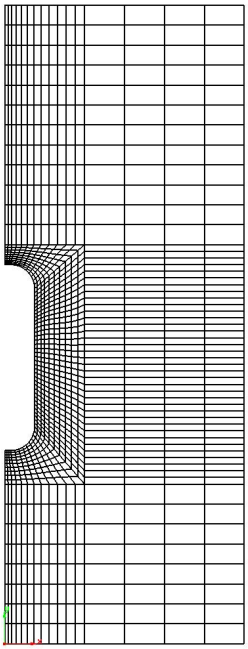

Figure 3.4: Finite element mesh discretisation

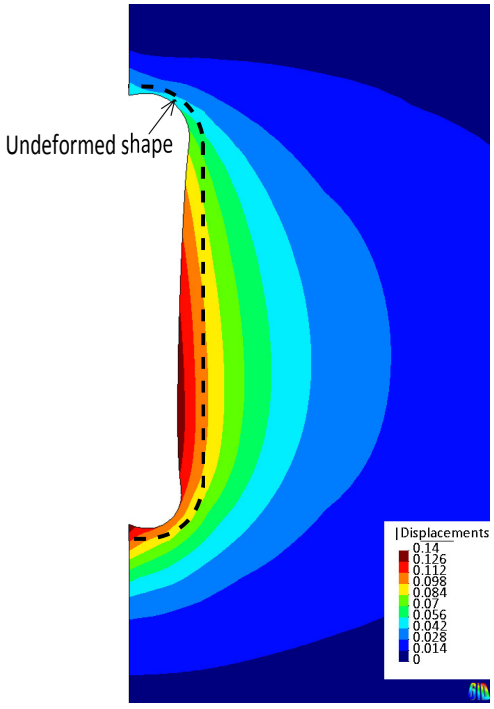

Figure 3.5: Scaled deformed shape of mid deep cavern under 4 MPa internal load

Fig. 3.6 displays the scaled stress path of the wall of cavern in the invariant stress plane, respectively. As Fig. 3.6 clearly shows the stress paths of node at the wall of shallow cavern under 4 MPa internal pressure is below the C/D line. Whereas for a deep cavity, minimum operating pressure equal to 4 MPa leads the stress state of salt formation around the cavern to dilatant region at the wall and ground of cavity as well. A comparison between the observed stress paths on the wall of the cavity and at its bottom shows, when observation point is at the bottom of cavern, minimum allowable internal pressure would be more critical. For example, consider stress paths at the mid depth under 4 MPa internal pressure at the cavern's floor and wall. The wall of cavity under this internal pressure is in the compressible zone, but the bottom of cavern experiences dilatant behaviour. Fig. 3.7 represents induced strain under different internal pressure along time for various depth of cavern. The strain of deep cavern shows higher value in each observation points compared to other cases. While at the shallow and mid depth caverns more amount of strain is induced during transient phase, at deep cavity secondary or stationary creep also has a considerable proportion in strain value. Horizontal and vertical strain at the wall and the floor of cavern respectively follow similar trend.

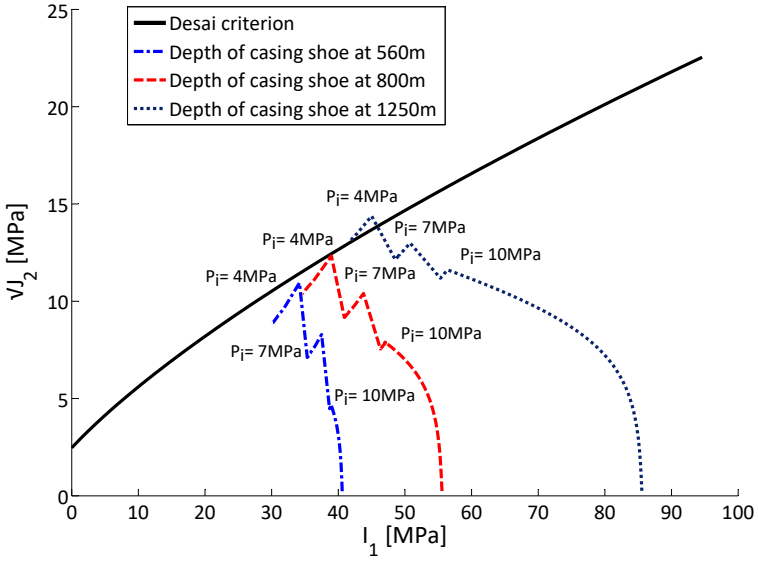

Figure 3.6: Stress path at the point A in Fig. 3.3

Fig. 3.8 shows the variation of deviatoric stress along a horizontal line at the mid height of cavity. As mentioned before in Sec. 3.2, far from the cavity's vicinity second invariant stress is negligible. For instance, the initial stress state of rock salt around the mid depth cavern does not change considerably farther than 4 times of cavern radius from the cavern's wall. The value of deviatoric stress around the cavern's wall increases for deeper caverns.

Moreover, variation of the deviatoric stress under various internal loads for the cavern in the depth of 800 m is presented.

3.4 Excavation simulation

Solution mining process is started by drilling a well into the salt structure, and then, leaching and withdrawal strings are hung into the cavern from the last cemented casing string (also called as casing shoe). The storage cavern is leached out from the salt formation by injecting fresh water at the bottom of the cavity and dissolving the salt. After the dissolution of salt, the brine is discharged through the withdrawal string to dissolve the salt in a controlled manner, progressively. The resulting saturated brine can be transported to a production plant to purify in a brine purification facility. During the leaching process, the density difference between injecting water and discharging brine forces circulation. At the end of the leaching process, the cavern is filled with brine that is

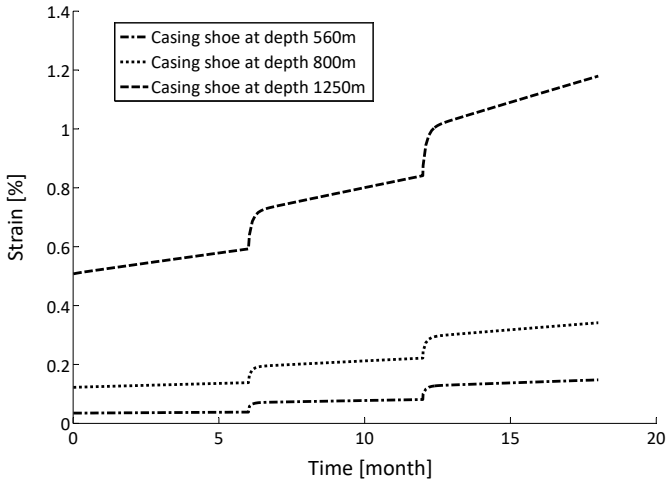

(a)

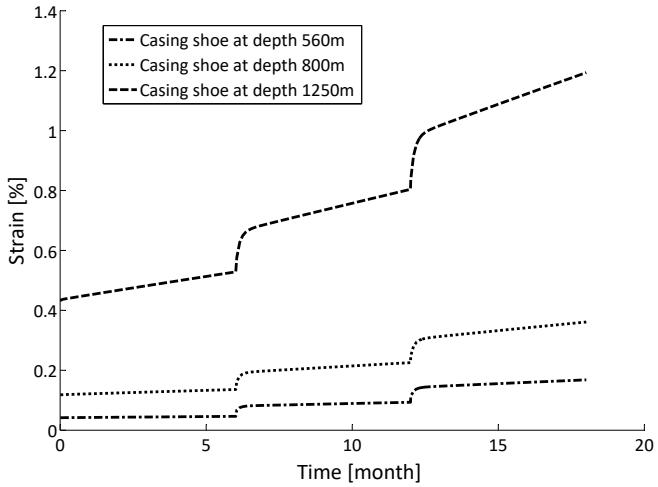

(b)

Figure 3.7: Evolution of strain along time for point (a) A and (b) B in Fig. 3.3

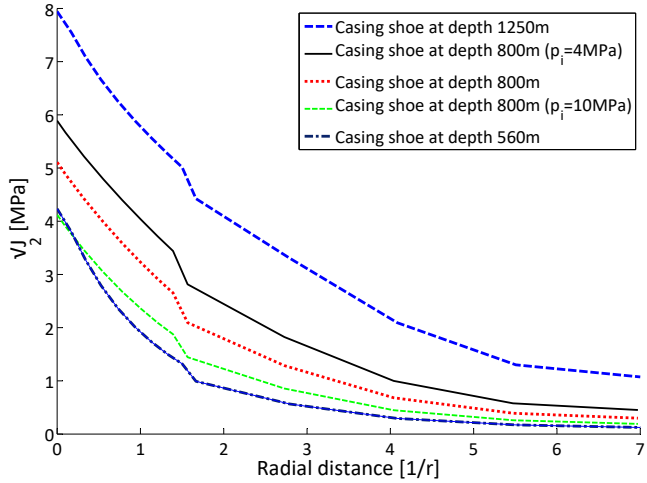

Figure 3.8: Deviatoric stress along CD section in Fig. 3.3 with $p_i = 7\,\mathrm{MPa}$ for various depths and under different internal pressure for deep cavern

usually replaced by injecting pressurised gas from the top of the cavern during the debrining phase. The direction of circulation, injection point of raw water and leaching rate are main parameters which control the shape of the cavern. Later, the injection/withdrawal cycles commence in order to balance out the consumption demands. Fig. 3.9 schematically shows the process of the solution mining. In this study, the solution-mining procedure is simulated by applying the internal pressure to the cavern's boundary in each step of excavation. In addition to using initial isotropic stress condition based on the weight of salt column, a ramp load equal to the initial isotropic pressure of rock salt medium is also applied to the cavern's wall to simulate intact rock with no deviatoric stress before the construction onset. After that, the internal pressure of cavern is gradually decreased to halmostatic pressure. This process, which starts from the deepest point of the cavern, is called leaching and is assumed to take place in 780 days. Extracting brine from the cavity is done by injecting a pressurised gas whose pressure is slightly higher than the weight of the brine column. Replacing the brine by gas, namely debrining process, is simulated in this study by increasing the internal pressure of cavern and happens within 264 days. In the last phase before the operation, the internal pressure in the cavity is adjusted to be equal to the maximum operating pressure (the first step of the operation phase). The explained process of simulating the solution mining consists of leaching, debrining and the first step of the operation, hereafter will be noted as stepwise excavation. In this study, stepwise excavation is assumed to take place in a total time duration about three and a half years.

To simplify the numerical model, the entire excavation and debrining process can be simulated by changing the internal pressure of cavern in one time step with the same total duration as the stepwise excavation. Therefore, the geostatic stress is reduced gradually to the maximum internal pressure of the cavern within the same time interval as mentioned above for the stepwise approach. Fig. 3.10 illustrates the schematic loading pattern imposed to the cavern's boundary during the excavation and the cyclic loading operation phases. The solid line shows the pressure variation within the stepwise excavation approach while dashed line shows its changes during the simplified simulation strategy. In Sec. 3.5, the results of a comparative study between these two approaches to model the excavation procedure is given.

3.5 Stress-strain status

Fig. 3.11a shows a typical geological profile of a rock salt strata where a storage cavern may be excavated. As previously mentioned, the excavation procedure of a rock salt cavern is simulated by two different simulation strategies, the first one models the whole phases stepwise, and a second approach simulates the excavation procedure in one step in a simplified way. The simplified procedure can be justified by the following statements: *i*) Figs. 3.12a and 3.12b show that the stress path related to the leaching, the debrining and the beginning part of the first step of the operation is located inside the initial yield surface, thereupon in these steps, the viscoplastic component of Eq. 2.6 equals to zero. Based on that, observed deformations are due to elastic and viscoelastic behaviour (i.e., steady state creep). *ii*) Fig. 3.13a displays the stress paths of the two different methods of modelling the excavation process. It is observed that both paths experience a different stress state during the excavation procedure, but they finally reach the same point in the $(I_1, \sqrt{J_2})$ plane. Also, the excavation-induced horizontal displacement of N_3 on the cavern's wall is drawn in Fig. 3.13b for both simulation methods. As mentioned before, the main part of the excavation-induced strain is due to elasticity and creep, which is a time-dependent behaviour. Therefore, since the same time interval is considered for both processes, the computed values of the horizontal displacement as well as the stress state at N_3 show in both modelling methods similar results. One can conclude that simplifying the numerical analysis by modelling the whole excavation phase in one time step, when its responses during operation are addressed, makes no remarkable difference in the initial system response. Thereupon, the simplified simulation strategy is applied. At the end of the excavation phase, two different operation protocols are investigated: (*i*) cyclic loading and (*ii*) long-term loading. In the first protocol, the internal pressure of the cavity is

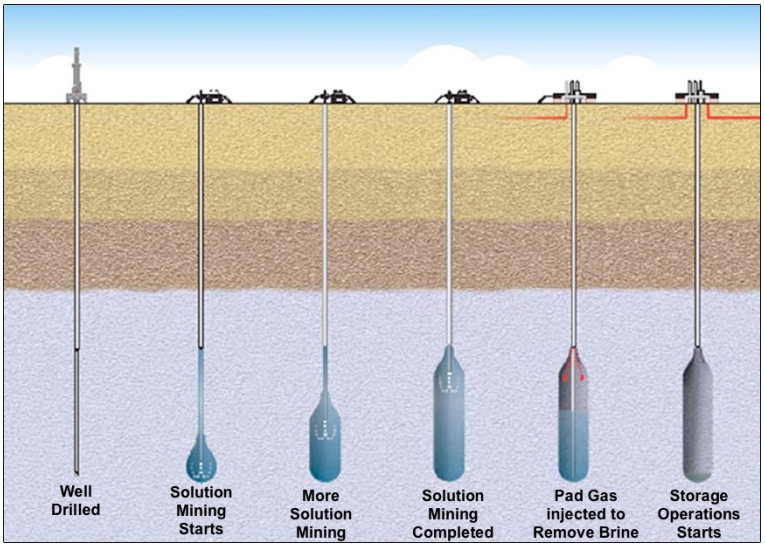

Figure 3.9: Solution-mining process (www.cadincadout.com)

set to 10 MPa, after that it is decreased to 7 MPa during 12 hours, and then it is kept constant for 12 hours. The cyclic loading simulation is followed by raising the internal pressure gradually to 10 MPa within 12 hours time interval. It is assumed that the salt cavern has no leakage or discharge during different phases.

Furthermore, for observing the volume convergence of the rock salt cavern induced by creep behaviour of rock salt, a long-term loading protocol is considered. After the completion of the excavation phase, the internal pressure is kept constant for six months in minimum level. This loading protocol is used for evaluating the reliability of the cavern against the volume loss in **Chapter. 5**.

Figs. 3.12a and 3.12b show the stress path of two nodes in the wall and the bottom region around the cavern, namely N_3 and N_5 in Fig. 3.11, respectively. Moreover, C/D line, the failure boundary and the initial yield surface are drawn in $(I_1, \sqrt{J_2})$ plane. In the following, contour plots of the horizontal strain and the deviatoric stress around the cavern under 7 MPa internal pressure at the end of the 10^{th} cycle are presented in Figs. 3.14a and 3.14b, respectively.

3.6 Stability of the cavity

The integrity and functionality of the rock salt cavern is a fundamental prerequisite in its design and are considered as the safety measures of such a repository. In general, the performance of the storage caverns is carefully monitored to prevent any environmental and financial risks, based on authorisation demands. There are follow-up procedures

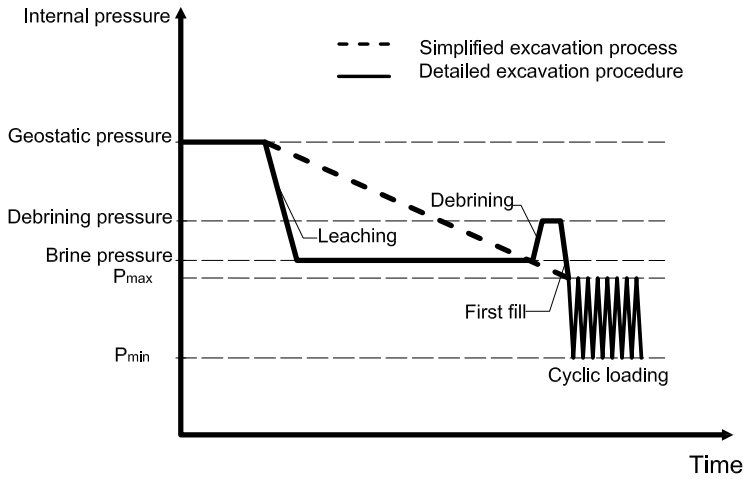

Figure 3.10: The changes of the internal pressure of the cavern during excavation and cyclic operation phases

to ascertain a sustainable storage volume of such a cavity, including bottom pressure and temperature logging, cavern thermodynamic modelling from well-head measurement. Some of the continuous or periodic monitoring procedures as seismic monitoring, subsidence survey, cavern bottom sounding and sonar survey are planned to examine the cavern stability. The integrity of the solution mined storage can be tested by corrosion monitoring and annular tubing pressure monitoring observations. Tab. 3.1 presents a standard monitoring program, determining the objectives of each observation for a geomethane storage cavity. Also, the proper frequency for periodic operations is suggested. The intact rock salt under isotropic stress conditions has no connected pore space (Bräuer et al., 2011), but within excavation procedure, as well as during operation phase, some microscopic fractures may propagate due to the dilatancy and tensile stresses. When a deep fracture develops, especially at the roof of the cavern, the integrity losses and product leakage occurs. Within a numerical design, the stability and serviceability of the rock salt cavity can be investigated by considering the following criteria,

- no-dilatancy,
- no-tensile region,
- no-damage region,
- limited volume loss,
- limited subsidence.

The mentioned criteria have been utilised in several research projects and case studies in order to ascertain the stability and serviceability of a rock salt cavern either in design or

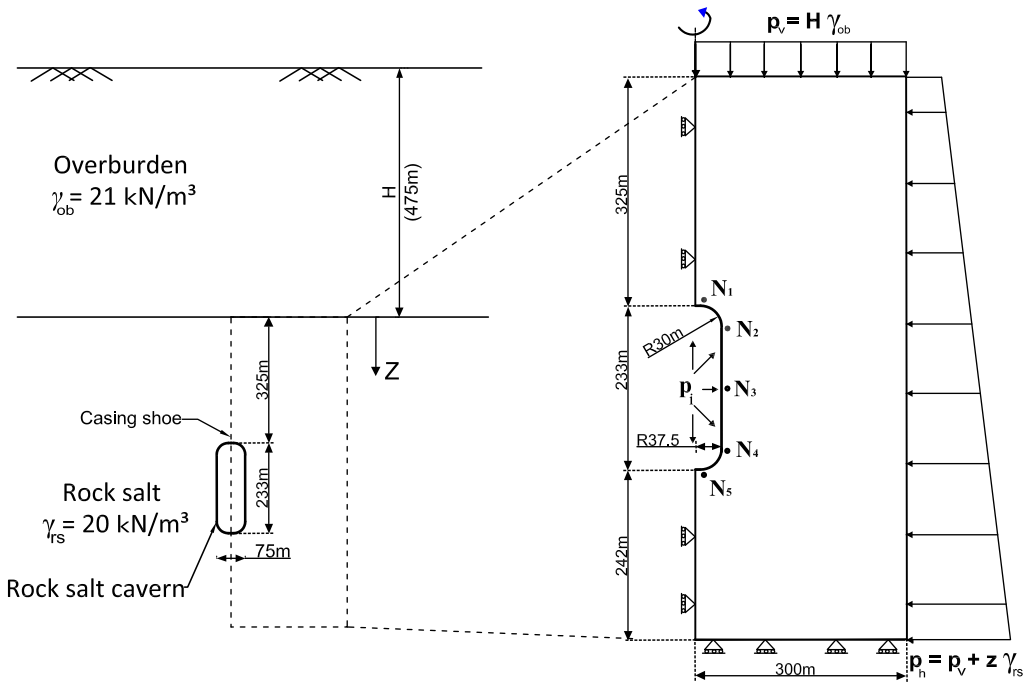

Figure 3.11: Geometry and boundary condition of the salt cavern model

operational phase. For instance, Nieland & Ratingen (2006) investigated the structural integrity of two natural gas storage caverns located in a Gulf Coast salt dome, considering limited volume loss, no tensile zone and no dilation zone and recommended a safe gas storage and withdrawal rates and minimum gas pressure. Also, a rock mechanical calculations performed by Jafari et al. (2011) to study the effects of the seasonal and micro-cycling operation modes on different failure criteria, namely, no-dilation, no-tension, no-damage and limited volume convergence. For more examples, see Bérest et al. (2008); Bérest (2011); Lux (2013), and Wang et al. (2016).

3.6.1 No- dilatancy criterion

The rock salt under high deviatoric stress undergoes dilatancy, and the permeability and acoustic emission increase due to the initiation and growth of the micro-cracks. Therefore, the dilatant zone in the rock surrounding the cavern should be avoided, to accomplish this no-dilation criterion is defined. No-dilation criteria employed the C/D boundary introduced in Sec. 2.4 as the limit state. In addition, the second variant of the stress state of the surrounding rock salt is evaluated to define a quantity as below to identify the location of the stress state to the dilatancy boundary. For this reason, a quantity DF is defined to identify the location of the stress state relatives to the dilatancy boundary as

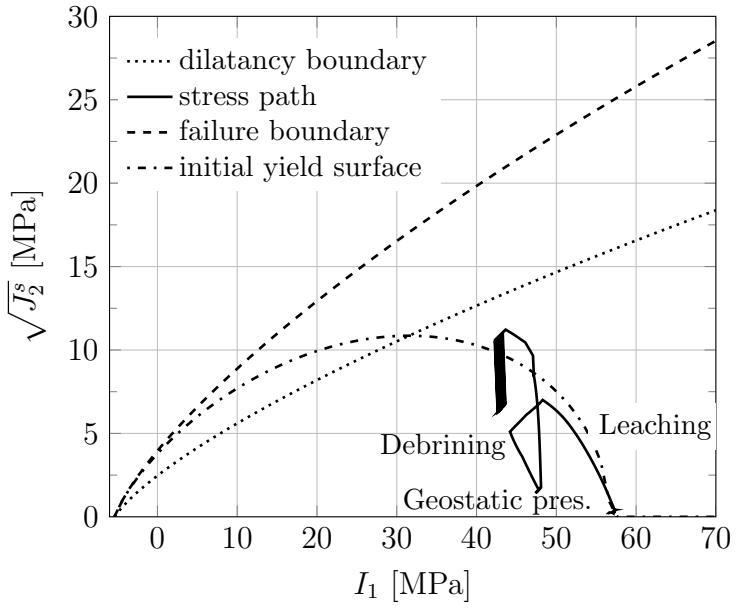

(a)

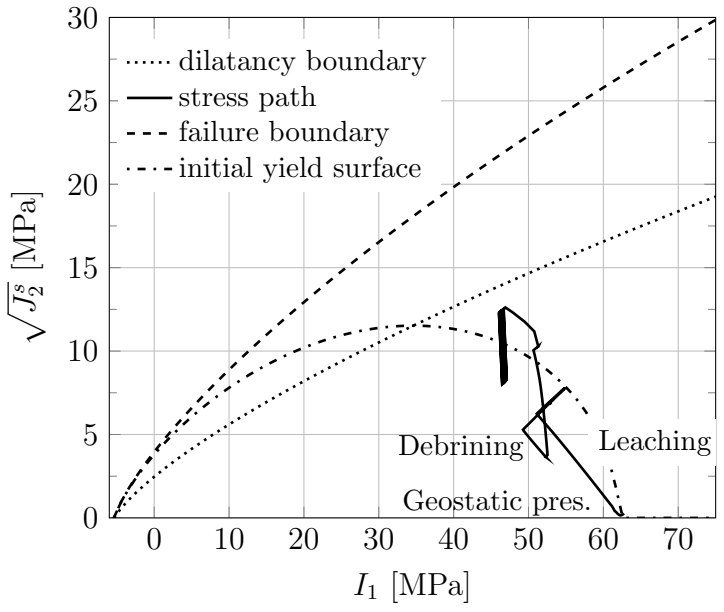

(b)

Figure 3.12: Stress path in $I_1 - \sqrt{J_2^s}$ plane at (a) the cavern wall and (b) the cavern's bottom

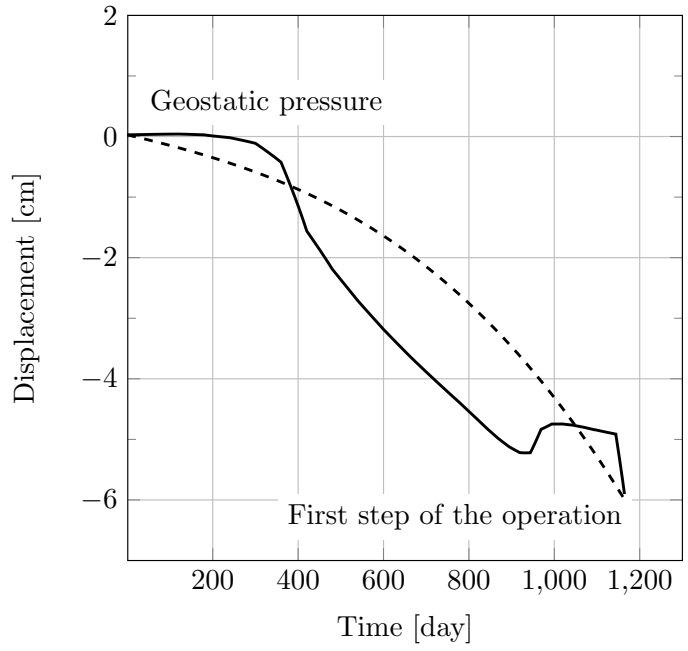

(a)

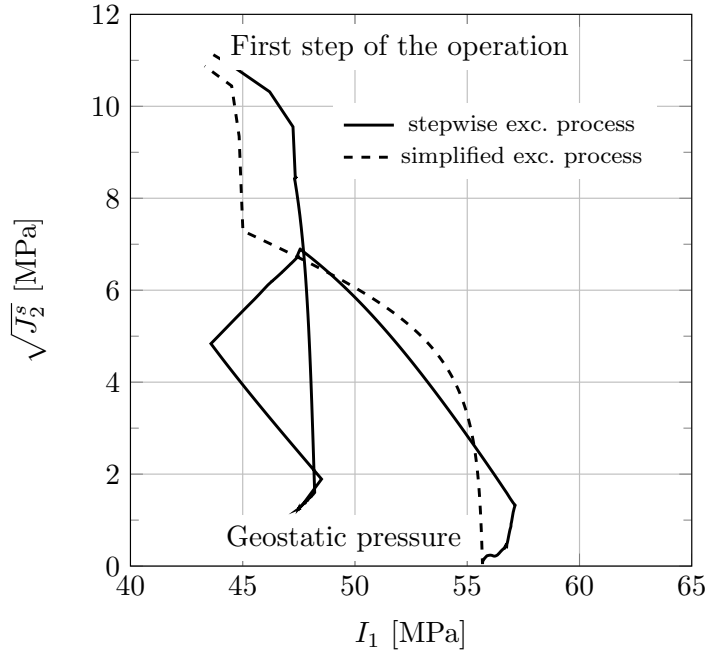

(b)

Figure 3.13: Comparison of the excavation-induced (a) horizontal displacement and (b) stress path in point N_3 w/wo implying the detailed excavation process

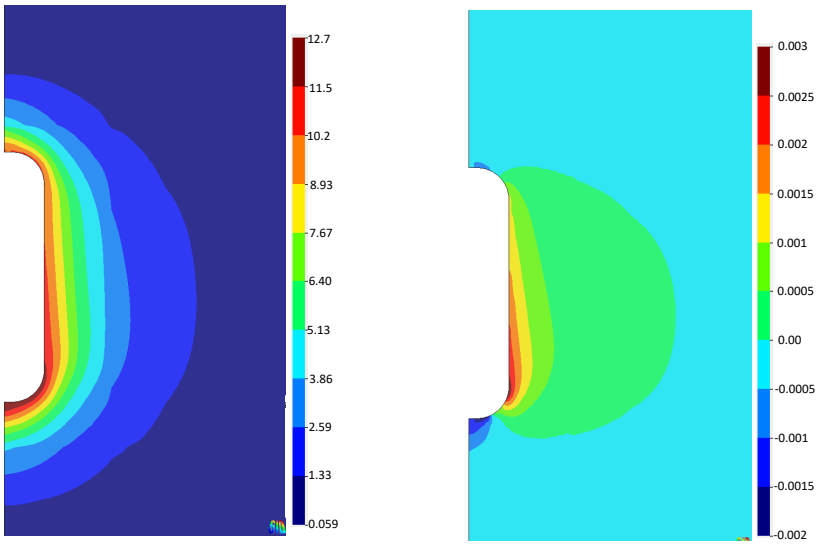

(a) (b)

Figure 3.14: Contour plots of (a) deviatoric stress ($\sqrt{J_2}$) and (b) the horizontal strain at the end of cyclic loading (simplified loading)

follows:

$$DF = \frac{\sqrt{J_2}}{\sqrt{J_2^{dil}}}, \tag{3.1}$$

here, $\sqrt{J_2^{dil}}$ indicates the distance of the dilatancy boundary from the isotropic condition in the π-plane. When $DF \geq 1$, it means that the present stress state of the cavern lies above the C/D line, and, subsequently, the corresponding areas around the cavity experience dilatancy, which increase the permeability. In this dissertation, the DF is used in the probabilistic study in **Chapter 5** as a pre-failure criterion to determine the minimum allowable pressure of the cavern. Although, violating the criterion in a node does not mean that the whole zone will be prone to collapse. For the sake of simplicity and because the walls of the cavity are considered smooth, we assumed that the defined nodes in Fig. 3.11 reflect the response of the zone, where they located. Figs. 3.15a and 3.15b show the contour plot of DF around the cavern when the internal pressure is fixed to 7 MPa and 4 MPa, respectively. Figures clearly illustrate that, decreasing internal pressure, causes dilatant regions around the cavity ($DF > 1$).

It is worth to mention that the maximum value of the deviatoric stress in the cavern's boundary is mainly affected by applying the minimum internal pressure (Mahmoudi et al., 2015*a*). Thereupon, when the internal pressure drops down drastically, the stress-state moves above the dilatancy boundary. The minimum storage pressure corresponds to high deviatoric stresses which may exceed the dilatancy boundary and leads microscopic

Table 3.1: Monitoring plan for a rock salt cavity storage (adjusted from Jafari et al. (2014))

Technique	Cavern stability	Well integrity	Gas inventory	Frequency
Seismic monitoring	X			Continuous
Subsidence survey	X			5 years
Bottom depth sounding	X			3 years
Cathodic protection		X		Continuous
Annuals pressure monitoring		X		Continuous
Sonar survey	X		X	10 years
Well-head pressure monitoring	X		X	Continuous
Downhole temperature measurement			X	<3 years
Gas metering			X	Continuous

cracks in the host rock. Hence, determining an appropriate value for the minimum storage pressure is substantial in the concept of stability of this structure.

3.6.2 No-tension criterion

In a gas storage cavity, specifically in the CAES ones, where the amplitude of charge-withdrawal cycles is high, rapid pressurisation and thermal stresses due to the cooling may cause tension stress state in some regions around the cavern. Since the tensile strength of the rock salt is very low (i.e., 1.8 MPa (Cristescu & Hunsche, 1998)), the integrity of the rock salt around the cavern may be imperilled if tensile zones form in the cavern's vicinity (Berést, Djizanne, Brouard & Hévin, 2013). Hence, the influence of fast cooling and induced thermal contraction on the minimum principal stresses should be examined within a thermo-mechanical analysis.

Moreover, the effective tensile stress may be developed when the internal cavern pressure exceeds the minimum comprehensive stress in each zone around the cavern (Brouard et al., 2007; Bérest, 2011; Djizanne et al., 2012). Thereupon, in the all international experience in cavern design, the maximum internal pressure is set between 80 and 90 % of the primary stress at the cavern roof (Lux et al., 2002; Hou et al., 2010; Xing et al., 2015).

3.6.3 No-damage criterion

The rock failure around the cavern does not propagate to the surface unless the rock salt above the cavern's roof elevation is breached (Allen et al., 1982). Such a case may happen after a network of micro-cracks which are built up due to the dilatancy, are connected.

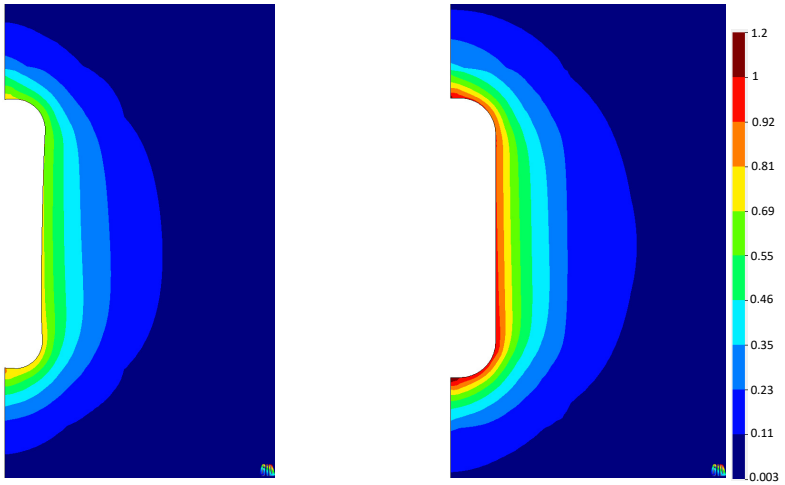

(a) (b)

Figure 3.15: Contour plot of DF under the minimum internal pressure (a) P_i =7 MPa and (b) $P_i = 4$ MPa

There are different approaches to describe and formulate the damage in geomaterials. For instance, Khaledi, Mahmoudi, Datcheva & Schanz (2016*b*) used an energy-based quantity defined to quantify the energy of micro-cracking. When the released energy due to micro-cracking reaches to a threshold value, the material failure occurs. In this regard, one may use the long-term failure ratio (LFR) introduced by Cristescu & Gioda (1994) to evaluate the micro-cracking and damage propagation around the cavern. The LFR is defined as the ratio of released volumetric inelastic work per unit volume (w_{vol}) due to the dilatancy of rock salt, to a threshold value (w_f).

$$LFR = \frac{w_{vol}}{w_f}, \tag{3.2}$$

here w_f is the maximum released energy in which the material failure takes place. In the case that LFR becomes greater than zero, the damage will initiate to progress. As previously mentioned, the surrounding rock salt under low internal pressure exhibits more tendency to dilatant, hence damage is also more likely to occur under low-pressure loading scenarios.

Based on the conducted analyses by Khaledi, Mahmoudi, Datcheva & Schanz (2016*b*), when cavern is operated under very low pressure loading scenarios, LFR raises by increasing the number of load cycles. In this thesis, the damage is not surveyed.

3.6.4 Limited volume convergence criterion

In the concept of the geomechanical design of an underground rock salt storage, in addition to the mechanical stability, its serviceability also should be assured. The serviceability of a rock salt cavern corresponds to fulfilling the requirements of the storage plant, e.g., the prescribed internal pressure, volume and temperature. In every rock salt cavern, the deviatoric stress due to the difference between the geostatic pressure and the cavity internal pressure, forces creep into the cavern as soon as the leaching process begins. The extent of creep in the rock salt is relatively high, compared to other common host rocks (Cristescu & Hunsche, 1998), therefore, creep induced deformations may cause large amounts of volume convergence. Consequently, the required storage space for running the turbine generators can not be provided. Evidences of large losses of storage space were represented by Thomas & Gehle (2000) and Bérest & Brouard (2003). Hereupon, the deformation of the cavity in the long term should be evaluated and restricted in a manner that may not endanger the serviceability of the storage plant. The amount of volume convergence increases drastically when the internal pressure of the cavity keeps low for a long period. Displacement contours of surrounding rock salt under long-term loading protocol under different internal load pressures are shown in Fig. 3.16a and 3.16b, respectively. As stated previously, decreasing internal pressure induces more deviatoric stress, which the creep strain is affected by, therefore, reducing internal pressure may encounter the cavity with extreme volume convergence values.

3.6.5 Limited subsidence criterion

Compared to the conventional underground structures, the ground settlement is markedly less in rock salt cavities. In other words, no significant damage at the ground level resulting from the convergence of deep caverns has been experienced. For instance, Ratigan & Yogt (1993) reported results of a survey on the ground level settlement rates on an LPG storage plant in Mont Belvieu, Texas, in which the average subsidence at 124 storage cavities in the site was 2.64 ± 1.02 cm. Also, at the Tersanne site, in contrary to the relatively large cavern convergence, the amount of subsidence was negligible. The settlement rate was reported approximately 1 cm per year in this salt formation (Nguyen et al., 1993). However, the ground subsidence in shallow rock salt cavities is relatively higher. Besides the depth of cavern, other factors as internal pressure, running time, excavation rate, etc. can effect on the settlement extent. Bérest et al. (2008) studied 1873 collapse of the Varangeville salt mine, France which caused 3.3 m subside in the ground level and proposed the occurrence of massive subsidence as an indicator for collapses. Since the

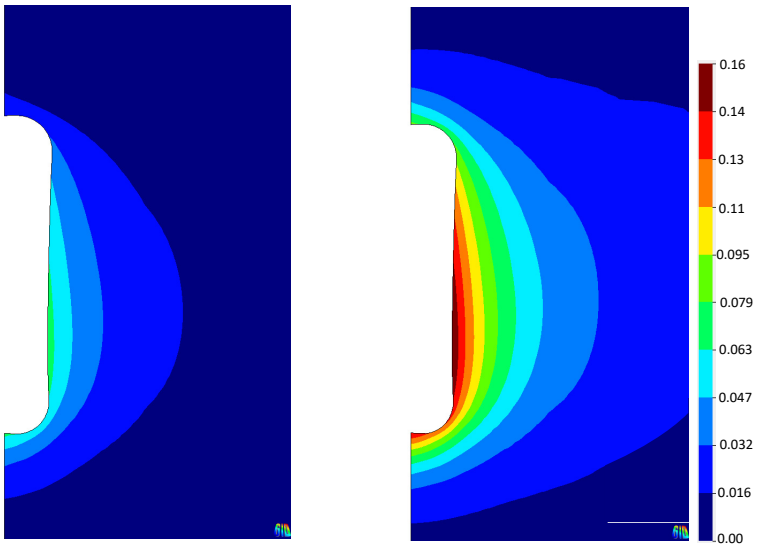

(a) (b)

Figure 3.16: Contour plot of displacement around the cavern under the minimum internal pressure (a) $P_i = 7\,\text{MPa}$ and (b) $P_i = 4\,\text{MPa}$ in long-term loading protocol

massive ground subsidence may cause sinkholes and surface failure, the value of subsidence above the opening should be evaluated, attentively (Jafari et al., 2008).

All above-mentioned failure criteria can be investigated along a reliability analysis. In this thesis, the no dilation and limited volume convergence are surveyed in **Chapter 5**.

3.7 Summary and conclusion

Analogous to most geotechnical engineering concepts, where the numerical methods are widely used, here the behaviour of rock salt under particular geomechanical conditions is numerically analysed. To do this, the finite element method, simulating excavation and different operation scenarios, is employed to evaluate the behaviour of a typical rock salt cavern under different loading protocols. Moreover, this chapter presented a numerical investigation on the mechanical behaviour of rock salt in distinct excavation depths. A typical geometry for caverns with three various locating depth has been analysed by a finite element code. To identify the minimum allowable internal pressure, considering no dilatation criteria, stress state of the various region of cavern vicinity are compared with the Desai dilatancy boundary. To conclude, the minimum permissible internal pressure is governed by the depth of locating the cavity. In deeper caverns, more internal pressure should apply to prevent irreversible volumetric change due to dilatancy.

Moreover, a comparative study on different simulation strategies of solution mining was conducted. The results approved that the differences produced by simplifying the numerical analysis by modelling the whole excavation phase in a single time interval are negligible.

4 Sensitivity Analysis

4.1 Global sensitivity analysis

The response of a system is not affected equally by all the involved factors. On the other hand, reducing the associated uncertainty in some input parameters may decrease noticeably the uncertainty measures in the model response, compared to the others. Hence, identifying those dominating input variables enables an effective selection of the measurement design. In this regard, the Sensitivity Analysis (SA) can be employed to detect the key input factors which have the greatest impact on the model output variation. In practice, two main categories of SA methods can be distinguished, the local SA category and the global one. In the local approach, the effect of a small variation of a single input parameter on the model output is investigated, while all the other factors are fixed. This approach also is known as one at a time and involves partial derivatives. The local methods can be considered as the historically first attempts to conduct SA and they provided valuable results. In general, numerical implementation of differential analysis and the demanding computational effort for local methods is affordable, hence they will be effective, specifically in the analysis of large systems. For a review of different local SA methods, see Cacuci (2003). Evaluation of partial derivatives of the model at the base point can provide a sensitivity measure. Hence, the calculation cost of this approach is low, and the demanding number of model evaluations is limited. Nevertheless, calculating derivatives around the base point cause some limitations in local methods as the necessity of linearity, monotonicity or additivity assumptions. However, calculating derivations around a base point in the space of an individual input factor makes this methodology model-dependent. Therefore, when the system deals with non-linear/ non-monotonic models, the local approach of SA may not provide a reliable importance ranking of the input factors. In this regard, the derivatives should be substituted with an exploration of the entire input parameter space. To accomplish this, the second category of sensitivity analysis methods, i.e., Global one is developed. The global methods consider the entire variable space of inputs to estimate their impacts on the model responses. Besides eliminating the local

methodology limitations, using the global sensitivity makes the identification of interactions between the input parameters also feasible (Cacuci, 2003). With the advancement of computational capabilities, comprehensive numerical approaches are increasingly used for simulating different geotechnical problems. These sophisticated simulation models of underground structures are supposed to model coupled and highly non-linear phenomena involved in the geomaterials behaviour. On this subject, the global sensitivity analyses techniques can be considered as a proper alternative to such models. In general, a global SA enforced a larger number of model evaluations rather than the local methods. To overcome this drawback of the global sensitivity analysis, metamodelling concept (see Sec. 4.8) can be employed.

However, in the last five decades, a diverse range of SA techniques have been developed in different scientific disciplines. Thereupon, for the choice of an appropriate SA method, among all the available methods, a non-expert SA operator (designer, who has a prior knowledge about the variety of methods), may be confused or even misled. In this regard, some attributes of the model of interest can be considered as key features to facilitate the choice of proper method. In the following, in addition to introducing some common global SA methods, a number of general fundamental aspects of employing an appropriate method, considering system features are discussed.

In this chapter, four alternative global SA methods, namely, Regression methods, Random Balance Design (RBD), Sobol'/Saltelli, and Elementary Effect (Morris) are introduced and applied to a geotechnical task solved by a finite element model. Here, the response of a rock salt cavity employed as a compressed air energy storage is investigated. The rock salt formation, as a porous media with low permeability and creep features, has been used as host rock of the hydrocarbon storage for decades. Nowadays there is a new trend to use them as the storage for the excess electrical energy produced by renewable resources in the form of compressed air or Hydrogen. Consideration of the uncertainty in the mechanical properties of such a huge structure (the storage volume may reach to 1 million m^3), which is extended vertically downward more than hundred meters from the ground level is substantial. Here, the stress state around the cavity is regarded as the interested model output. Firstly, a deterministic model of a typical compressed air storage in rock salt is generated. In the following, the performance of different SA techniques is compared in the aspect of required computational effort and result conformity. Furthermore, provided sensitivity indices by various methods are used to achieve a better understanding of the system behaviour, in the aspect of the probable interaction and non-linearity.

In general, global SA techniques are developed to detect the most important set of parameters which dominate the system output and require additional measurement or ob-

servation efforts for strengthening the knowledge base. Moreover, global SA may object to detect ineffective input variables. Hence, it enables the designer to fix their values based on a simplified experience in statistical analyses and reduces the model complexity for any further deterministic or probabilistic investigation.

To decrease the extent of existing uncertainties in the numerical approximation, the computational model is usually calibrated by back analysis methodologies, e.g., global optimisation algorithms and Bayesian inverse techniques (Meier et al., 2009; Miro et al., 2015). Nevertheless, the available measurements of geotechnical projects as a rock salt cavern are limited which may restrict the possibility of taking advantage of back analysis techniques. Besides, the location where a certain sensor is placed to monitor the system output will influence the outcomes of the parameter identification considerably. Thereupon, the concept of optimal experimental design can be utilised to decrease the uncertainty measures of the input factors. Numerous publication explored the methodologies to obtain an optimum experimental design in various fields of science, e.g. Bardow (2008) in chemical engineering, Ucinski (2005) in environmental processes and Joshi et al. (2006) and Schenkendorf et al. (2009) employed the optimal experimental design in system biology. Also, Lahmer (2011) used this strategy to find out the best positioning plan of sensors in gravity dams. In this regard, global SA can be applied in the subject of optimum experimental design. For instance, to find the optimal sensor positions for parameter identification, the variance-based sensitivity analysis can be used to identify areas in which the model outputs are most sensitive to the unknown parameters of interest. Doing so, the arrangement of sensors can be evaluated and optimised. The author has employed this feature of the global SA in Hölter et al. (2015) and Hölter et al. (2017) to investigate the optimal experimental design for a loading experimental setup and a mechanised tunnelling project, respectively.

As mentioned previously, there are several well-developed global SA techniques, which can evaluate the uncertain input factors and rank them using different statistical measures. Since these methods have their own definition of importance or significance, their obtained importance ranking may disapprove each other and lead to confused or inconclusive results, subsequently (Rocquigny et al., 2008). Thereupon, the term of "important factor" in the model of interest should be predefined. A so-called setting can provide such a definition (for a general review of the different settings, the reader is referred to Saltelli et al. (2008)). Among the others, two standard settings are:

- The Factor Prioritisation setting: it is defined to detect a factor which enforced the greatest reduction in the output variance when its real value is identified. On the basis of this setting, when an "important" uncertain variable can be determined

precisely, the variance of output would lessen significantly. Therefore, when the designer is interested in reducing the output variance, this setting can detect and rank those factors which are the most deserving of a proper investigation through more measurements and observations.

- The Factor Fixing setting: it can detect parameters, which fixing them at any given value over their range of uncertainty makes no meaningful reduction in the output variance. It can detect non-influential factors. This setting is a proper choice to simplify the model of interest when it is dealing with many input variables, while it can identify non-influential factors, which represent some specific features in the system behaviour.

Among the available global sensitivity analysis methodologies, in this thesis three different class of methods are investigated in detail: *i*)Regression-based methods, *ii*) the quantitative sensitivity indices (a.k.a. the importance measures techniques), and *iii*) the screening methodology. In the following, an overview of different methods of global sensitivity analysis, namely Regression-based technique, Sobol'/Saltelli and Random Balance Design (classified as the importance measures techniques), and Elementary Effect (as a screening method), is presented. Also, a comparative assessment is conducted to evaluate the performance of the given techniques in various aspects as, the cost in the number of system evaluations, the model complexity and the type of provided information.

4.2 Regression-based methods

In order to address non-linear models, we have to move from derivatives into the exploration of the input factors space, e.g. using Monte Carlo. Global sensitivity analyses are conducted by generating a matrix samples of input factors, evaluating the corresponding output vector, and assessing the relative importance of each input factors on the output. The most popular method to do this is to try a linear regression on the sampled input matrix through an appropriate sampling method, and the evaluated vector of outputs. In general, regression analysis is employed to build response surfaces that approximate computational models (Hamby, 1994). On the other hand, regression analysis can provide sensitivity measures, as their application in SA is reviewed in Helton et al. (1991) and Helton (1993). To provide general form for a regression equation of the generic model of $y = f(X_i)$, we generated via Monte Carlo a set of model evaluations $y_i, i = 1, ..., N$, corresponding to N different sampled values X_i ($X_i = x_1, x_2, ..., x_k$) of input factors are

considered.

$$\hat{y} = b_0 + \sum_{i=1}^{k} b_i \cdot X_i, \tag{4.1}$$

where the hat notation flags the model estimates, and b_i are regression coefficients. The estimated model is known as a fitted response surface, and SA measures can be derived from this fitted model. As the simplest approach, the coefficient b_i can be treated as importance measures for different input factors. Nevertheless, their values depend on the considered units for the input variables X_i. Therefore it is necessary to normalise these coefficients to generalise them as assessment indices. A standardisation process can address the issue of units and the relative magnitudes of parameter values. Standardisation can be done in the form of the ratio of the parameter's standard deviation to the output's standard deviation. To compute the standardised regression coefficients (a.k.a. SRC), defined as

$$\beta_i = \frac{b_i \sigma_i}{\sigma_y}. \tag{4.2}$$

The β_i can give an insight to the relative importance of the input factor X_i (Saltelli et al., 2000). The use of the regression technique can be classified as Factor prioritisation which allows the sensitivity ranking to be determined based on the relative magnitude of the regression coefficients (Hamby & Tarantola, 1999). Therefore, one may conclude, when $\sum \beta_i^2$ is close to one, then the regression model is considered the most of the variability in the y, and flags a linear model (Saltelli et al., 2004). Although this method is working efficiently for the linear models, it is still model-dependent, i.e., the degree of linearity of the model of interest is a significant factor.

As an example to illustrate the SA regression estimation, a linear test function is considered with three independent uniformly distributed variables X_i, where $i = 1, 2, 3$

$$y = x_1 + x_2 + x_3 + x_4; \quad \text{where,} \begin{cases} x_1 \sim U(0.5, 1) \\ x_2 \sim U(1, 3) \\ x_3 \sim U(3, 12) \\ x_4 \sim U(12, 36) \end{cases} \tag{4.3}$$

Generating a randomly sampled $(500, 3)$ matrix, the first-order sensitivity index, are estimated as $\beta_1 = 0.0188, \beta_2 = 0.077, \beta_3 = 0.34, \beta_4 = 0.93$; and the $\sum_{i=1}^{3} \beta_i^2 = 0.986$ estimates the fraction of linearity of the model. It should be pointed here that, using a local SA method, i.e., derivatives in such a test model evaluates the same relative importance of all

the variables, although considering their different distribution, they have various impacts on the model output.

However, the effectiveness of the β_i's as sensitivity measures is judged by the model coefficient of determination

$$R_y^2 = \frac{\sum_{i=1}^{N}(\hat{y}_i - \bar{y})^2}{\sum_{i=1}^{N}(y_i - \bar{y})^2}, \tag{4.4}$$

where $\hat{y_i}$ is the regression model prediction and $R^2 \in [0, 1]$. If R_y^2 is close to 1, then the regression model is accounting for most of the variability in the y_i, and the β_j can be used to gain insight into the relative importance of the input factors. Conversely, low values for R_y^2 suggest that the model has non-linear behaviour.

Helton et al. (1986) presented the standardised rank regression coefficients method, which is able to assess the system sensitivity analysis for non-linear, but monotonic, models (Saltelli & Sobol', 1995). In the rank-based version of the Standardised Regression Coefficients, both the input and the output values are replaced by their ranks, when no extra computational cost is required (Saltelli et al., 2000). In many of other applications, different regression based techniques as the Standardised Rank Regression Coefficients and the Partial Rank Correlation Coefficients are performed (for instance see Saltelli & Sobol' (1995); Helton et al. (1991)). Saltelli & Homma (1992) pointed out the inadequacy of this schemes to deal with non-monotonic relationships.

However, regression methods were extended with the main idea of express fractional contributions to the total variance of Y. Albeit these techniques were applied successfully, their performance depends on the degree of linearity or monotonicity of the model of interest. This idea can be considered as the basis of developing another group of SA methods classified as variance based methods, which are model-independent.

4.3 Variance-based methods

In general, variance-based estimates the output variance and the contribution of the uncertainty of each input factor and their probable interaction in this variance. Variance-based methods are independent of linearity, monotonicity, additivity, etc. (i.e., model independent), and they can evaluate the interaction effects among the input factors. Variance-based methods for SA were first employed by chemists in the 1970s (Cukier et al., 1973, 1975, 1978). Later, Sobol' (1993) developed the work of Cukier et al., to calculate the sensitivity measures, using a Monte Carlo-based implementation. A review

of different variance-based methods with their recent developments can be found in Chan et al. (1997) and Saltelli et al. (2004).

The method of Cukier and colleagues, known as FAST (Fourier Amplitude Sensitivity Test) was quite effective in calculating the first-order (main effect) measures of variance-based methods but has its limitations as difficulties in implementation and no consideration of higher order indices. Tarantola et al. (2006) addressed the first drawback by employing RBD methodology to simplify FAST calculation, which is adopted in the present thesis. Moreover, the computation of higher-order indices was later made possible by extensions proposed by Saltelli et al. (1999). The method of FAST was generalised later by Sobol' (1993) to compute the sensitivity measures, employing a Monte Carlo implementation. The work of Sobol' constitutes a milestone in the development of variance-based methods.

In general, one may conclude the features of variance-based methods as:

- capable of capturing the influence of the full range of variation of each input factor,
- consider the interaction effects of input factors,
- they are model independence and compute the model-free sensitivity measures.

In the following, the methodology of analysis of variance based on variance decomposition is briefly presented. Let us consider a generic model of $Y = f(X_i), \forall i = 1, ..., k$, where k is the number of input parameters, and adopt factor prioritisation setting. In this regard, parameter X_i is fixed at x_i^* and the conditional variance of model $V_{X_{\sim i}}(Y|X_i = x_i^*)$ is evaluated. The notation V is the variance value, and $X_{\sim i}$ is the vector of all input variables but X_i. This conditional variance is generally less than the corresponding total variance $V(Y)$ (i.e. in non-linear models one may reach $V_{X_{\sim i}}(Y|X_i = x_i^*) \geq V(Y)$), but still influenced by the chosen value for x_i^*. This drawback can be overcome by taking the average and variance of this measure over all possible values x_i^*, and calculate $E_{X_i}(V_{X_i}(Y|X_i))$ and $V_{X_i}(E_{X_{\sim i}}(Y|X_i))$. Based on the following algebraic rule,

$$E_{X_i}(V_{X\sim i}(Y|X_i)) + V_{X_i}(E_{X_{\sim i}}(Y|X_i)) = V(Y) \tag{4.5}$$

averaging the conditional variance will assure $E_{X_i}(V_{X\sim i}(Y|X_i)) \leq V(Y)$ for all models. In this equation, the term $V_{X_i}(E_{X_{\sim i}}(Y|X_i))$ is known as the first-order effect of X_i on Y, or as McKay (1997) called, correlation ratio. The term $E_{X_i}(V_{X\sim i}(Y|X_i))$ is known as a residual and indicates the variance of the expected value of Y over all but X_i, which has been fixed.

Normalizing the term of $V_{X_i}(E_{X_{\sim i}}(Y|X_i))$ on model variance, provides the first-order sensitivity index as follows,

$$S_i = \frac{V_{X_i}(E_{X_{\sim i}}(Y|X_i))}{V(Y)}, \tag{4.6}$$

S_i is known as first-order effect of X_i on $V(Y)$. A high value of S_i, and hence higher $V_{X_i}(E_{X_{\sim i}}(Y|X_i))$ indicates an important input variable. An important factor here denotes a variable which decreasing its variance will reduce the uncertainty of model output most. It should be pointed out here that $\sum_{i=1}^{k} S_i \leq 1$, and $\sum_{i=1}^{k} S_i = 1$ will be held for additive models, then this measure also can be employed to determine non-additive models.

For non-additive models or models with interaction effect between input parameters where $\sum_{i=1}^{k} S_i < 1$, the higher order of sensitivity indices due to the interaction between X_i and the other parameters, is also involved in the variance of output. For a non-additive model evaluating S_i will not recover 100% of the variance, hence one should add the higher order sensitivity indices to get

$$\sum_i S_i + \sum_i \sum_{j>i} S_{ij} + ... + \sum_i \sum_{j>i} \sum_{l>j} ... \sum_k S_{ijl..k} = 1. \tag{4.7}$$

Computing the higher order indices, when there are many interactions between parameters is not feasible, specificity when the number of associated parameters is high the Eq. 4.7 has $2^k - 1$ terms. Thereupon, another sensitivity measure denoted as S_{Ti} was introduced which considers a full set of all terms including X_i. This index entitled as total-effect sensitivity index, can be evaluated as

$$S_{Ti} = 1 - \frac{V(E(Y|X_{\sim i}))}{V(Y)} = \frac{E(V(Y|X_{\sim i}))}{V(Y)}. \tag{4.8}$$

By definition, the term of $V(E(Y|X_{\sim i}))$ includes effect of all inputs but i^{th} factor. Also, the term of $E(V_X(Y|X_i))$ indicates the average of the remaining variance of Y, when the X_i is fixed, which is known as the residual term as well. S_{Ti} covers a full set of terms that consist parameter X_i. Hence, S_{Ti} denotes the total effect of all terms with any orders that includes X_i. Recalling the definition of the factor fixing setting, S_{Ti} can be contemplated as an index for this setting.

To estimate the above-mentioned sensitivity indices (a.k.a Sobol' indices), Monte Carlo sampling based methods have been proposed firstly by Sobol' (1993). However, the proposed method was computationally expensive in term of the number of model calls to reach precise estimates of sensitivity indices (i.e. kN^2 model runs are needed). An extension of Sobol' method was developed which using quasi-Monte Carlo sequences instead of

crude Monte Carlo samples to calculate both first and total-effect indices along reduced number of model evaluations (Saltelli, 2002; Saltelli et al., 2008). Moreover, Marzban & Lahmer (2016) proposed a conceptual implementation for calculating the Sobol's first order effects using limited model evaluations. The performance of this implementation is stable and accurate in the case of large models with limited available data.

4.3.1 Random Balance Design

One of the well-designed methods for conducting sensitivity analysis, which could explore the entire input space for monotonic and non-monotonic models is FAST (Saltelli et al., 1999). The core feature of FAST is that the multidimensional space of the input factors is explored by a suitably defined search-curve introduced in the 70's Cukier et al. (1973) and computationally upgraded by Koda et al. (1979). FAST method computes the major effect of each input factor to the variance of the output; it can be considered same as the first-order measure S_i in Sobol' method (Iman & Hora, 1990; Homma & Saltelli, 1996; McKay, 1997). Nevertheless, Mara (2009) mentioned that estimating sensitivity indices of any order is also possible and Saltelli et al. (1999) extended FAST to calculate the higher order sensitivity measures. The RBD and Hybrid FAST-RBD methods, proposed by Tarantola et al. (2006), modified FAST method using a new sampling technique based on Satterthwaite's random balance designs (Satterthwaite, 1959). Recently, Plischke (2010) derived a new method known as Effective Algorithm for computing global Sensitivity Indices, which estimates first-order sensitivity index based on FAST technique, as a post-processing module for model evaluations.

FAST employs Parseval's relationship to decompose the variance of a model response in the frequency space (Mara, 2009). Recalling the generic model of $Y = f(X_i), \forall i = 1, ..., k$, Y can be obtained by an analytical representation of a system or the output of a computational model. The factor values are sampled in N sample points from a periodic curve exploring the space of a k-dimensional cube, with a different frequency ω_i assigned to each factor. The frequencies should be selected such that they are free of interferences up to a given order of higher harmonies, M (commonly is assumed to be equal to 6). Afterwards, the Fourier spectrum is calculated on the model output at each sample point for the frequency of ω_i. The parametric curve is defined as,

$$X_i = T_i sin(\omega_i d_j) \quad \forall i = 1, ..., k; \quad \forall j = 1, ..., N \tag{4.9}$$

where d_j is a scalar variable varying over the range $-\infty < d_j < +\infty$, and sampled over its range using N sample points. T_i is the transformation function which is chosen according to the desired probability density function of the input parameter of X_i, and ω_i are the frequencies, associated with each factor. Homma & Saltelli (1996) proposed the following transformation to provide a uniformly distributed sample for the factors

$$X_i = \frac{1}{2} + \frac{1}{\pi} sin^{-1} sin(\omega_i d_j), \tag{4.10}$$

which is a set of straight lines oscillating in the range of $[0 - 1]$, while $-\pi < d_j < +\pi$. The classic FAST method forces a sophisticated algorithm to set all the frequencies free of interferences (Tarantola et al., 2006; Tarantola & Koda, 2010). Moreover, FAST is unstable when the number of inputs increases, due to its discrete harmonic analysis feature (Tissot & Prieur, 2012). Tarantola et al. (2006) simplified the procedure of FAST method by including random balance designs in FAST. In this method, the input space is explored using an arbitrary frequency ω for all input factors. Although this assumption avoids the complex calculation of different frequencies involved in the original FAST method, the generated curves do not cover the entire input space. This limitation is addressed by employing random permutation of sample points to assure a full coverage of the input space. The model is evaluated N times

$$Y(d_j) = f(X_1(d_{1j}), X_2(d_{2j}), ..., X_k(d_{kj})) \qquad \forall j = 1, 2, ..., N. \tag{4.11}$$

Then, the sample points are ranked on X_i are re-ordered in increasing order and the associated evaluated model outputs $Y(d_j), j = 1, ..., N$, as well. Then, the frequency ω and its higher harmonies (i.e., $2\omega, 3\omega, ..., M\omega$) will be applied to calculate the Fourier spectrum of the model output $F(\omega)$.

$$F(\omega) = |\frac{1}{\pi} \sum_{j=1}^{N} Y^R(d_j) e^{(-i\omega d_j)}|^2, \tag{4.12}$$

where $(Y^R(d_j))$ is re-ordered model output such that the corresponding values of $X_1(d_{ij})$ are ranked in increasing order. In the following, an estimate of the first-order sensitivity index (a.k.a. importance measure (Iman & Hora, 1990; Ishigami & Homma, 1990) is evaluated as

$$S_i = \frac{1}{V_Y}(V(E(Y|X_{\sim i})) = \sum_{l=1}^{M} F(\omega|_{\omega=l}). \tag{4.13}$$

Afterwards, the ranking process mentioned above is repeated for each X_i, using the same initially N sampled points. Due to the use of random permutation, the calculation cost of this method is decreased to N model evaluations. For more details, the reader is referred to Tarantola et al. (2006). However, the RBD method merely computes the first-order term, therefore it just able to decompose the 100% of output variance in the case of additive models. In this regard, one may use $\sum_{i=1}^{k} S_i$ to identify whether the model is additive or non-additive. If the sum is noticeably smaller than 1, we must use another algorithm to compute interactions or total-effect terms. An advantage of RBD is that it is relatively easy to implement. Also, the sample size N, being independent of the number of factors k, makes it an affordable technique even for computationally expensive models. It also should be emphasised that FAST and RBD estimate positive sensitivity measures. This methodology applied previously by Nguyen-Tuan et al. (2017) to investigate a thermo-hydro-mechanical geotechnical problem.

The main features of RBD in comparison with the FAST method can be summarised as

- better convergence properties rather than FAST
- no need to search for frequencies free of interferences
- avoiding the problem of aliasing in FAST which can be due to a small sample size N
- the sample size N, is independent of the number of factors k and
- it is relatively easy to encode.

Later in the next section, we test the performance of the RBD in evaluating the sensitivity indices of nine constitutive input factors considering the dilatancy behaviour of a rock salt cavity.

4.3.2 Sobol's method (Monte-Carlo based implementation)

The main idea of variance-based methods is to evaluate how the variance of inputs contribute to the variance of the model output. Recalling the Sobol' indices, the S_i as the first-order sensitivity measure which evaluates the sensitivity of model Y to input factor X_i without considering the interaction between input parameters. The total-effect sensitivity index S_{Ti} estimates the effect of input factors and their interactions with the other input factors. Sobol' (1990, 1993) proposed the Monte-Carlo based numerical procedure for the calculation of the first and total-effect sensitivity indices. Saltelli and colleagues modified the crude Monte Carlo based method by Sobol' with the much less computational burden (Saltelli et al., 1993; Homma & Saltelli, 1996). This technique was modified later,

in such a way that estimation of the full sets of first and total order sensitivity indices is about 50% cheaper considering the number of model evaluations (Saltelli, 2002). In the following, this procedure is presented for a model of k factors $Y = f(X_i); \forall i = 1, ..., k$.

Firstly, two randomly sampled $(N, 2k)$ matrices C_1 and C_2 are generated, N is the number of samples, and k is the number of input parameters. Afterwards, a new matrix R_i is defined with re-sampling all arrays from C_2, but its i^{th} column which is identical with C_1 matrix. Then, model output for C_1 and C_2 are evaluated as

$$\boldsymbol{y}_{C_1} = f(C_1) \quad \boldsymbol{y}_{C_2} = f(C_2) \quad \boldsymbol{y}_R = f(R_i). \tag{4.14}$$

Finally, with (4.15) and (4.17) variance-based indices for model inputs evaluate.

$$S_i = \frac{\boldsymbol{y}_{C_1} . \boldsymbol{y}_{R_i} - f_0^2}{\boldsymbol{y}_{C_1} \boldsymbol{y}_{C_1} - f_0^2}, \tag{4.15}$$

here $\boldsymbol{y}_{C_1}$, $\boldsymbol{y}_{C_2}$ and $\boldsymbol{y}_{R_i}$ are vectors containing model evaluations for matrices C_1, C_2 and R_i respectively. While the symbol $(.)$ denotes the scalar product of two vectors, the mean value f_0 is defined as

$$f_0 = \left(\frac{1}{N} \sum_{j=1}^{N} \boldsymbol{y}_{C_1}^{(j)} \right)^2. \tag{4.16}$$

In the following, a similar method is adapted to estimate the total-effect index,

$$S_{Ti} = 1 - \frac{\boldsymbol{y}_{C_2} . \boldsymbol{y}_{R_i} - f_0^2}{\boldsymbol{y}_{C_1} . \boldsymbol{y}_{C_1} - f_0^2}. \tag{4.17}$$

The total-effect index accounts for the total contribution to the output variation due to factor X_i, i.e., its first-order effect plus all higher-order effects due to interactions (Homma & Saltelli, 1996). It should be emphasised that the aforementioned equations used to compute the SA measures only when the input factors X_i are independent.

Running the program to obtain the $\boldsymbol{y}$ vectors in Eq. 4.14 is the most costly step of the proposed procedure. The cost of this approach to estimate both Sobol's indices, is equal to $N(k+2)$ times model evaluations. We need $k \times N$ model calculations for $R_i; \forall i = 1, ..., k$ matrices, and N times for matrices C_2 and C_1, separately.

Table 4.1: Sensitivity analysis techniques

Method		**Model requirement (additional info.)**	**Setting**	**Cost of analysis**	**Number of runs (N)**	**Number of Parameters (k)**
LSA		Linearity	-	k+1	-	>100
Regression		Linearity/Monotonicity	FP	N	500 - 1000	<100
Screening	Morris	(Nonlinearity-Interaction)	FF	N(k+1)	4 - 10	20-100
	Random sampling	(Nonlinearity-Interaction)	FF	N(k+1)	100 - 500	
Variance-based	RBD	(Just S_i)	FP	N	500 - 1000	<20
	Sobol'/Saltelli	(Interaction)	FP (S_i) FF (S_{Ti}	N(k+2)	100 - 1000	

4.4 Elementary Effect

Screening methods exploring the model behaviour based on a discretisation of the input space, provide a fast exploration of the system response. The main idea of screening is originated from the local SA techniques. These methods can be adapted to the sophisticated models with tens of input parameters to identify the non-influential factors with a relatively small number of design evaluations (Hamby, 1994). Afterwards, the model can be simplified before using other more accurate but more costly SA methods; Morris (1991) presented the Elementary Effect method as a global SA methodology. This approach is referred to as Morris method hereafter. This method allows to identify inputs are having negligible effects, and variables that express large non-linear and interaction effects, as well. Based on the proposed technique by Morris, each parameter range is normalised and discretized into a p-level grid. Therefore the parameter space of a model with k parameters is converted to a k-dimensional unit cube.

To estimate the Elementary Effect of the i^{th} parameter ($EE_i, \forall i = 1, 2, ..., k$) for a given point in this grid $X = (X_1, ...X_i, ...X_k)$, Δ as a small perturbation is added to the i^{th} input parameter in a random order. With this, Δ is an increment equal to $p/2(p-1)$ and EE_i is calculated by

$$EE_i = \frac{Y(X_1, X_2, ..., X_i + e_i\Delta, ..., X_k) - Y(X_1, X_2, ..., X_i, ..., X_k)}{\Delta}, \tag{4.18}$$

here e_i is a unit vector in direction i, which is selected randomly. To compute EE_i for k parameters, Morris proposed an efficient methodology which crosses a trajectory of $k+1$ points in the normalised parameter space. Each trajectory provides one EE for each input parameter, and by considering r trajectories ($r \approx 10 - 500$), the total number of required simulations is $r(k+1)$. Now there is a collection of r EEs for each parameter. Since the mean of EE represents the average effect of each parameter over the parameter space, the mean EE can be regarded as a global sensitivity measure (Wainwright et al., 2014). The mean and the standard deviation of EEs denoted as μ and σ, respectively, are calculated as

$$\mu_i = \frac{1}{r}\sum_{j=1}^{r} EE_j^i \tag{4.19}$$

$$\sigma_i = \sqrt{\frac{1}{r}\sum_{i=1}^{r}\left(EE_j^i - \frac{1}{r}\sum_{i=1}^{r} EE_j^i\right)^2} \tag{4.20}$$

where, μ_i and σ_i are considered as the sensitivity indices. μ_i represents the average effect of each variable over the parameter space, and σ_i can notice the existence of any interaction between parameters and/or non-linearity of the model. Small σ_j is identifying a linear relationship between the studied input and the output. Also, μ_i may provide information about the sign of the input's effect on the system behaviour, which helps to realise the nature of the problem. Nevertheless, different signs of EE_i, e.g., in some models, may lead to significant changes in their mean value μ, and an imprecise parameter ranking, subsequently. In this regard, Campolongo et al. (2007) suggested using the mean of absolute Elementary Effect indices $|EE_i|$, denoted as μ^*. The smaller μ^* of a factor identifies a less contribution to the output uncertainty. This measure is suitable for the factor fixing setting. Moreover, as Saltelli et al. (2008) mentioned, a lower value of σ_i, which is due to similar values of the Elementary Effects, reveals that the effect of X_i is almost independent of the values taken by the other factors. Therefore, it can be used as an identification measure to detect the interaction/non-linearity effects between input factors. Then, a graph depicting μ_i and σ_i may offer information to distinguish the linear factors, non-influential ones, and also factors with interaction/non-linear effect.

The elementary effect is numerically efficient and can be applied to sets of factors. Moreover, it is a proper choice for factor fixing setting. This method can also be used before employing a costly variance-based technique to prune the number of factors to be considered. This global SA methodology used previously by the author, in other publications as Mahmoudi et al. (2015*b*); Khaledi, Mahmoudi, Datcheva, König & Schanz (2016).

4.5 Choose a proper SA method

Tab. 4.1 concludes the above-mentioned attributes of the introduced SA techniques, i.e., their related setting, the cost of analysis, the required number of runs, and the additional information that each of them may provide.

As a conclusion of all introduced methods, one may provide a primary guideline to choose an appropriate method. Fig. 4.1 depicts such a decision tree which leads to the most appropriate technique based on the system features as model complexity, demanding computational costs and the dimension of the input space. Based on illustrated graph in Fig. 4.1, one should firstly consider the complex features of the model, the local approach is the best choice for linear systems, for the others, global techniques must be employed. In a linear regression, the value of the standardised regression coefficient is the same as the correlation coefficient or first-order sensitivity measures. At the further steps, the

number of associated parameters and the regarded computational costs in a single model evaluation, are decisive factors. In general, using screening methods for the models with a high number of input parameters and computationally expensive ones is recommended. Also, one may use the grouping techniques as recommended in Saltelli et al. (2000) to shrink input space. Afterwards, one may fix a set of non-influential inputs and further evaluates the variance-based sensitivity measures suggested by Sobol'. Nevertheless, in the following, we applied all three techniques on the same model of a rock salt cavern to compare their outcomes' conformity and abilities to provide additional information about the model response.

4.6 Numerical example

A typical salt cavern with a simplified geometry is modelled using a finite element model. Since the cavern has a cylindrical shape, only half of the geometry has been simulated. The axisymmetrical model has a height of 800 meter and a width of 300 meter. A detailed description of the simulated excavation and operation process was given in **Chapter 3**. As mentioned previously in Chapter2, in order to guarantee the stability and serviceability of the cavity, dilatant zones caused by excessive shearing should be avoided. The dilatant behaviour is defined by the beginning of the irreversible volumetric expansion, and may initiate the damage progress and leads to long-time failure (Hunsche & Hampel, 1999). In this regard, the stress state of the rock salt around the cavern is considered as the interested model output. Here, the stress state in different observational points around the cavern wall (as shown in Fig. 3.11), are investigated. The finite element model is constituted based on an elasto-viscoplastic creep material model, presented in Sec. 2.3 (Mahmoudi et al., 2017). For the sake of simplicity, we assume that the shape of the yield surface in the π-plane remains unchanged. Therefore, related parameters, namely b, β and β_1 are kept constant. Hereupon, this example considers nine independent constitutive parameters as uncertain parameters in the governed material model introduced in Sec. 2. These uncertain parameters are E and ν as parameters of the elastic behaviour, as well as six viscoplastic parameters in the constitutive model (namely N_f, n, λ, a_1, γ and η) in addition to $\overline{\eta}_M^*$ which controls the steady state strain rate. It should be indicated that the investigated constitutive parameters in this study are considered as independent variables, which have no correlation.

Nine constitutive parameters are regarded as the uncertain parameters. Tab. 4.2 represents the definition and the assumed statistical measures of these uncertain parameters.

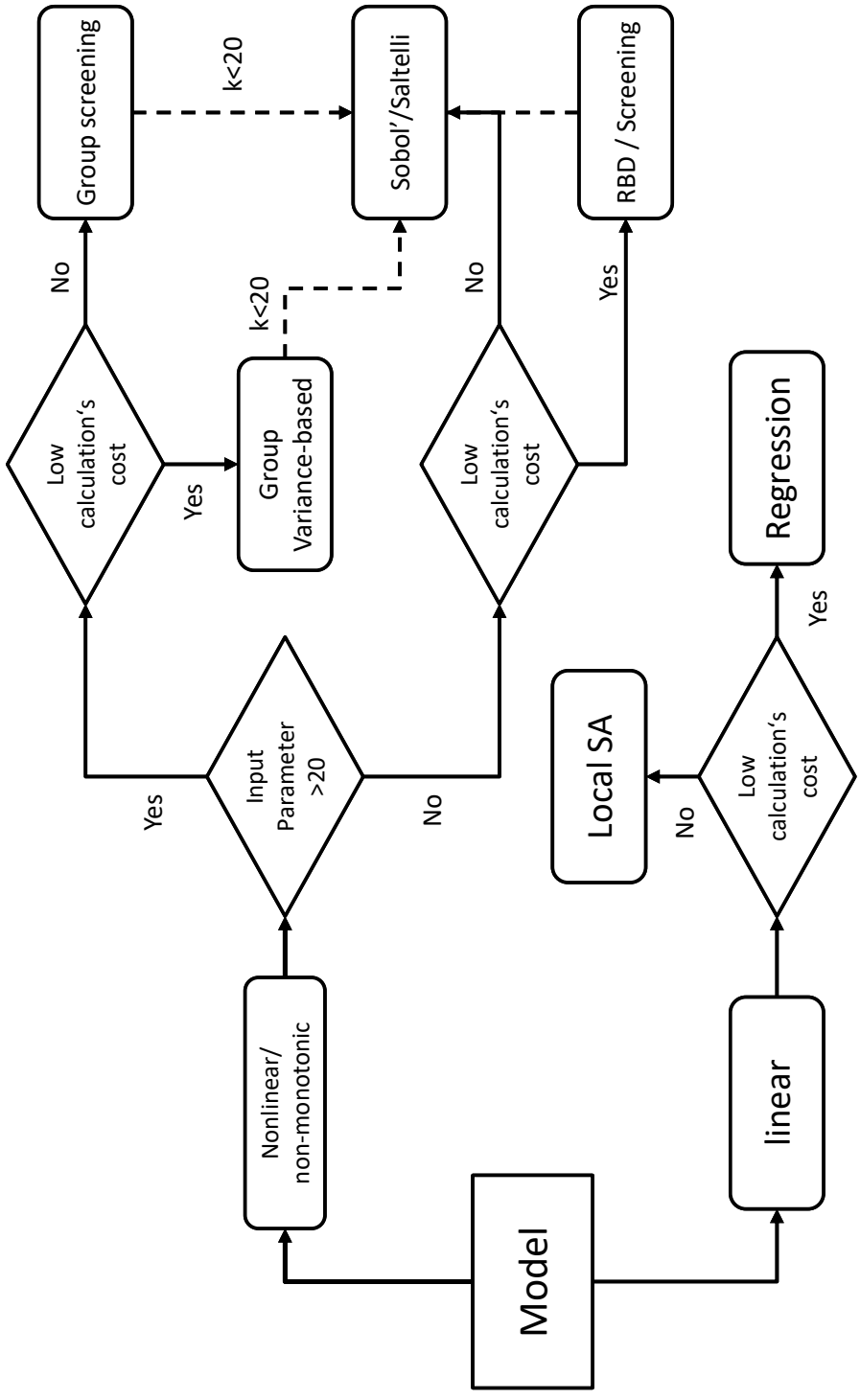

Figure 4.1: Diagram for the choice of sensitivity analysis method (adjusted from Rocquigny et al. (2008))

It also should be mentioned that all the regarded uncertain parameters are assumed to follow a Gaussian probability distribution.

Baecher & Christian (2005) did an analysis investigating the effect of different probability density function of geomaterials on the reliability measures. They concluded that the assumption of a Normal distribution in the absence of further information is conservative and such an assumption will probably overestimate the probability of failure.

Also, the further argument for using the Normal distribution is that the geological and geotechnical phenomena are determined by the combined contributions of a wide variety of small effects and, considering the Central Limit Theorem, the distribution of the overall effect ought to be Normal. Based on this theory, for a wide range of conditions, the distribution of the sum of a vast number of variables, while no one variable dominates, converges to a Normal distribution. The only drawback of using a Normal distribution is that it allows negative values, which is unrealistic for many of the material properties of rock and soils. However, because of the usually small considerations for the value of the coefficient of variation, the portion of the Normal distribution that has negative values is so small that it has almost no effect on the obtained results. Among the other distributions which can be applied to geotechnical variables, as Exponential Function, Gamma and Beta distributions, considering lognormal distribution for geomaterials is also very common. Assuming lognormal distribution can be adjusted by this argumentation that the combinations of different random variables are commonly represented by their product not the sum of individual effects. Hence the resulting distribution should reflect the sum of their logarithms (Baecher & Christian, 2005). Moreover, using the lognormal distribution can settle the issue of negative values. However, for the sake of simplicity and considering the fact of delivering conservative outcomes, in this thesis, the normal distribution is considered for all the constitutive parameters. In Sec. 6.4, where the higher variations are assumed, the lognormal distribution is applied.

4.7 Results

The aforementioned SA techniques in Sec. 4.1 are applied to the model introduced in Sec.4.6. The obtained results and remarks are presented in the following.

4.7.1 Convergence Analysis

As mentioned previously, the required number of model evaluations in the Monte Carlo based approach proposed by Saltelli can be adjusted within a convergence analysis; this

Table 4.2: Uncertainty representation of constitutive parameters

Parameter	Description	Dimension	Boundaries	COV(%)
E	Elastic modulus	MPa	[19000 , 25000]	15
ν	Poisson Ratio	[-]	[0.25 , 0.28]	5
n	Transition parameter	[-]	[2.4 , 3.5]	15
N_f	Flow exponent	[-]	[2.4 , 3.5]	15
λ	Fluidity parameter	s^{-1}	[0.5e-14 , 0.5e-11]	10
a_1	Hardening parameter	$MPa^{(2-n)}$	[0.3e-4 , 0.35e-3]	10
γ	Ultimate parameter	[-]	[0.085 , 0.11]	10
η	Hardening parameter	[-]	[0.7 , 0.9]	10
$\overline{\eta_M^*}$	Maxwell coefficient	MPa s	[1e12 , 3e12]	15

analysis is adapted from Yang (2011). To conduct a convergence analysis, firstly R replicas (in this study $R = 50$) of a base sample of dimension m should be generated. Then the corresponding sensitivity measures for each replica is evaluated. In this step, the statistical measures of the indices (namely, mean and coefficient of variation) are evaluated. These steps are repeated for various sample size (N) till its coefficient of variation (COV) converges. Fig. 4.2 depicts the convergence of the S_{Ti} regarding the required number of samples (N). For accurate estimations of the sensitivity measures, we assumed N is equal to 1500, and subsequently the required number of model evaluation is 22000.

Fig. 4.3b and 4.3a show the confidence intervals (as boxplots) of the estimated sensitivity indices, μ^* and S_{Ti}, respectively. To evaluate S_{Ti} index, we considered $N = 1500$ and the number of trajectories, r is assumed to be equal to 300, the estimation process are repeated 50 times for each estimated indices. As figures shown, the variation of estimated indices, in Morris method is higher than those evaluated any Sobol'/Saltelli technique. Moreover, increasing the relative importance of input factors raises the related variation in the estimation process.

4.7.2 Sensitivity measures

Fig. 4.4 and 4.5 present the outcomes of Sobol'/Saltelli technique of DF with respect to the constitutive parameters, namely S_i and S_{Ti}. The first order sensitivity indices that are estimated using RBD method are illustrated in Fig. 4.6. It should be noted that for those non-effective variables, in some analyses the negative values are also obtained as their first-order sensitivity index. Negative signs are due to numerical errors in the estimates.

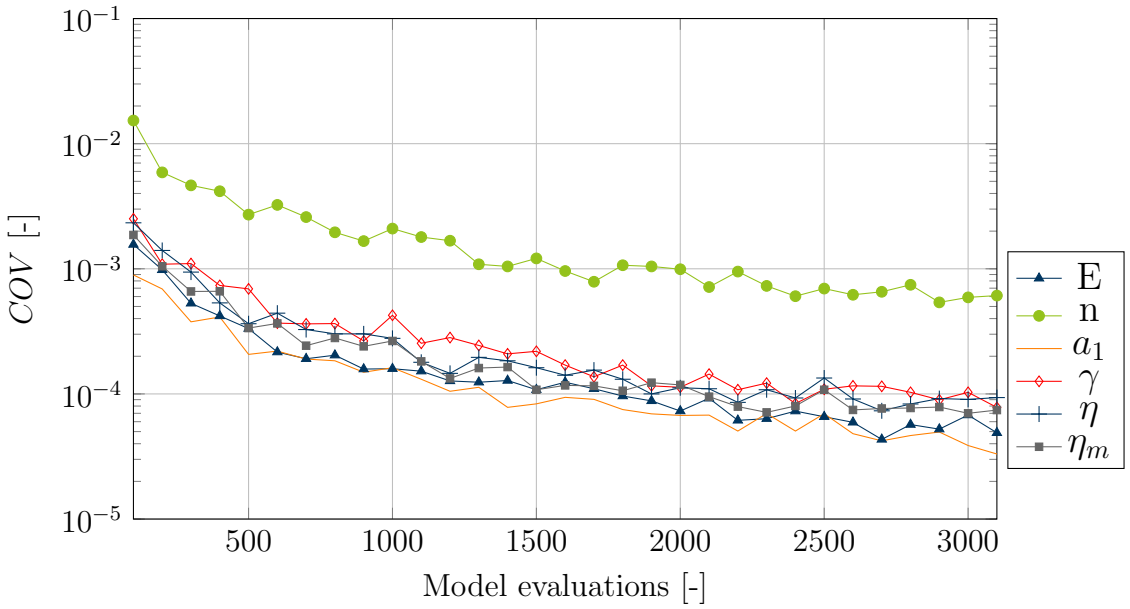

Figure 4.2: Convergence S_{Ti}

Such negative values can often be encountered for the Saltelli method when the analytical sensitivity indices are close to zero (i.e. for unimportant factors). Increasing the sample size of the analysis reduces the probability of having negative estimates. FAST and RBD estimates are always positive, by the construction.

Results obtained by Morris method are presented in Fig. 4.7. The sensitivity analysis is carried out at various points around the cavity wall, $N_i, \forall i = 1, ..., 5$ illustrated in Fig. 3.11. Based on these results, n has the most impact on the variation of DF as a measure for dilatancy occurrence in the system. Also, the parameters ν, N_f and λ have the least influence on the outputs, therefore, in the next steps of this chapter their variations are neglected, and they are fixed to the values mentioned in Tab. 2.3. The sensitivity of volume change of the cavern is also estimated considering the same constitutive parameters and provided in Fig. 4.7b. As expected, the most sensitive constitutive parameter to the volume change is the Maxwell coefficient. The estimated major effect for the Maxwell viscosity coefficient can be adjusted to the fact that it governs the time-dependent behaviour (i.e., steady state creep) of the system and the period considered in the model is relatively long (more than 3.5 years).

4.7.3 Temporal sensitivity analysis

Since the thermo-mechanical behaviour of the rock salt is time-depended, thus in addition to studying the efficiency level of constitutive parameters in different zones around

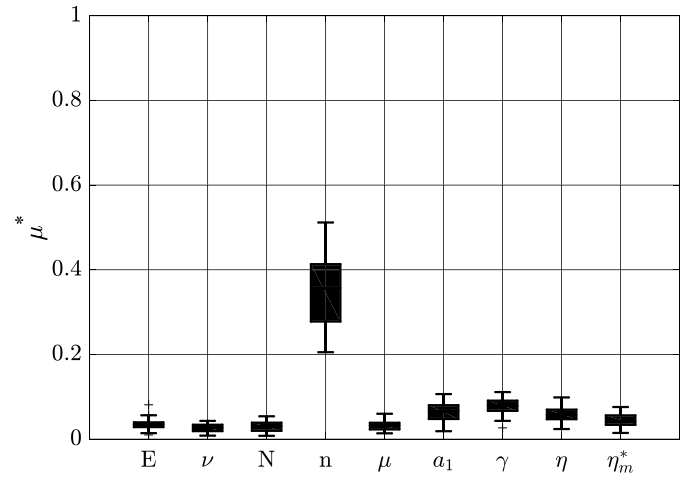

(a)

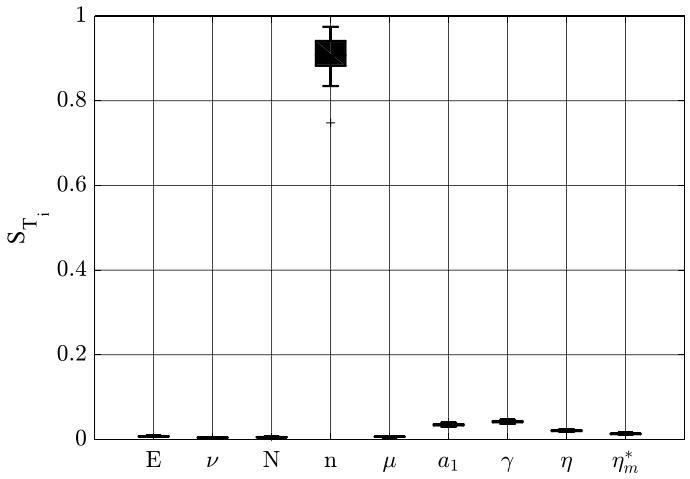

(b)

Figure 4.3: Estimation of a) μ^* and b) S_{Ti} in point N_4. (Each boxplot corresponds to 50 independent estimates)

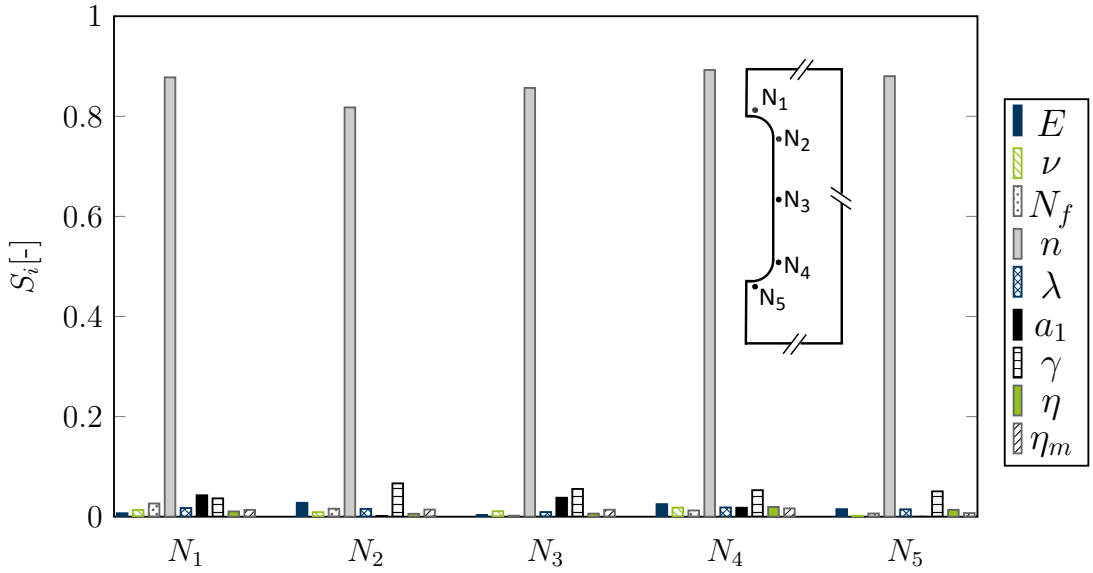

Figure 4.4: First-order sensitivity index S_i in different regions (N_1 to N_5 as displayed in Fig. 3.11) around the cavern, calculated by Sobol'/Saltelli approach

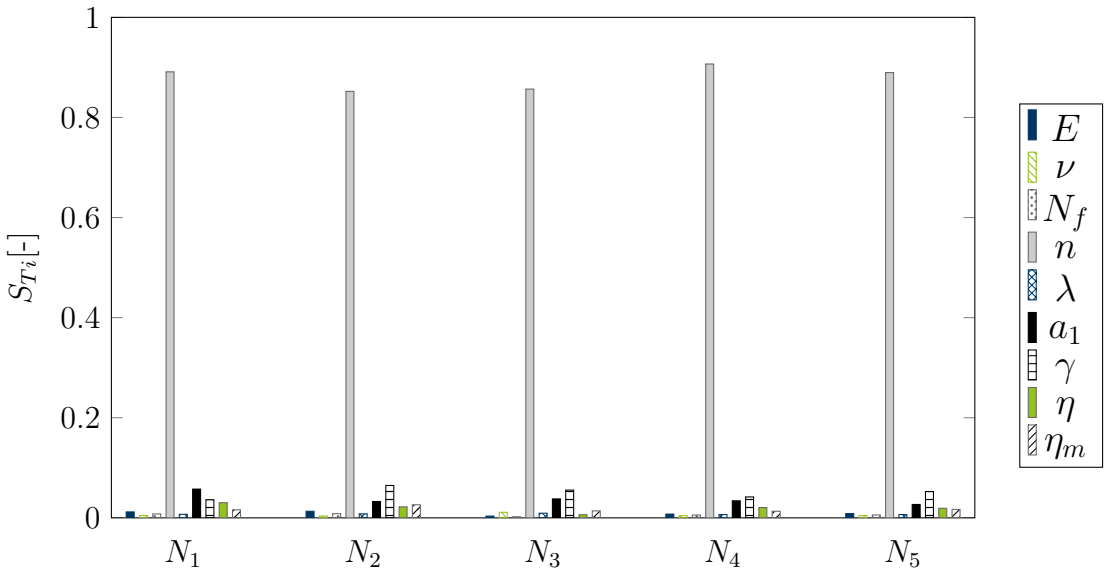

Figure 4.5: Total-effect sensitivity index S_i in different regions (N_1 to N_5 as displayed in Fig. 3.11) around the cavern, calculated by Sobol'/Saltelli approach

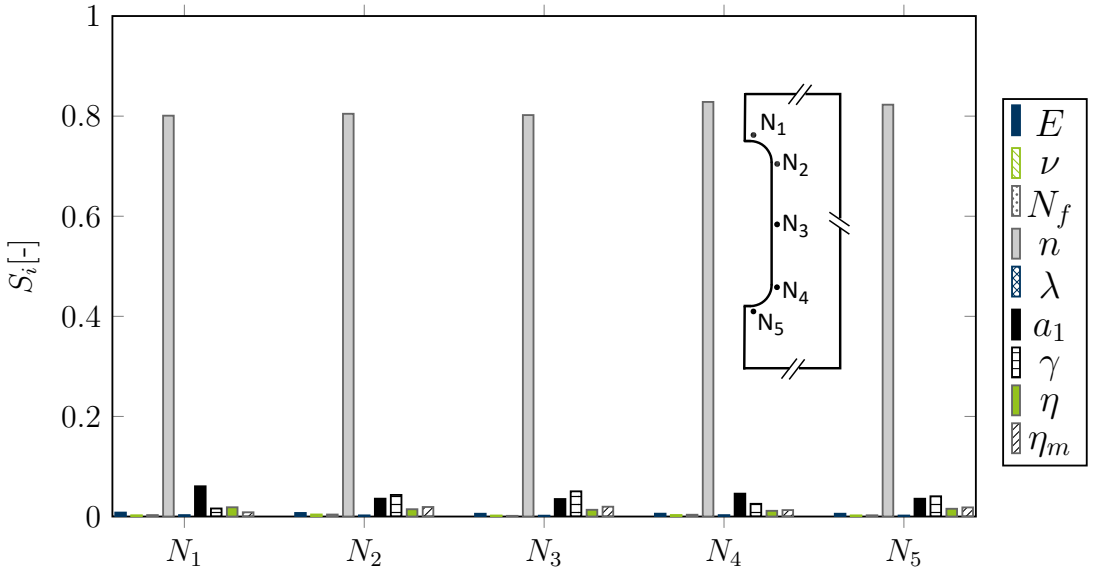

Figure 4.6: First-order sensitivity index S_i in different regions (N_1 to N_5 as displayed in Fig. 3.11) around the cavern, calculated by RBD approach

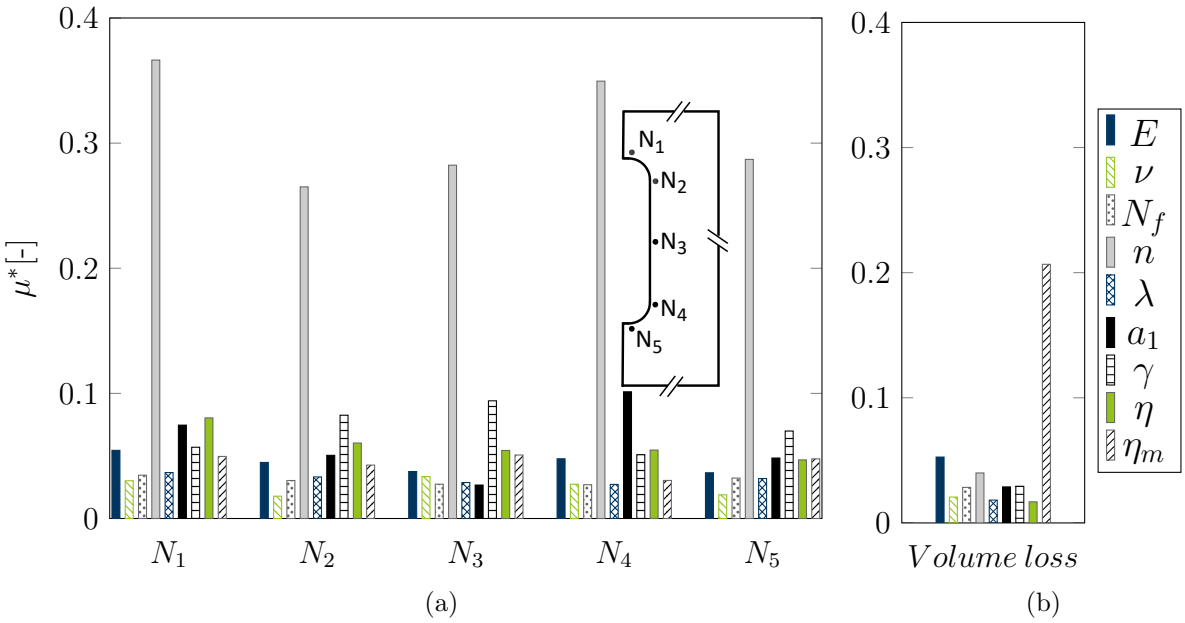

Figure 4.7: Elementary effect sensitivity indices of (a) *DF* in different regions (N_1 to N_5 as displayed in Fig. 3.11) around the cavern and (b) volume loss to constitutive parameters

the cavity, one may survey the change in their importance level during excavation and operational time. In this regard, the effect of various parameters of the creep, as the most time-dependent component of the constitutive model is surveyed in Mahmoudi et al. (2015*b*). In this section, the effect of variation in three material constant values on horizontal displacement of point N_3 in Fig. 3.11 is investigated. For this purpose, the horizontal displacement of the point N_3 within 60 days is observed while the finite element model used the LUBBY2 constitutive model (For more detail see Sec. 2.1). The uncertainty measures of the constitutive parameter values of the LUBBY2 model are presented in Tab. 4.3 (Mahmoudi et al., 2015*b*). Morris and VB methods have analysed the sensitivity of model outputs to input data. Two variance-based measures S_i, S_{Ti} and one elementary effect index μ^* calculated versus time of loading represent in Fig. 4.9, 4.10 and 4.8, respectively. Based on results, the sensitivity measures of the mechanical response of the cavity to various constitutive parameters changes versus time. In the short term the most important parameter in LUBBY2 model is Kelvin dashpot coefficient. During the first day of analysis its sensitivity is considerable, but after one day decrease, as varying its value does not change the displacement of cavern's wall. Also, the Kelvin spring's coefficient in first steps of calculation does not have a significant role in cavern's wall displacement, but its sensitivity indices in the early loading steps increase and reduce slightly. Moreover, the coefficient of Maxwell dashpot as a part of constitutive model which describes the steady state creep phase, during time shows a rising tendency (Khaledi, Mahmoudi, Datcheva, König & Schanz, 2016). Therefore, it is necessary to be more careful about obtaining its value in long term analysis, more accuracy rather than other parameters for this parameter is needed.

4.7.4 The comparative study

The calculated first-order indices S_i for different constitutive parameters by Sobol'/Saltelli and RBD methods are shown in the Fig. 4.11. The results are mostly identical, while the RBD technique merely needs about 500-1000 model evaluations compared to the 22000 required ones in Sobol'/Saltelli technique. The other comparison can be done between the calculated sensitivity indices provided by Morris and Sobol'/Saltelli methods. Fig.4.7 illustrates the result of μ^* considering no-dilatant zone and volume loss in left and right side, respectively. Besides, Fig.4.5 shows the result of S_{Ti} considering no-dilatant zone and volume loss in left and right side, respectively. Based on the gained results, the importance ranking of input parameter obtained by Morris method is more visible than S_{Ti}. In this study, Morris method enforced 3000 model evaluations (r) is assumed relatively high

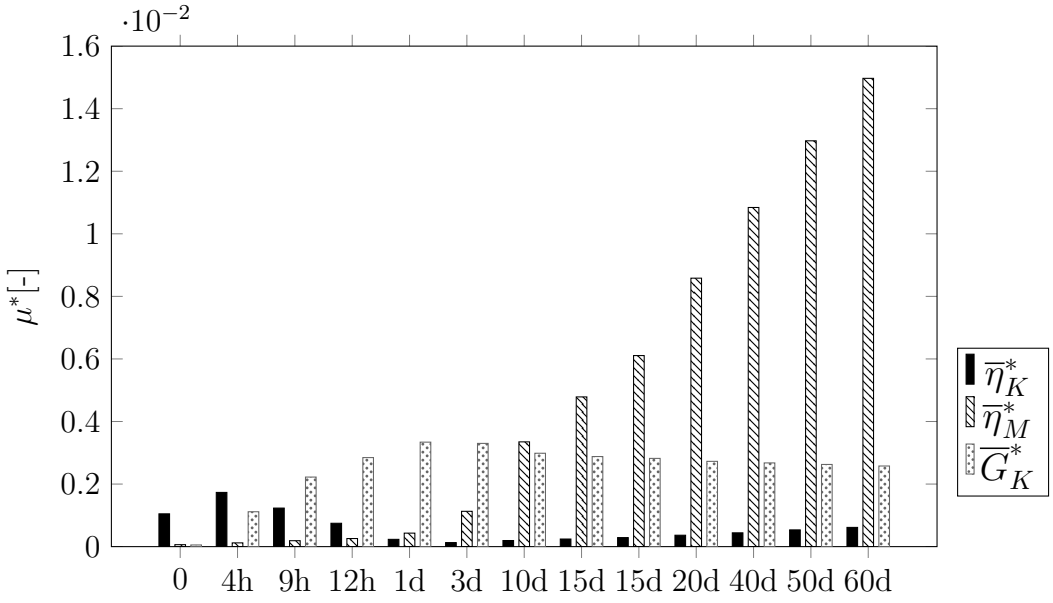

Figure 4.8: μ^* index along loading time

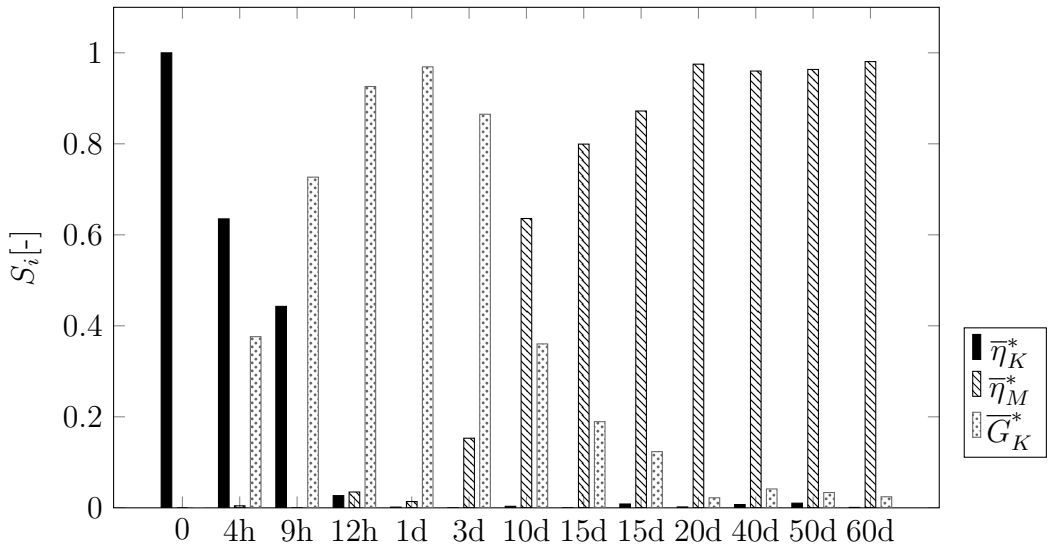

Figure 4.9: S_i index along loading time

Table 4.3: Uncertainty representation of the LUBBY2 constitutive parameters

Parameter	Description	Dimension	Boundaries
$\overline{G_K^*}$	Kelvin spring coefficient	MPa	[3e5 , 6e5]
$\overline{\eta_M^*}$	Maxwell viscosity coefficient	MPa s	[0.5e12 , 2.5e12]
$\overline{\eta_K^*}$	Kelvin viscosity coefficient	MPa s	[4e9 , 9e9]

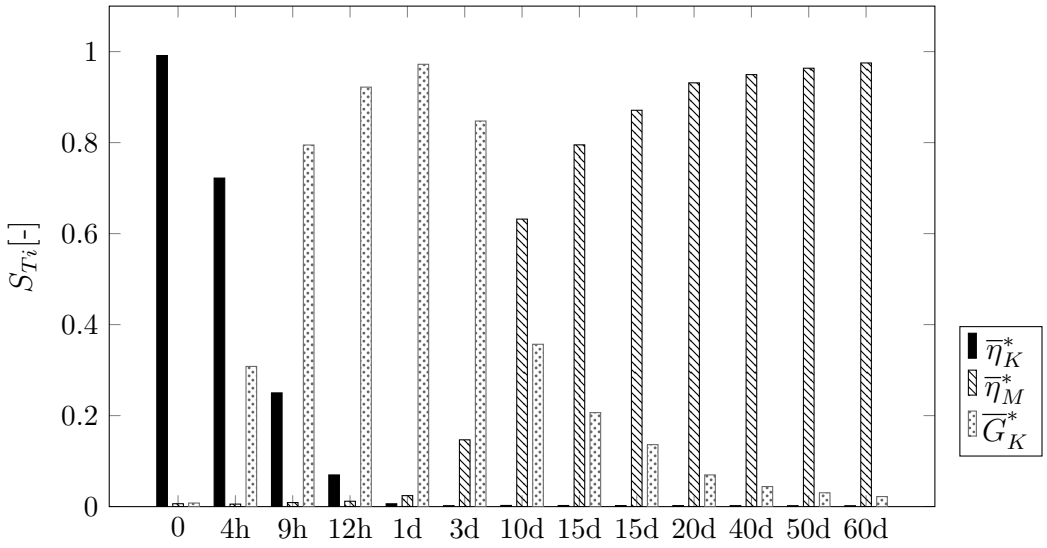

Figure 4.10: S_{Ti} index along loading time

but could be chosen less). Although the scale of provided SA measures is different, the obtained ranking is mostly same. One may conclude that the three input parameters of Poisson ratio ν, the flow exponent N_f, and the fluidity parameter λ have the least contribution in the stress state of the different zones in Fig. 3.11 and can be treated as fixed values for further investigations. The author used these results in Khaledi, Mahmoudi, Datcheva, König & Schanz (2016) to reduce the dimension of the parameter space to perform a reliability analysis.

4.7.5 Detecting non-linearity and interaction effects

As mentioned in Sect.4.1, the Morris and Sobol'/Saltelli methods, are both able to provide some more additional information about the model features. For instance, Fig. 4.12 displays results of five conducted SA at different points around the cavern's wall in the frame of a cross plot of $\sigma - \mu$. Based on the obtained results, transition parameter n shows the most standard deviation, which indicates the existence of non-linearity/interaction effects between this parameter and the others. In addition, the almost zero effect of the

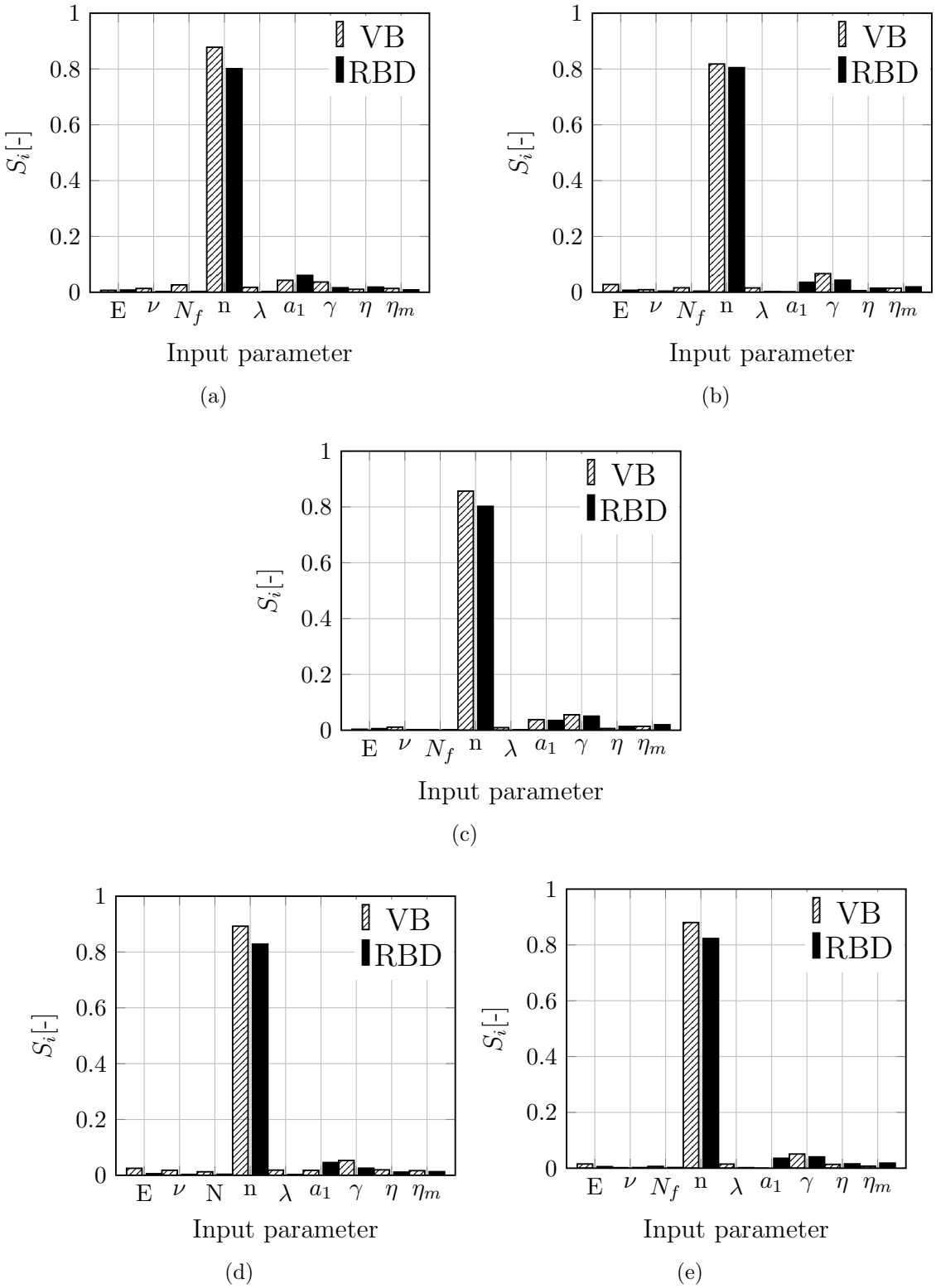

Figure 4.11: Comparison between the RBD and the VB approaches in point a)N_1, b)N_2, c)N_3, d)N_4 and e)N_5

parameters ν, N_f, and λ, which already have been identified as the non-influential ones is shown, also the regarded σ is negligible. As additional information one can extract from such a graph is the sign of the input parameter's effect on the model output. As clearly shown in Fig. 4.12, n has a negative effect on the stress state of the cavern's wall. This is justified based on the definition of this parameter, which assigns the dilatancy boundary (For more details about the constitutive model see **Chapter 2**). Moreover, on the Fig. 4.13 the obtained S_i as a function of the S_{Ti}-S_i is depicted. According to the Fig. 4.13, one can identify the ratio between the first-order effect and the interaction effects, as it shows a large interaction effect for parameter n. Also, comparing the graphs in Figs. 4.13 and 4.12 enables the designer to distinguish the non-linearity and interaction effects involved in the model, since the right one just reveals the interaction effects and the left one includes both. For example, parameters n and a_1 show the same interaction effect but n has a higher non-linear effect.

4.8 Metamodelling

The main aim of metamodelling is to reduce the computational costs of high-dimensional stochastic problems, which require hundreds of deterministic model evaluations. For instance, the execution time of a comprehensive numerical model of a rock salt cavity, considering excavation and operation phases is relatively high.

In general, any probabilistic analyses as global sensitivity analysis technique one needs to generate a relatively large number of the input-output set of data. Thereupon, in the case of comprehensive computational models, performing such analyses seem infeasible. For instance, in variance-based methods, which are developed based on Monte Carlo simulation, one need to run a large number of the computational model. Therefore, using such numerical models that explained in **Chapter 3**, which is computationally expensive, makes such analysis infeasible. Consequently, a proper solution to overcome this issue is utilising a *metamodel* to substitute the original numerical model. A metamodel is an analytical model that replaces the original simulation with sufficient accuracy and evaluates the behaviour of a multivariate complex system while it is computationally inexpensive and plausible, see Fig. 4.14.

Among the other well-established methods, Proper Orthogonal Decomposition with Radial Basis Function (POD-RBF) is carried out in this thesis. Radial Basis Function were first used by Hardy (1971) for multivariate data interpolation. He proposed Radial Basis Functions as approximation functions by solving multi-quadratic equations of topogra-

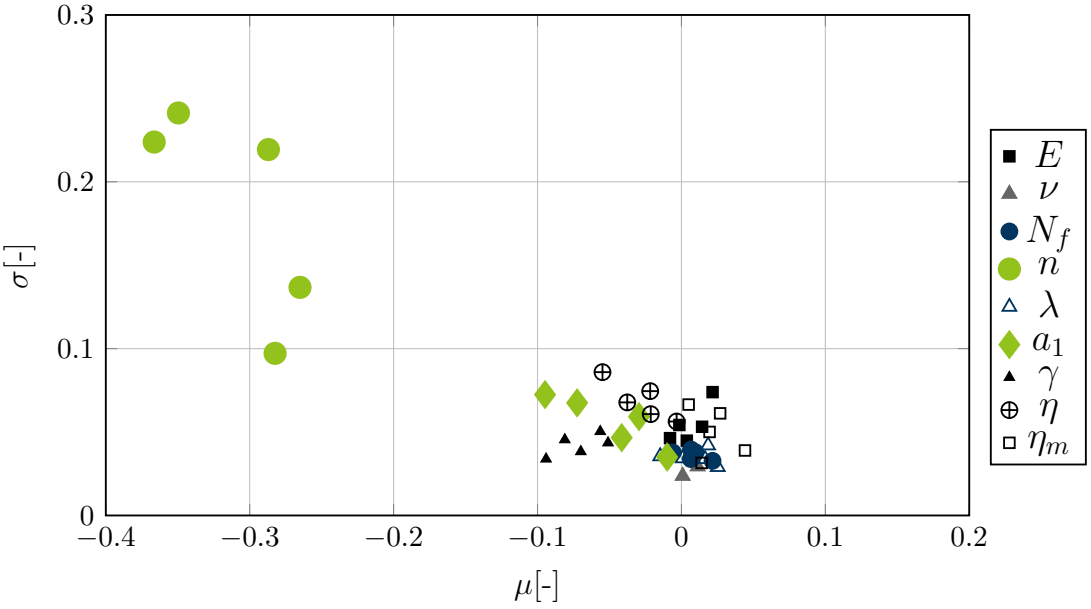

Figure 4.12: Standard deviation of elementary effect (σ) approach vs. mean EE (μ)

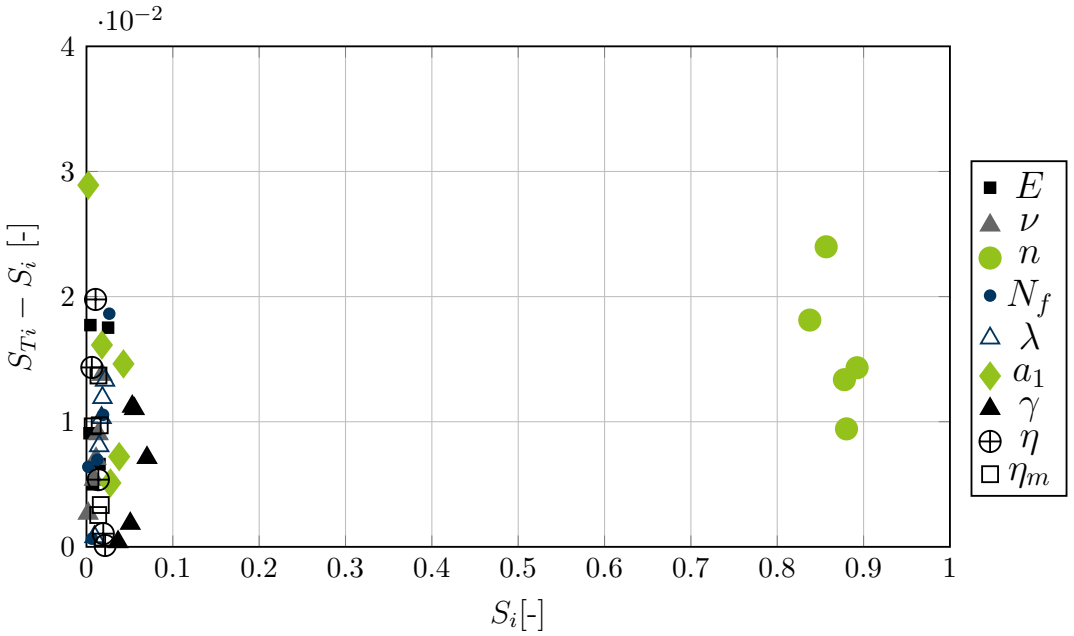

Figure 4.13: First-order index of sensitivity (S_i) vs. S_{Ti}-S_i

phy based on coordinate data with interpolation. Buljak (2010) developed POD-RBF to make a metamodel for scattered points in multidimensional space. This model uses orthogonality in the vector spaces to reduce the dimension of the problem and simplify the approximation procedure. POD-RBF firstly decompose the matrix of the system response into a reduced space, and then the radial basis functions interpolate the reduced amplitude matrix. For generating a metamodel, a limited number of computations have been done with the original model and their input-outputs use as input data for training metamodel.

In order to develop a POD-RBF metamodel, firstly 100 uniformly distributed sample sets of the input parameters are generated, and subsequently, the FE numerical model is run for each sample set and the relevant output is recorded. After that, the generated input-output sets, are used for constructing the metamodel. To examine the accuracy level of the metamodel, the original numerical model is executed to determine the DF value in the point N_4 for 20 additional input parameter sets, and the corresponding results are compared to the outputs obtained by the metamodel. Here, two error measures, namely the coefficient of determination, and the Normalized Root-Mean-Square deviation, are employed. The error measures known as the model coefficient of determination and denoted as R^2 is equal to the fraction of the variance of the original data which come from our model, see Eq. 4.4. where $\hat{y}_i$ is the regression model prediction and $R^2 \in [0, 1]$. It should be mentioned that for a perfect approximation R^2 reaches 1 and NRMSD reaches 0. For instance, the computed error measures for point N_4 are estimated as follow

$$R^2 = 0.98858, \qquad NRMSE = 0.001791. \tag{4.21}$$

4.9 Conclusion

In the framework of system performance analysis, SA techniques may provide an assessment of the uncertainty involved in the system outcomes, and identify the sources of this uncertainty. In this chapter, different SA methods and techniques, their corresponding results and settings are briefly introduced. A guideline to select a proper technique based on the attributes of the model including complexity, computational costs and the number of parameters involved is presented. The decision tree introduced may guide the user to select the most appropriate technique among the others. Since the expensive SA methods as Sobol'/Saltelli provide measures to have a better understanding of the system

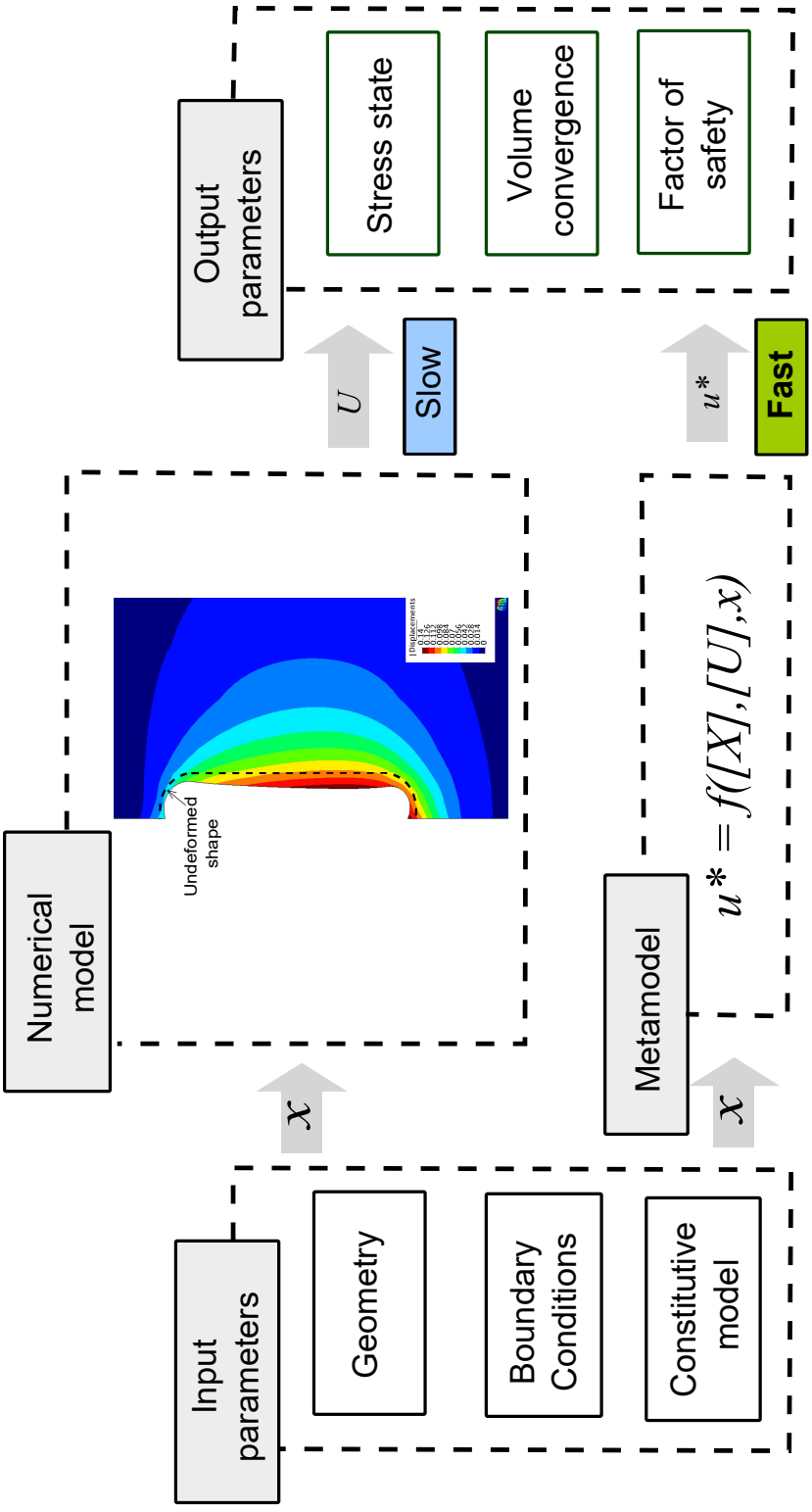

Figure 4.14: The Information flow of metamodeling process

behaviour, sometimes the designer may afford the expensive methods to achieve such a sophisticated knowledge. In the following, different global SA methods are applied on a geotechnical model, namely an underground energy storage in rock salt. The particular level of construction and the massive geometry of such an underground structure confront the design process with a significant amount of uncertainties. Hence, to reduce the involved uncertainties through model calibration or further observations, conducting SA techniques is appropriate. The performance of different methods and the conformity of the provided results are discussed. The study reveals that the applied SA methods assign same parameter importance rankings in the considered simulation model. Furthermore, it can be concluded that the RBD, which requires less computational effort rather than Sobol'/Saltelli technique, provides a suitable option for S_i. Moreover, the comparative study demonstrated that Morris method might offer an appropriate alternative for the S_{Ti} as a variance-based index. It also can detect the positive or negative effects of parameters and non-linearity and interaction effects.

5 Probabilistic Analysis

5.1 Introduction

In this chapter, different methodologies to perform a probabilistic analysis are presented. In general, a non-deterministic analysis is utilised by designers to ensure the decision makers about a certain range of the serviceability and stability of the system of interest. Moreover, the reliability design concept alongside the engineering design codes can be employed to assess the design parameters' values in a way that the system safety is warranted.

The interested level of reliability for each specific system is subject to different issues like economic and social benefits or costs. However, the performance of each system during its lifetime can be defined through opposite terms as load-strength, force-resistance or demand-capacity. The difference between capacity and demand, which is usually referred to as the safety margin, determines the state of the system. Without loss of generality, the term of reliability can be defined through the following description presented by Kottegoda & Rosso (2008).

"Reliability is the probabilistic assessment of the likelihood that a system will perform adequately for a specified period under known operating conditions." On the other hand, the reliability of a system is defined as the probability of non-failing in fulfilling the demands, over a predefined time interval.

To assess the safety state of a system, one needs to determine the resistance of the structure and the maximum forces that a system may experience. The values of the maximum forces and the strength of a structure are not constant during its lifetime. Apart from this, the prediction process of these values is subject to uncertainties. A standard engineering solution to overcome this issue is utilising the safety factors. The determination process of safety factors mainly relies on the previous experiences on the behaviour of similar systems. Hence, a significant level of uncertainty can be involved in their values, that considering them leads to conservative (and probably expensive) designs. Thereupon, the probability of a system ability to properly perform under the imposed burden requires

probabilistic analyses to take into account the associated uncertainties with the considered values for model parameters. Accordingly, the response of the system for each set of the input factors' value (from the assumed range of the variation) may take place in the safe or the failure state. The boundary between these two states is known as the limit state surface, denoted as G_x. The function of this surface is formulated such that $G_x > 0$ indicates the safe state and $G_x \leq 0$ determines the failure state. The probability that a system does not accomplish the requirements P_F is defined as

$$P_F = 1 - R_F = P(G_x < 0) = \int_{G_x<0} f_x(X)dx \tag{5.1}$$

where R_F, as the corresponding probability of non-failure states, indicates the reliability of the system. $f_x(X)$ is the joint probability density function of the relevant demands and resistance parameters $X = (x_1, ..., x_k)$. The performance function denoted as $G_x = G(x_l, x_2, ..., x_k)$, is the mathematical relationship between these variables. The failure or the limit state surface can then be defined as $G_x = 0$. A schematic representation of a simple system with two normally distributed parameters and the related limit state surface is illustrated in Fig. 5.1.

Every probabilistic analysis technique is designed to provide various information about the system of interest. For instance, it may calculate the statistical moments of the system response, or the failure probability and the reliability index, accordingly. The reliability index of a system, denoted by β_r, is defined as the ratio between the mean and standard deviation of the safety margin of the system (Baecher & Christian, 2005). On the other hand, β_r is the number of standard deviations between the mean value of the safety margin and its critical value (see Fig. 5.2).

$$P_F = 1 - \Phi(\beta_r) = \Phi(-\beta_r) \tag{5.2}$$

where $\Phi(.)$ denotes the standard normal cumulative probability. To perform a reliability analysis, one needs to calculate the integral of Eq. 5.1. However, the joint probability density function of the random variables $f_x(X)$ is practically impossible to obtain and subsequently, directly evaluating the regarded integral is difficult. However, many techniques and methods are developed to accomplish a reliability analysis. Li et al. (2015) divided these methods based on their approaches into two main categories.

i) There are methods that approximate the limit state surface by a Taylor series expansion (either first or second order) (Ditlevsen & Madsen, 1996; Hasofer & Lind, 1974). Many studies have been utilised such methods in structural reliability problems, e.g., Rackwitz

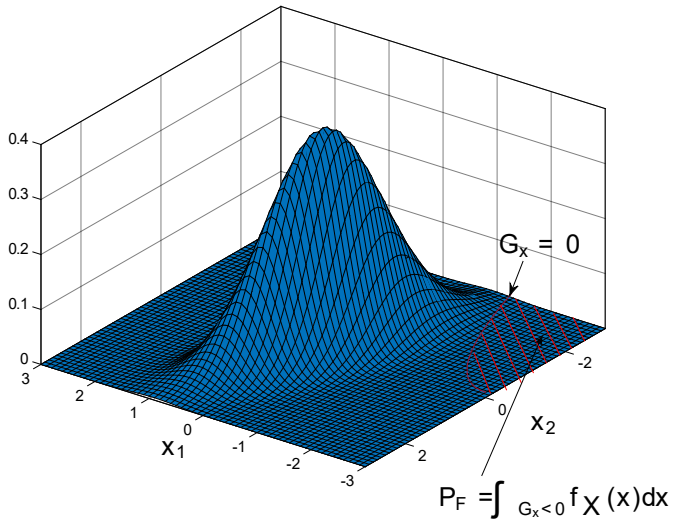

Figure 5.1: Reliability analysis concept

& Fiessler (1978); Wang & Grandhi (1996); Zhao & Ono (1999). A collection of formulae represents the First-Order Reliability Method (FORM) that approximate (linearise) the performance function G_x by the first order Taylor expansion. One may mention the name of First-Order Second-Moment (FOSM) and Advanced First-Order Second-Moment (AFOSM) methods (Hasofer & Lind, 1974) as the members of this class of methods. While the FOSM ignores the information on the distribution of random variables, in AFOSM, the distributional information is appropriately used (Haldar & Mahadevan, 2000). In the AFOSM (a.k.a. Hasofer-Lind method), the assessment of the reliability index is mainly based on the transformation/reduction of the problem to a standardised coordinate system.

Employing the first order Taylor expansion can fulfil nearly all practical needs, and its numerical accuracy is sufficient. Considering that a second-order expansion of the limit state surface can approximate the limit state surface more accurately than a first-order expansion (Fiessler et al., 1979), Second Order Reliability Methods are developed and employed (Breitung, 1984; Breitung & Hohenbichler, 1989; Köylüoglu & Nielsen, 1994). The concept and calculation procedure of this class of methods are simple, and they also were observed to be efficient in many previous studies. However, results presented by Valdebenito et al. (2010) indicate that approximation methods may be inappropriate for treating high-dimensional, non-linear problems.

ii) The second class of methods for estimating the failure probability are collectively referred to as simulation-based methods. The crude Monte Carlo simulation (Rubinstein, 2008), important sampling methods, and subset simulation belong to this class. Crude

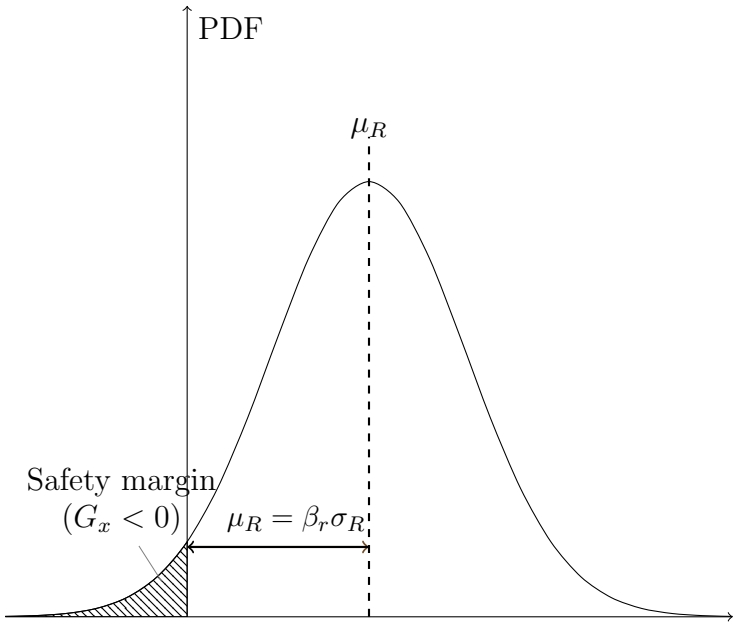

Figure 5.2: Probability density function of system response and safety margin

Monte Carlo uses statistical averaging over random samples generated from the probability density function of the parameters to evaluate P_F. It is a well-known and robust procedure to address models of different complexities. The Monte Carlo simulation is employed widely in the geotechnical field to conduct reliability analyses, Tang et al. (1976); Phoon & Ching (2014); Miro et al. (2015).

Importance sampling schemes are developed to make results arbitrarily exact at the expense of some more numerical effort. Shinozuka (1983) introduced the importance sampling concept to the reliability community. The basic idea of importance sampling method was choosing an importance sampling distribution to generate samples that lead to failure more frequently. Successful applications of this method to various engineering problems have been reported in Schuëller & Stix (1987), Bucher (1988) and Au & Beck (1999). Rosenbluth (1975) proposed the point estimate method, a simple method to assess the moments of the performance function by evaluating it at a set of specifically chosen discrete points. This method requires that the performance function is evaluated for a vast number when the number of uncertain parameters is large.

For efficiently computing small failure probabilities encountered in civil engineering, Au & Beck (2001) developed the subset simulation as an advanced Monte Carlo simulation method. This approach expresses a small failure probability as a product of larger conditional failure probabilities and channelises the problem of simulating a rare failure event into several problems that involve the conditional simulation of more frequent events. To

generate the conditional samples, the Markov chain Monte Carlo simulation is used. A detailed description of this method is presented in Sec. 5.2.1.

In the following, the crude Monte Carlo and subset simulation techniques are presented in detail and applied to the finite element computational model of a rock salt cavity presented in Sec. 3.2.

5.2 Monte Carlo Simulation

The Monte Carlo simulation can be regarded as a well established and the most common method in probabilistic studies. The Monte Carlo simulation which is named after the gambling complex in the city of Monte Carlo in Monaco is an easy to use method even for those engineers with basic statistical knowledge (Fishman, 1996). Nevertheless, the Monte Carlo simulation is a robust method that its accuracy can be assured regardless of the complexity of the system (Hammersley, 1960; Hammersley & Handscomb, 1964; Rubinstein, 2008). Its accuracy can be easily adjusted with the adequate number of model simulations. Also, this method is not affected by the number of involved input variables, which is beneficial in large models. In this approach, the failure probability in 5.1 can be rewritten as

$$P_F = \int I_F(X) f_x(X) dx \tag{5.3}$$

where the indicator function $I_F(X)$ is a Boolean description of the system state

$$I_F(X) = \begin{cases} 0 & \text{system is safe,} \\ 1 & \text{system failed.} \end{cases} \tag{5.4}$$

The Monte Carlo simulation performs random sampling and conducts a large number of model calculations (N). In each sampling process, the possible values of the input random variables $X = (x_1, x_2, ..., x_k)$ are generated according to their distributions. System outputs corresponding to the different sets of random parameters are calculated. Then, the system state is evaluated through the performance function of G_x. With a number of model evaluations, a set of samples of output variable Y are available to estimates the characteristics of the system output. The failure probability can be regarded as an expectation value of $I_F(X)$. Accordingly, the P_F is estimated by the fraction of the number of samples that lead to failure, therefore

$$\hat{P_F} = \frac{1}{N} \sum (I_F(X)) = \frac{N_f}{N}, \tag{5.5}$$

where N_f is the number of samples that derive the performance function as $G_x \leq 0$. Hereafter, the estimated value for the failure probability ($\hat{P_F}$) is denoted by P_F, as well.

The required number of samples (N) to achieve a given accuracy is inversely proportional to the failure probability (Au & Beck, 2001). The accuracy of the failure probability estimated by Monte Carlo simulation can be assessed by the following equation proposed by Ang & Tang (2007)

$$C\hat{O}V_F = \sqrt{\frac{1-P_F}{NP_F}} \approx \frac{1}{\sqrt{NP_F}}, \tag{5.6}$$

where $C\hat{O}V_F$ is the coefficient of variation of the estimated P_F. Smaller values of COV_F point out more accuracy in the estimation. Based on Eq. 5.6, the required computation time for a given COV_F, can be calculated as

$$N \approx \frac{1}{COV_F^2.P_F} \quad \Rightarrow \quad t_{MC} \approx \frac{t_0}{COV_F^2.P_F}, \tag{5.7}$$

where t_0 is the required time for a single model evaluation. Hence, in spite of being computationally robust and applicable for complex models, it is computationally expensive for reliability analysis, because the higher the reliability is, the larger the number of needed simulations (i.e., a large value for N). In other words, small failure probabilities corresponding to rare samples which lead to failure (very small hatched area in Fig. 5.1). Thereupon, conducting a reliability analysis in such cases requires many samples and model evaluations before such a rare failure sample happens. Variance reduction schemes as importance sampling (Shinozuka, 1983) or subset simulation are developed to subject this issue.

On the other hand, Monte Carlo simulation can be impractical when the simulation model is expensive to execute (i.e. t_0 is large). Utilising approximation methods as it has been introduced in Sec. 4.8 and methods as AFOSM and SORM which uses Taylor series expansion to provide a rough estimate of the first two statistical moments (mean value and variance) of the system response, can address this issue (Au & Wang, 2014).

5.2.1 Subset Simulation

As mentioned previously, the number of the numerical simulation runs required to achieve a given probability of failure (P_F) is proportional to $1/P_F$. Hence for a small failure probability, a huge number of numerical simulations is needed. Subset simulation is an advanced Monte Carlo simulation method that combines the conditional probability and the Markov chain Monte Carlo (MCMC) method to calculate small values of probabilities

by a few number of deterministic model executions. This methodology was developed by Au & Beck (2001). The subset simulation method is based on a simple idea that the failure probability of a rare event can be represented as the product of some more likely conditional failure probabilities. Different steps of conducting the subset simulation method, presented by Au & Wang (2014), are illustrated in Fig. 5.4.

The efficiency of the subset simulation method in estimating small failure probabilities with much less computational effort made it a widely used method in engineering reliability analysis (for instance see Au & Beck (2003*b*,*a*); Schuëller & Pradlwarter (2007); Hsu & Ching (2010); Mahmoudi, Khaledi, König & Schanz (2016)). Ahmed & Soubra (2012*a*) combined the SS approach with the Collocation-based Stochastic Response Surface Method to provide information about the probability density function of the system response and the contribution of each uncertain input parameter in the variability of this response. Also, Li et al. (2015) developed the generalised Subset Simulation approach to estimate the failure probabilities of multiple stochastic responses using a single run of Subset Simulation. Ching et al. (2005) and Katafygiotis & Cheung (2007) also proposed different variants of the subset simulation.

Consider a failure event F defined by the condition $G_x \leq 0$, where G_x is the performance function, and let $s_1, ..., s_m, ..., s_Z$ be a sample of Z realisations of a vector s, where s is composed of k random variables. In the subset simulation method, the space of uncertain parameters is divided into l levels with an equal number of Z_s realisations $(s_1, ..., s_m, ..., s_{Z_s})$ in each level. A sequence of nested failure regions $F_1, ..., F_j, ..., F_l$ of decreasing size are defined where $F_1 \supset ... \supset F_j \supset ... \supset F_l = F$. An intermediate failure region, F_j can be defined by $G < y_j$, where y_j is an intermediate failure threshold whose value is larger than zero. Thus, there is a decreasing sequence of positive failure thresholds $y_1, ..., y_j, ..., y_l$ corresponding to $F_1, ..., F_j, ..., F_l$, respectively. It should be noted that, $y_1 > ... > y_j > ... > y_l = 0$. An intermediate level, j contains a safe region and a failure region defined on a given failure threshold y_j. The failure probability corresponding to the intermediate level of j is calculated by

$$P(F_{j+1}|F_j) = \frac{1}{Z_s} \sum_{m=1}^{Z_s} \mathbf{I}_{Fj}(s_m), \tag{5.8}$$

here $\mathbf{I}_{F_j}(s_m) : \mathbb{R}^n \rightarrow [0,1]$ is an indicator function, which is equal to one if the system output, related to the vector of s_m, is located in the failure region with respect to F_j, otherwise $\mathbf{I}_{F_j}(s_m) = 0$. The first Z_s realisations are generated using the Monte Carlo simulation methodology according to a target PDF.

The concept of the subset simulation approach is schematically illustrated stepwise in Fig. 5.3 for the case of a bi-dimensional problem. Filled symbols with the same colour represent safe samples in each conditional levels, and the others are located in the failure zone, which are used as seeds to generate the samples of the next level. In order to compute the failure probability in this study, a prescribed conditional failure probability $P(F_{j+1}|F_j)$ is considered for all levels and y_j in each level is evaluated, separately. In the following, the values of performance functions for each sample are calculated and sorted in ascending order. Subsequently, the ratio between the number of realisations for which $G < y_j$ and the number of samples Z_s is equal to the prescribed value of the conditional failure probability, y_j will be the intermediate threshold (Ahmed & Soubra, 2012*b*). In other words, y_j is equal to the value of the prescribed value of n^{th} component in the ascending order,

$$n = (P(F_{j+1}|F_j)Z_s) + 1. \tag{5.9}$$

In the next step, the parameter sets corresponding to those $Z_s \times P(F_{j+1}|F_j)$ realisations, which are located in the failure zone of F_j, are used as seeds in MCMC analysis. Seeds generate Z_s new samples for the next level of subset simulation. This procedure to generate new levels of intermediate failure regions is repeated up to reaching $y_j \leq 0$.

The failure probability of the failure region F, denoted as P_F, is calculated from the sequence of conditional failure probabilities

$$P_F = P(F_1) \prod_{j=1}^{l-1} P(F_{j+1}|F_j), \tag{5.10}$$

where l is the number of levels required to reach the limit state surface.

5.2.2 Modified Metropolis-Hastings

The Markov chain Monte Carlo methodology generates efficient random samples according to an arbitrarily given probability distribution. This method has been utilised in statistical estimation problems, like Bayesian system identification or rare events simulations. One of the well-known algorithms to carry out the MCMC methodology is Metropolis-Hastings (Metropolis et al., 1953; Hastings, 1970). This algorithm proceeds by generating new sequences of the Markov chain from a proposal distribution conditional ($q(.|\mathbf{x}^{(h)})$) on the current samples $\mathbf{x}^{(h)}$. Then, it accepts or rejects these new samples with a certain acceptance probability which is based on the current and the proposed state. Fig. 5.5 shows the steps of a modified Metropolis-Hastings algorithm, suggested by Santoso et al.

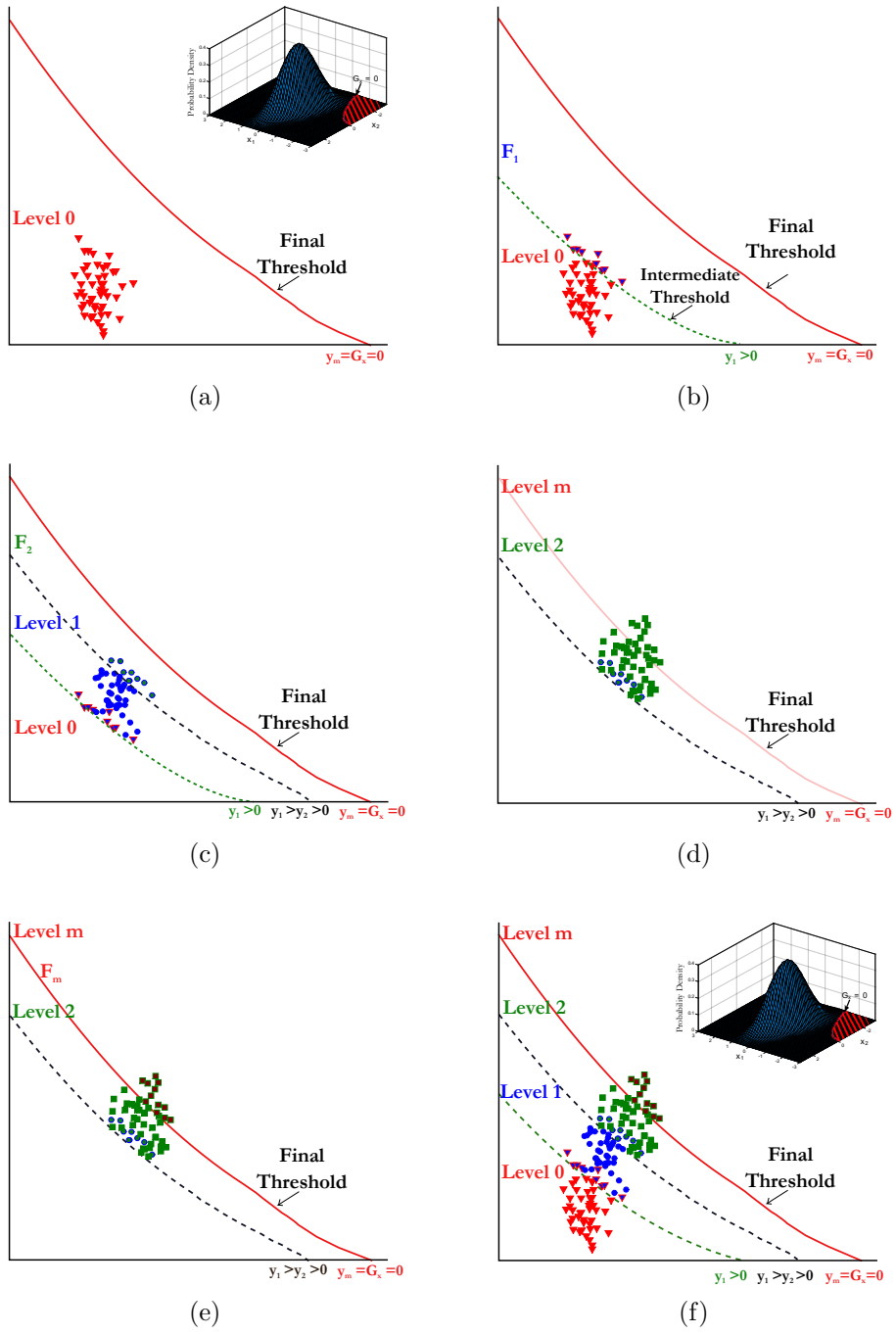

Figure 5.3: Illustration of the main steps of subset simulation approach

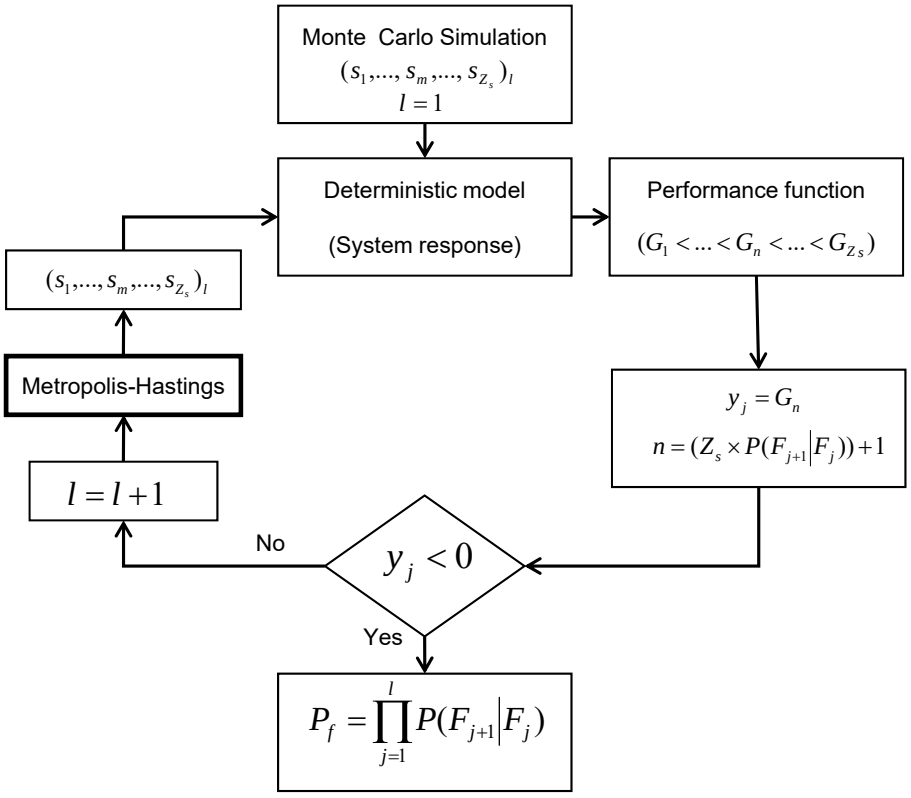

Figure 5.4: Flowchart of subset simulation method

(2011). In order to obtain the next sample $\mathbf{x}^{(h+1)}$ from $\mathbf{x}^{(h)}$, a candidate sample $\mathbf{x}^{(*)}$ from a proposal PDF is generated, firstly. Then, factor B is calculated,

$$B = \frac{P(\mathbf{x}^{(*)})q(\mathbf{x}^{(h)}|\mathbf{x}^{(*)})}{P(\mathbf{x}^{(h)})q(\mathbf{x}^{(*)}|\mathbf{x}^{(h)})}. \tag{5.11}$$

If $B \leq 1$, then $\mathbf{x}^{(h+1)} = \mathbf{x}^{(*)}$, otherwise the first step is repeated to generate a new candidate. Afterwards, $G(\mathbf{x}^{(h+1)})$, i.e., the performance function for $\mathbf{x}^{(h+1)}$ is evaluated. In case $G(\mathbf{x}^{(h+1)}) < y_j$, which means $\mathbf{x}^{(h+1)}$ is located in the domain F_j, $\mathbf{x}^{(*)}$ is accepted as the new sample. Otherwise, $\mathbf{x}^{(*)}$ is rejected and $\mathbf{x}^{(h+1)} = \mathbf{x}^{(h)}$.

According to the suggestion made by Santoso et al. (2011), in this study, the target probability distribution is assumed to be Gaussian, and the proposal PDF was chosen to be uniform.

5.2.3 Error Assessment

In this section, the formulas that assess the error associated with the subset simulation probability estimation is presented. As in many other error assessment techniques, here the coefficient of variation is regarded as the error measure. COV_{P_F} depends on the correlation among the MCMC samples within a given level. In this thesis, the following approach which was introduced by Au & Wang (2014) is employed.

For the level i it is denoted by COV_{F_i} and given by

$$COV_{F_i} = \sqrt{\frac{1 - P_c}{P_c Z_s}(1 + \kappa_i)}, \quad P_c = P(F_{j+1}|F_j), \tag{5.12}$$

where κ_i indicates the correlation among the MCMC samples at the level i.

$$\kappa_i = 2 \sum_{k=1}^{Z_{sc}-1} (1 - \frac{k}{Z_{sc}})\rho_i(k) \quad \forall i = 2, ..., l, \tag{5.13}$$

here $Z_{sc} = Z_s/Z_c$. It is assumed that at each intermediate level, $Z_c = P_c Z_s$ a Markov chain is developed, each having Z_s/Z_c samples. It should be noted that the value of $\kappa_1 = 0$, and the error for the first level should be calculated based on the formulation of the COV of the Direct Monte Carlo in Eq. 5.6 (Ang & Tang, 2007).

Here, ρ_i is the correlation coefficient of samples along a chain at k steps, where $\mathbf{I}_{F_i}(\theta_{j,k}^{(i)}) : k = 1, ..., Z_t/Z_c$, and $\theta_{j,k}^{(i)}$ denotes the k^{th} sample along the chain started from the j^{th} seed

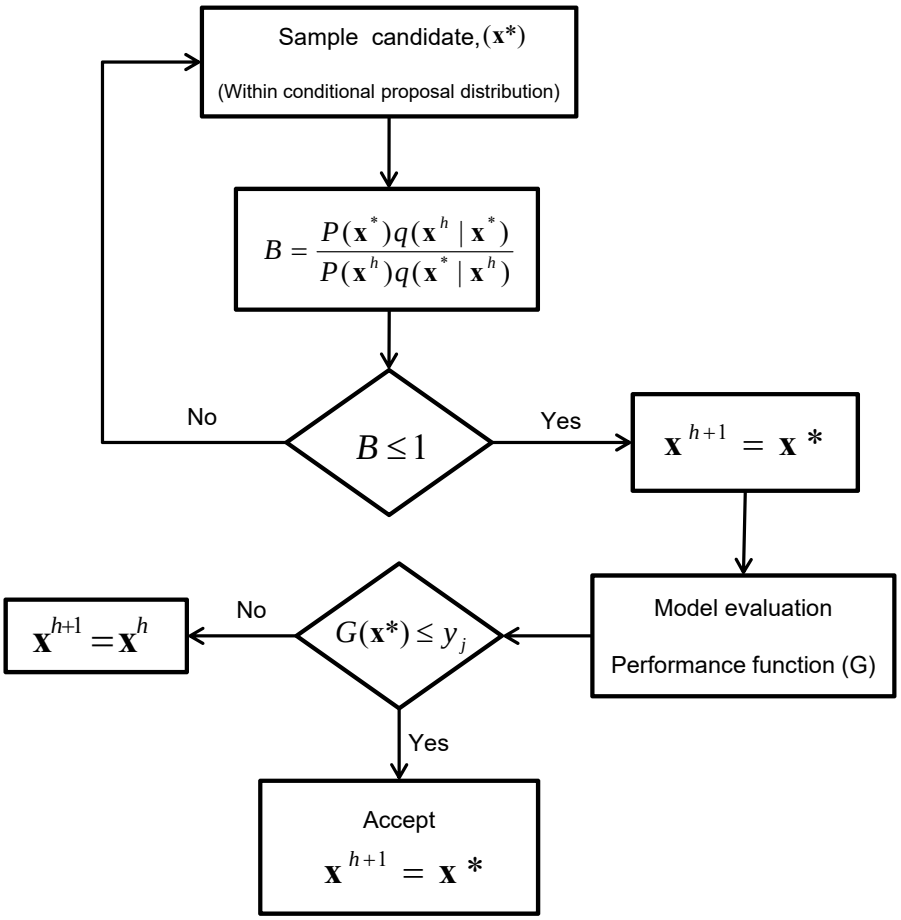

Figure 5.5: Work flow of the modified Metropolis-Hastings sampling method

at the i^{th} simulation level (Au & Beck, 2003a).

$$\rho_i(k) \approx \frac{1}{P_c(1-P_c)} \left[\frac{1}{Z_c(Z_{sc}-k)} \left[\sum_{j=1}^{Z_c} \sum_{r=1}^{Z_{sc}-k} \mathbf{I}(G_{j,r}^{(i)} < 0)\mathbf{I}(G_{j,r+k}^{(i)} < 0) \right] - P_c^2 \right] \tag{5.14}$$

Therefore, one can evaluate the coefficient of variation of the probability failure value using,

$$COV_{P_F} = \sum_{i=1}^{l} COV_{F_i} \tag{5.15}$$

The scaling of the COV_{P_F} with small P_F has significant impacts on the applicability of the method to rare events. For crude Monte Carlo, $COV_{P_F} \propto P_f^{-1}$ for small P_F and so it grows drastically when a very small P_F is expected.

In the following section, this value will be utilised in the finite element computational model of a rock salt cavity presented in Sec. 3.2 to assess the sufficient number of model evaluation in each level.

5.3 Numerical example

In the following, results of conducting reliability analysis on the typical rock salt cavern described in Sec. 3.4, considering an elasto-viscoplastic creep model in Sec. 2.3 is presented.

5.3.1 Uncertainty propagation

After introducing the governing constitutive model presented in Sec. 2.3, the distribution of the associated uncertainties for each input parameter should be described. The probabilistic modelling of geotechnical parameters is usually carried out by taking into account the uncertainties of material properties using random variables or random fields modelling. In this chapter, the quantity of the constitutive parameters is considered to be constant within the entire rock media which is regarded as homogeneous host rock. This assumption can be justified by this fact that salt dome formations include a very little amount of impurities, and can be assumed nearly homogeneous. Accordingly, the existence of any heterogeneity or spatial correlations is neglected. The uncertain input parameters which are modelled as random variables are characterised by their statistical moments, the mean value and standard deviation, besides their probability density functions.

Since there is not enough information available about the variability of these constitutive parameters, three different probabilistic scenarios, optimistic, neutral and pessimistic are defined to represent different possible circumstances. In the optimistic scenario, the construction site is assumed to be well-known, which could be because of the high number of in-situ and laboratory experiments carried out. In the neutral scenario, we assume that there is an acceptable amount of explorations and experimental tests about the target site. While for the pessimistic scenario the variation of the parameters is assumed to be higher than the previous scenarios, because of a lack of test and observation data.

The minimum internal pressure, which has a key role in the mechanical stability of the rock salt cavern, may vary due to imperfections in operating and monitoring facilities and heat transfer between the rock and gas, among other factors. Therefore, the reliability-based design approach is utilised to quantify its reliable value in the long-term loading protocol.

In the case of long-term loading, in which the internal pressure is considered as the main variation parameter, various scenarios of uncertainty can be linked to the equipments' accuracy level that controls the internal pressure. All the regarded independent uncertain parameters are assumed to vary according to their statistical moments, which are provided in Table. 5.1. The uncertainties of these parameters are modelled by normal probability density functions distribution. The minimum and maximum values of the uncertain parameters are chosen based on previous experiences (Hansen et al., 1984; Desai & Zhang, 1987; Sane et al., 2008; Guo et al., 2012) and engineering judgement. The values corresponding to the Maxwell dashpot coefficient are chosen based on Heusermann et al. (2003) and Hou (2003).

5.4 Non-deterministic analysis

As mentioned previously in Sec. 3.6.1, the deviatoric stress, which can be induced by different internal pressures and in-situ stresses of the rock around the cavities, leads to creep deformation. A low internal pressure value may cause dilatancy. Because of dilation, the mechanical properties of the host rock can change drastically, which may initiate microcracks. In some cases, a widened microcrack network by dilatancy may cause leakage of the stored product in the cavity. Thereupon, those internal pressures leading the stress state to locate above the C/D line (namely dilatant zone) can be considered as unsafe states. Hence, the C/D line is considered as a failure criterion.

$$G_s = DF_u - DF_p, \tag{5.16}$$

Table 5.1: Uncertainty representation of the input parameters

Parameter	Description	Dimension	Mean	COV(%)		
				Pessimistic	Neutral	Optimistic
E	Elastic modulus	MPa	22000	20	15	10
ν	Poisson Ratio	[-]	0.27	10	5	5
n	Transition parameter	[-]	3	20	15	5
N	Flow exponent	[-]	3	15	15	5
μ	Fluidity parameter	s^{-1}	2.5e-12	15	10	5
a_1	Hardening parameter	$MPa^{(2-n)}$	0.2e-4	15	10	5
κ	Ultimate parameter	[-]	0.0975	15	10	5
η	Hardening parameter	[-]	0.8	20	10	5
$\overline{\eta_M^*}$	Maxwell coefficient	MPa s	2e12	15	15	10
P_i	Internal pressure	MPa	5.5	20	10	5

where G_s is the performance function related to the dilation criterion, DF_u is the allowable value in the system, and DF_p is the response of the system. As mentioned before, the cavern's volume loss is also considered as a probable failure mode, and hence, this failure mode is presented by the performance function G_v

$$G_v = VL_u - VL_p. \tag{5.17}$$

The prescribed tolerable volume convergence in this failure mode is presented by VL_u, and the amount of volume loss due to the applied parameters is given by VL_p. In addition, another performance function as G_l for the minimum internal pressure is defined as

$$G_l = \frac{P_u}{P_p} - 1, \tag{5.18}$$

here, G_l and P_u are the performance function of the internal load and the admissible minimum internal load, which may not cause dilation in the cavern vicinity. P_p is the amount of the imposed internal pressure. The variability of the system responses, as a result of the uncertain input variables, is described by assigning the probability density functions. To accomplish this, the probability distribution of the system response is evaluated by investigating the related probability density functions.

For instance, Figs. 5.6a to 5.6d present the PDFs of the value of DF for three different scenarios of parameters' value expectation, for the nodes N_2, N_3, N_4, and N_5 in Fig. 3.11, respectively. As an example, the probability density functions of the obtained DF values

which represents the no-dilation criteria are illustrated in Fig.5.6c for point N_4, when the internal load is considered as the variable in the long-term loading protocol.

Fig. 5.6 emphasises that, varying the dispersion of the input parameters, which is applied in the present work by three different probabilistic scenarios changes the dispersion of the model responses, significantly. This means that having good knowledge about the involved input variables such as those considered in the optimistic scenario, makes the PDF of the model output narrower (i.e., the variation in the system response becomes less). Investigating the generated PDFs of the *DF* for all observation points around the cavern demonstrates that less safety margin against the dilation exists at the points located at the bottom of the cavern. Also, Fig. 3.16 has already shown that the biggest values of *DF* occur in this region, which can be attributed to the high value of the induced deviatoric stress. For this respect, hereafter, merely the failure probability of point N_4 is investigated. In the following, the failure probability of the system versus the failure criteria defined in Sec. 3.6.1 is calculated. The failure is defined as the exceeding of a response quantity Y over threshold y_t, where the limit state surface is determined as $G_x = y_t - Y$. Hence, the failure probability $P(F) = P(Y > y_t)$ can be demonstrated as the value of the Complementary Cumulative Distribution Function (CCDF) of Y at y_t. In each failure mode, different allowable thresholds are defined, and the relevant P_F is calculated using samples from the input space of the uncertain constitutive parameters presented in Sec. 2.3.

Estimation of failure probability is done by the subset simulation technique. The required number of model evaluations in each level is determined in the following sections. Also, a comparative study is conducted in order to verify the obtained outcomes by subset simulation.

5.4.1 Sufficient number of model evaluation

As we consider the intermediate failure $P(F_{j+1}|F_j)$ amount in all intermediate levels to be the same, the corresponding intermediate thresholds depend on the generated conditional samples and vary in different runs. To ensure that the variations in the sample sets make no significant differences in the obtained value of P_F, the coefficient of variation of the probability failure value, COV_{P_F} (see Eq.5.7) can be a proper measure. COV_{P_F} may estimate that how accurate is the conducted analysis. For more details about the procedure of evaluating COV_{P_F}, see Au & Beck (2001).

In order to obtain the optimal number of required sample sizes, different Z_s are applied to calculate the probability of failure, and for each case, the COV_{P_F} is computed. Fig. 5.7

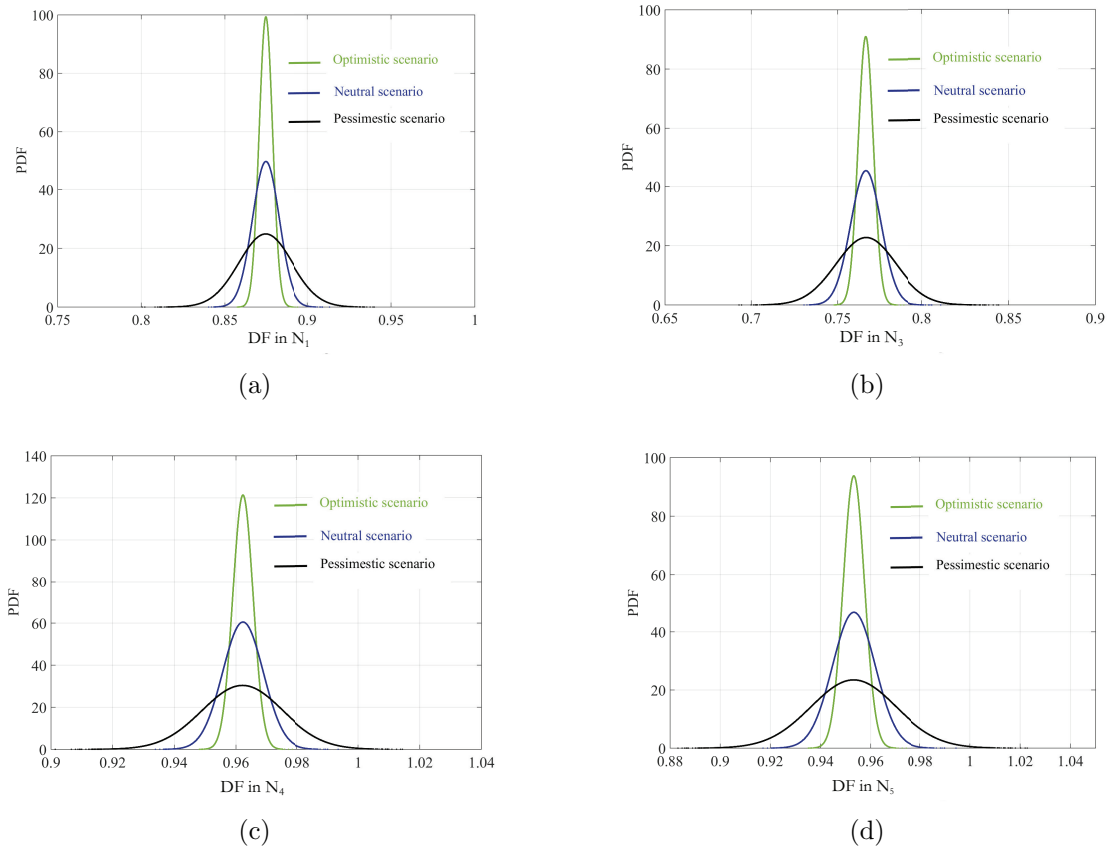

Figure 5.6: Probability density function of *DF* around the cavern (long-term loading protocol)

represents the considered number of realisations in each level of the subset simulation versus its corresponding COV_{P_F}. It demonstrates the dependency of the coefficient of variation of P_F on the number of samples. Based on this figure, raising Z_s from 1000 to 4000 makes no meaningful change in the COV_{P_F}, thereupon, the number of samples per level in the present study is chosen to be equal to 1000.

5.4.2 Validation by comparing with Monte Carlo simulation method

The efficiency of the subset simulation methodology is examined by comparing its results with the estimated P_Fs using a Monte Carlo-based analysis. The failure probability of the rock salt cavern's vicinity, considering no-dilation criteria, is calculated by conducting both methodologies. The comparison here is conducted for a point located on the bottom of the cavern, and the failure probability is computed against several prescribed DoU_u. Fig. 5.8 illustrates the obtained results, while in the Monte Carlo-based approach 100,000 samples are used. In the subset simulation method, the corresponding P_F is estimated by generating samples through three levels of intermediate failure probabilities. Thereupon, the final P_Fs are calculated by subset simulation using 3,000 realisations. These results show that, although the computational burden required in the subset simulation approach is significantly less compared to the Monte Carlo simulation, the differences between the obtained P_Fs are negligible.

5.5 Reliability-based design

The CCDF can be used directly for estimating the failure probability that the solution-mined cavity simulation exceeds for a specified threshold. The obtained CCDFs for three probabilistic scenarios are illustrated in Fig. 5.9. This figure shows the probability of failure as functions of the DF thresholds for the cyclic loading protocol.

The P_F of the long-term loading protocol, which considers the minimum internal pressure of the cavern as the only input variable, is calculated by the same procedure as explained above. In this protocol, the serviceability of the system is regarded as the limit state by evaluating the volume convergence value. The obtained results presented in Fig. 5.10 demonstrate that by applying different COVs, i.e., different uncertainty variations, the value of P_F changes enormously. In other words, the minimum values of the failure probability against different failure criteria are observed in the optimistic scenario.

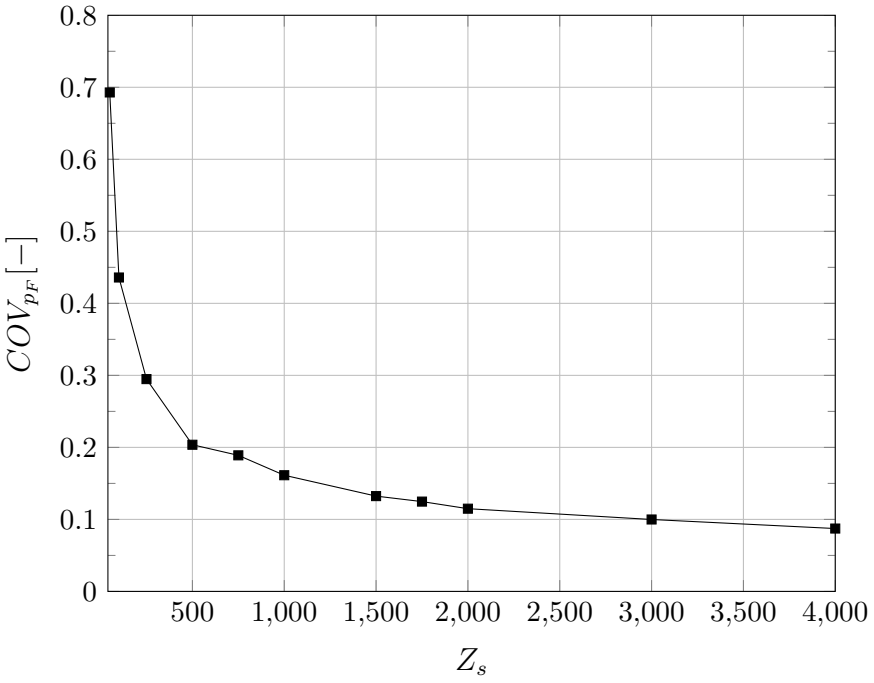

Figure 5.7: Coefficient of variation of failure probability versus the number of samples generated per level

Later, the forward simulation model introduced in Sec. 3.4 is used to estimate the minimum allowable internal pressure of the cavern for a prescribed set of constitutive parameters. The minimum allowable pressure is evaluated in a manner, such that in the first minimum pressure step of loading after the debrining phase, any stress state in the cavern's vicinity corresponds to $DF > 1$. Subsequently, the failure probability of the rock salt cavern is evaluated. P_F versus the minimum allowable pressure inside the cavern is drawn in Fig 5.11 as a function of the thresholds using samples of the uncertain constitutive parameters.

After determining the P_F, one can compute the proper value of the regarded input variable to satisfy a prescribed level of safety based on reliability analysis approaches, such as AFOSM. In design codes, the tolerable safety levels are categorised based on the probable consequences of a failure event. These categories are quantified by the reliability index values. Reliability index or safety index is denoted as β_r

$$\beta_r = -\Phi^{-1}(P_F), \tag{5.19}$$

here, $\Phi(.)$ represents the standard normal cumulative distribution function. For instance, *Eurocode* 7 considers the value of β_r to be equal to 3.8 for structures with moderate conse-

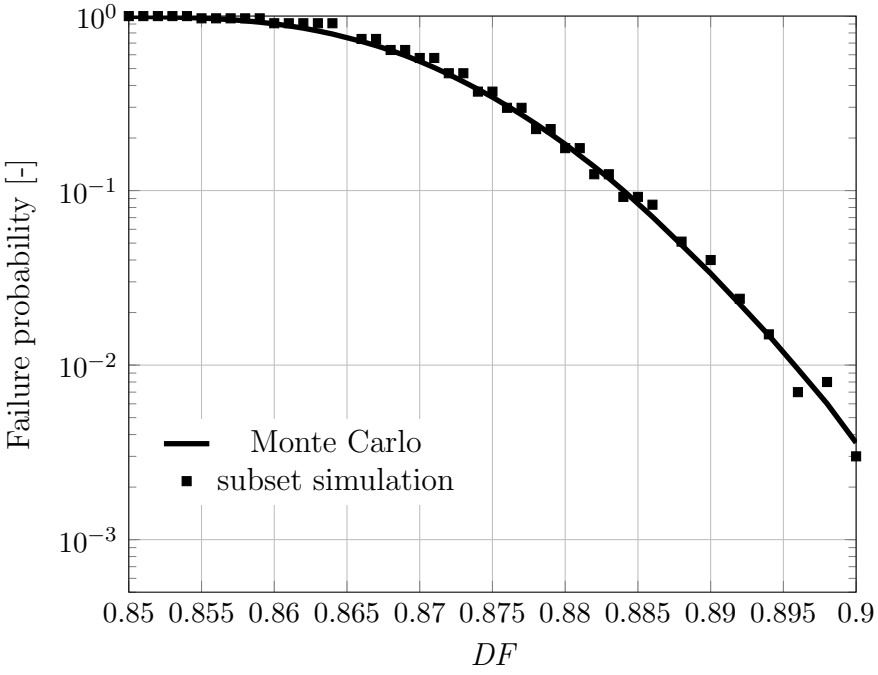

Figure 5.8: Comparison between the obtained CCDF computed by applying Monte Carlo simulation and subset simulation in Point N_5

quences in the case of failure (Phoon, 2008). Therefore, the moderate safety corresponds to a failure probability of $7.2348e-05$. This value is used to determine the appropriate minimum internal pressure as demonstrated in Fig. 5.11. For instance, as shown in Fig. 5.11 in the optimistic scenario, the applied pressure in a cavity with the prescribed geometry in Sec. 3.4, may not be less than 6.08 MPa. Otherwise, dilatancy may take place around the cavern. This approach can be applied to the other probabilistic scenarios as well, which leads to higher values for the safe minimum pressure, e.g. even to more than 7 MPa in the pessimistic scenario. Tab. 5.2 presents the obtained results for each probabilistic scenario. Moreover, Tab. 5.2 displays the minimum admissible internal pressure for different assumption for the levels of failure consequences. All the regarded reliability indices are chosen as proposed in *Eurocode* 7.

5.6 Conclusion

In this chapter, the stability and serviceability of the rock salt cavern have been explored considering different failure criteria, namely limited volume convergence and no dilatant zone. The probabilistic analyses are utilised to describe the involved uncertainties in ma-

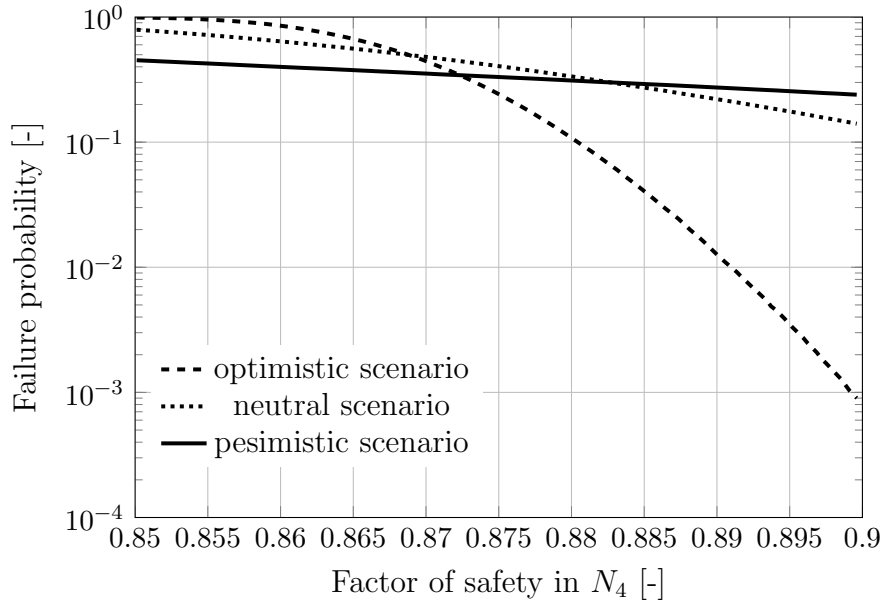

(a)

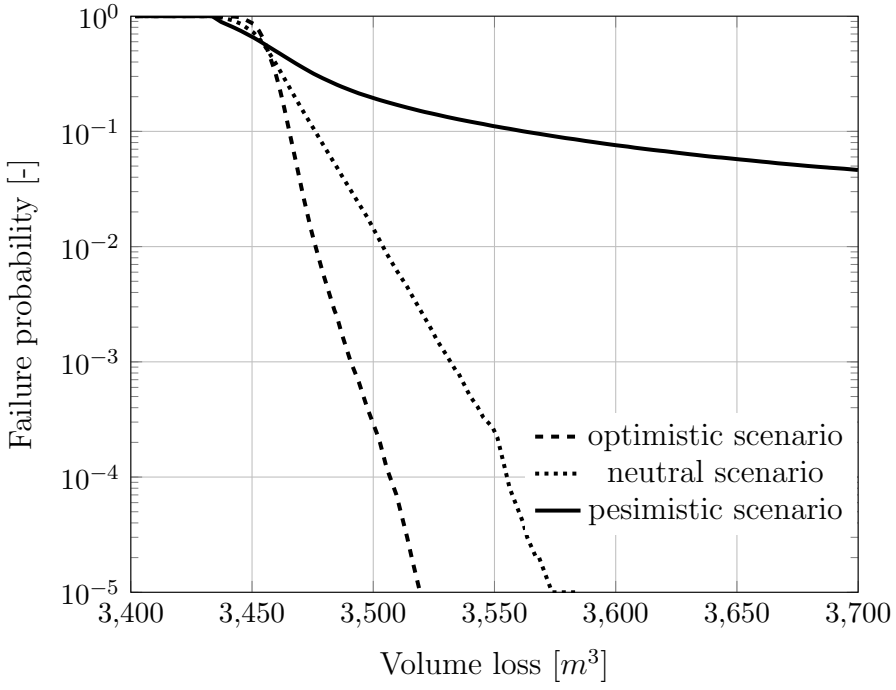

(b)

Figure 5.9: CCDF plotted in a logarithmic scale against a range of admissible thresholds (cyclic loading protocol)

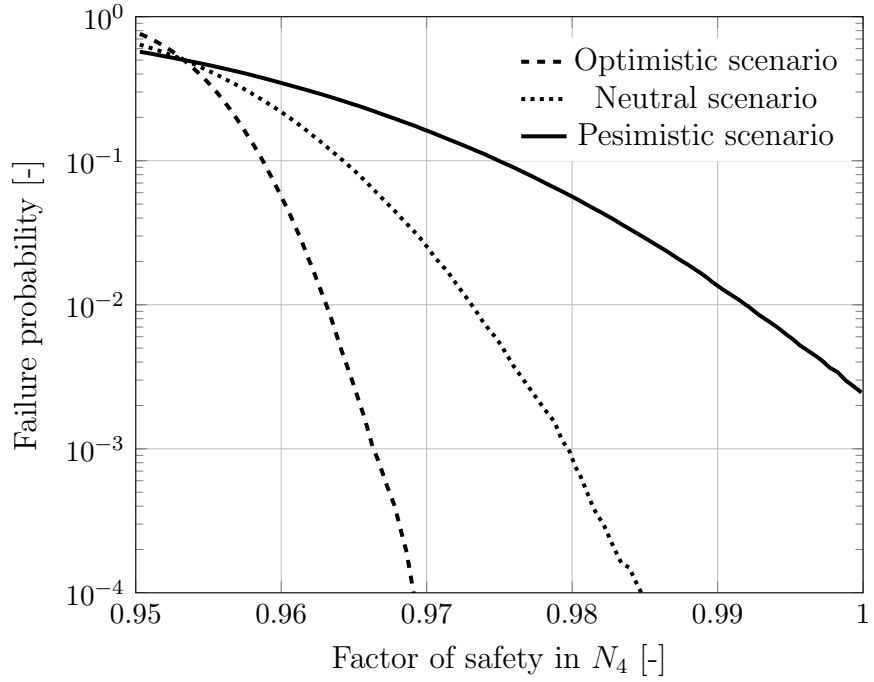

(a)

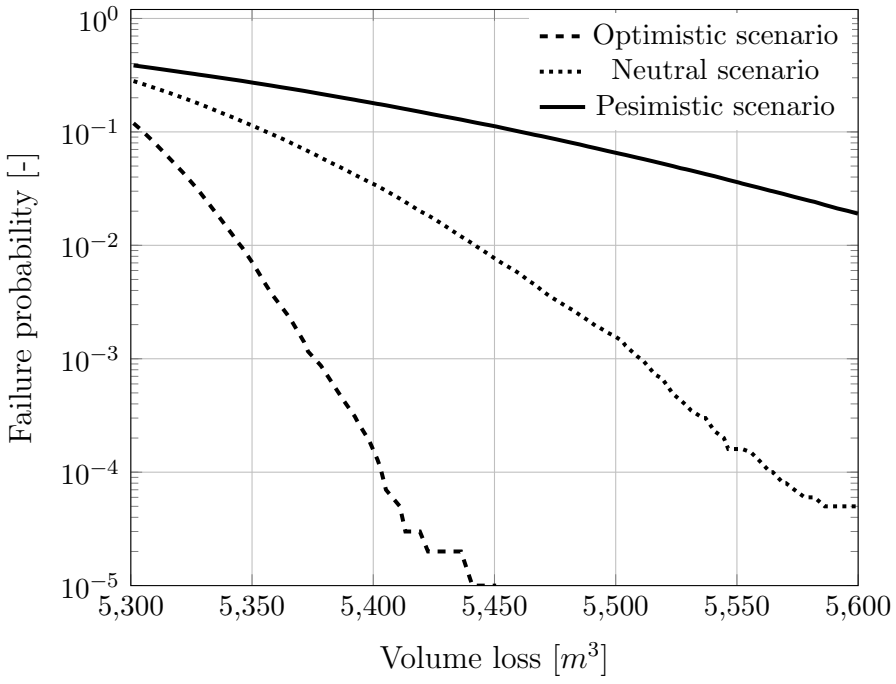

(b)

Figure 5.10: The obtained CCDF due to long-term loading protocol plotted in a logarithmic scale against a range of admissible thresholds

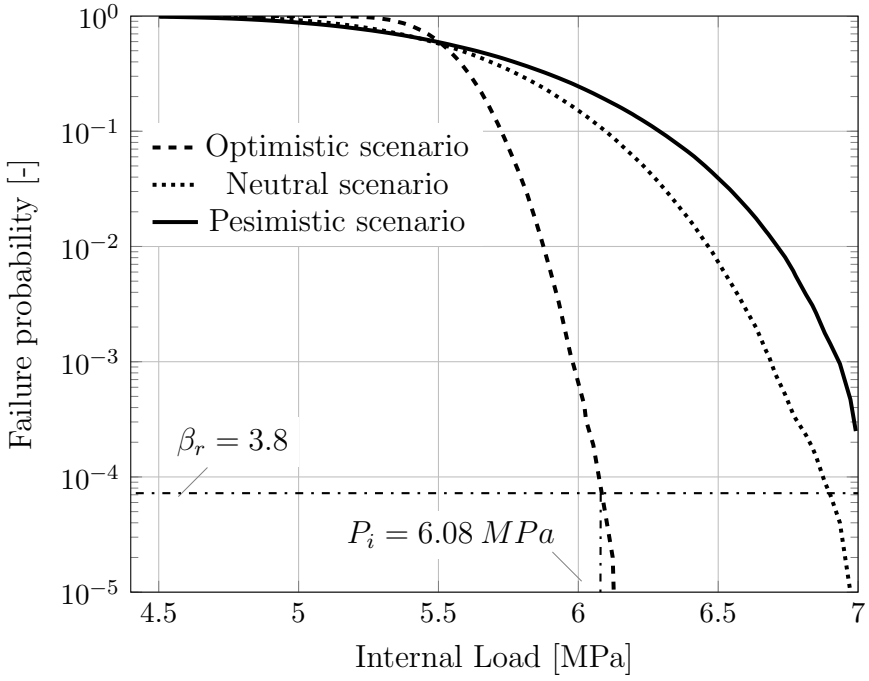

Figure 5.11: Failure probability against dilatancy versus the internal pressure of cavern

Table 5.2: Obtained reliability index β_r in different probabilistic scenarios

Consequence of failure	β_r	P_F	min. admissible P_i [MPa]		
			Pessimistic	Neutral	Optimistic
small	1.3	0.0968	5.72	4.83	6.29
some	2.3	0.01072	5.87	6.46	6.7
moderate	3.1	9.676e-4	5.96	6.69	6.93
great	3.8	7.235e-05	6.08	6.9	>7

terial properties of the rock salt and evaluate the impacts of their propagation. Their relevant uncertainties have been considered by three scenarios, using different coefficients of variation. This chapter also presents a computationally affordable reliability analysis method, called as subset simulation. Subset simulation can address small probabilities encountered in the practical reliability assessment of the complex systems while analysing their reliability with classical Monte Carlo-based methods is computationally expensive. A modified Metropolis-Hastings approach is employed to generate adaptive samples in a sequence of failure regions. Afterwards, the efficiency and accuracy of the subset simulation were justified by conducting a comparative calculation. Since the minimum internal pressure of the rock salt cavern governs the safety level of the system against dilatancy, the minimal allowable internal pressure has been evaluated to assure that no area around the cavern experiences dilatancy. Moreover, a reliability-based design approach has been

employed to identify the acceptable minimum internal pressure of the cavern when considering the uncertainty of the constitutive parameters. It should be noted that this case study is a synthetic one, nevertheless, the proposed method can be applied analogously to realistic problems.

6 Random field Analysis

6.1 Introduction

A clear picture of the rock salt characteristics may only appear by gathering different information sources as laboratory analyses, geotechnical in-situ measurements, and on-site observations. In practice, for such particular structures which are extended vertically downwards more than hundred meters from the ground level, only limited experimental and in-situ data is available. On the other hand, the inherent randomness of natural materials as rocks causes a wide extent of spatial distribution in their physical properties. Considering these facts, the measure of involved uncertainties in the rock salt properties cannot be neglected. Hence, a reliable design procedure cannot rely merely on deterministic approaches. In order to provide an adequately accurate computational model, stochastic analysis approaches must be utilized, as well. It should be pointed that a stratigraphic unit may consist of several different homogeneous zones. The graphs provided by Bräuer et al. (2011); Bornemann et al. (2008), which are derived from creep tests on two different shafts in Gorleben salt dome (north-east of Germany), indicate the existing of vertical heterogeneity in creep behaviour of this site (see Figs. 6.1 & 6.2). The present study considered a one-dimensional (vertical) spatially random field. Bräuer et al. (2011) shows that creep behaviour is significantly correlated with stratigraphic, fabric properties and tectonics.

Despite other geotechnical fields of study where the stochastic analyses are well established (e.g. Phoon (2008); Baecher & Christian (2005)), there are rare studies that investigate the involved uncertainties in the geotechnical design of rock salt cavities as Roberts, McCullough, Buchholz & DeVries (2015) and Mahmoudi et al. (2017). In the latter one, a probabilistic analysis on a compressed air rock salt cavity was performed, using the subset simulation methodology as a modern Monte Carlo approach. In that study, the involved input parameters were considered as the random variables, and the defined uncertainty measure applied to the entire medium and the spatial randomness was neglected.

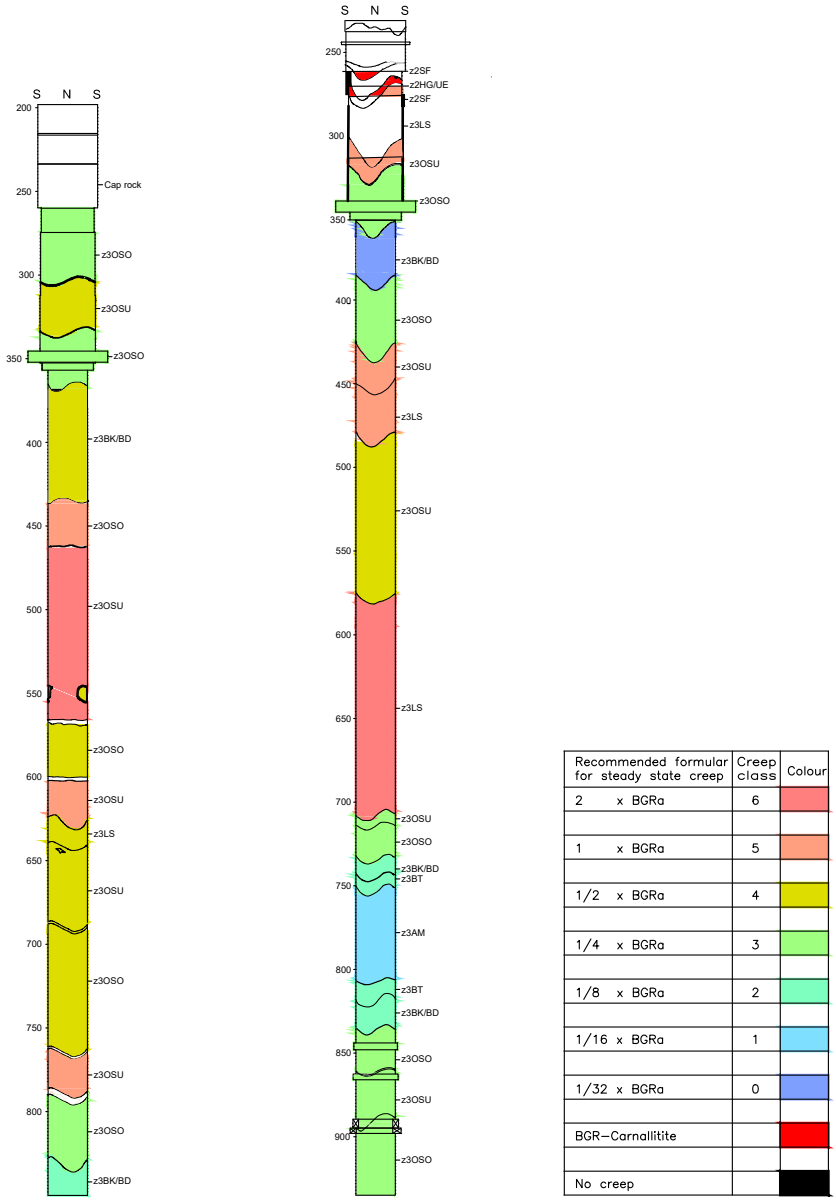

(a)

Figure 6.1: Assignment of homogeneous zones in shaft 1 (left) and 2 (right) (Bräuer et al., 2011)

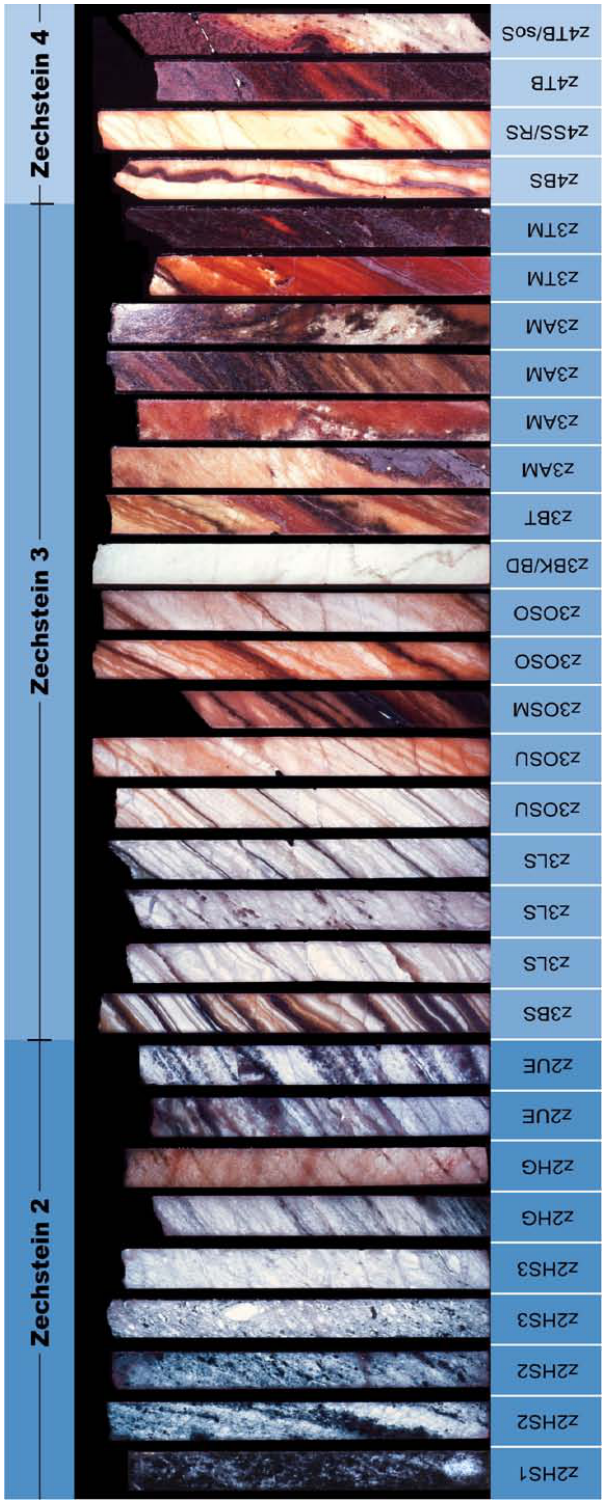

Figure 6.2: Lithological standard profile of the Gorleben salt dome (Bornemann et al., 2008)

To represent the real spatial variability of a field variable, a significant amount of information must be gathered from the field, which is an expensive or even infeasible project. Also, if not enough amount of data is gathered then the parameter identification and design process can be inaccurate. In this regard, a probabilistic analysis concept may be employed to minimise sampling costs while it is still being able to provide informative data. For this, random fields are appropriate as models of the spatially distributed uncertainty and they can be utilised to produce probability measures regarding design criteria (Griffiths & Fenton, 2007). In the random field models, the characteristics of the spatial distribution of mechanical parameters are simulated as functions of spatial location. In general, the main attribute of a random field representation is the concept of statistical dependence between input values in the spatial field. Applications of stochastic finite element analysis have been initiated in the 1970s (Kiureghian & Ke, 1988). A random field is defined by its mean and variance which may be spatially constant, or vary as a function of location to depict the degree of variation in the field. Moreover, the correlation arrangement in the random field is an important feature.

Various random field generator algorithms are available in the literature, which are shortly reviewed in Sec. 6.2. Among the others, the series expansion methods can approximate the random field by a finite sum of products of deterministic spatial functions and random variables. In this dissertation, the Karhunen-Loève expansion as a series expansion method, introduced in Sec. 6.3, is applied to generate random field realisations.

In the following, a typical natural gas rock salt cavern is simulated by finite element method. Within the numerical model, the rock salt behaviour is described by BGRa constitutive model (Hunsche & Hampel, 1999), a well-known creep model. In Sec. 6.4 the numerical model, boundary and loading conditions are presented. Sec. 6.5 presents the probabilistic analysis of the considered cavity mined in spatially varying rock salt. The effect of the uncertainties in the input parameters on the system responses is inquired by carrying out a global sensitivity analysis. In the present thesis, Sobol's method (Sobol', 1993) as a variance-based sensitivity technique is employed. After ranking the importance level of parameters, random field discretisation applied on the most governing one. In the following, the failure probability of the system considering dilatant behaviour is evaluated. At the end, a parametric study is conducted to investigate the effect of variations in the assumed auto-correlation lengths. The obtained results are concluded in Sec. 6.6.

6.2 Random field discretisation

Because of the differences of mineral ingredients, stress history, and other geological factors, constitutive parameters of rocks or soils show spatial differences and correlations as well. The characteristics of the spatial distribution of constitutive parameters can be simulated as a geological parameter field which exhibits spatial variability. Many studies has been applied different random field methodologies on civil and particularly geotechnical problems, among the others one may mention the work of Schweiger & Peschl (2005), where a slope stability analysis is performed taking into account spatial variability and using random field theory. Also, Griffiths et al. (2012) used random field, Monte-Carlo simulations and finite element concepts to evaluate the influence of porosity and void size on the probability of excessive settlement.

In general, a random field is characterised by its mean, variance, and its correlation structure. One of the major features of a random field representation of a material is the concept of statistical dependence between field values at different points, which is known as the correlation structure (Sudret & Der Kiureghian, 2000). The correlation coefficient between two points x_1 and x_2, $\rho(x_1, x_2)$ is decreasing gradually as the distance is increasing. On the other hand, when the distance between two realisation points approaches to zero, the material characteristics are identical. It should be pointed out that higher order moments of random field can also represent its characteristics, but due to difficulties in estimating them, random field models are often represented by information about the three mentioned measures. To accomplish this, firstly a relatively simple joint PDF (e.g., multivariate normal or lognormal distributions) for the field should be adopted. The correlation structure is often assumed to be a simple function of the distance between points.

A continuous random field $H(x, \psi)$ can be defined as a random function that describes a random quantity at each point $x \in \Omega$ of a continuous domain $\Omega \subset \mathbb{R}^n$. $\psi \in \Psi$ is a coordinate in the sample space Ψ. Hence, $H(x_0, \psi)$ denotes the random variable associated with point x_0, and $H(x, \psi_0)$ indicates ψ_0 realisation of the field. As mentioned before, a random field can be defined by its mean $\mu(x)$, variance $\sigma^2(x)$ and auto-correlation coefficient function that is

$$\rho(x_1, x_2) = \frac{C_H[H(x_1), H(x_2)]}{\sigma(x_1)\sigma(x_2)}, \tag{6.1}$$

where $C_H(.,.)$ is the auto-covariance function. A random field can be discretized by approximating $H(.)$ by $\hat{H}(.)$, described by means of a finite set of random variables $\{\chi_i,$

i = 1,...,n }

$$\hat{H}(x) \xrightarrow{\text{Discretisation}} \hat{H}(x) = F[x, \chi]. \tag{6.2}$$

Sudret & Der Kiureghian (2000) classified the most commonly used methods of random field discretisation into following main groups ,

- Point Discretisation

  In this group of methods, the random variables χ_i are selected values of $H(.)$ at specific points in a given spatial discretisation (e.g., mesh in finite/difference element methods). As example one can name the midpoint method, introduced by Kiureghian & Ke (1988) where the random field is approximated in each element by a single random variable at the centre of that element. The Shape Function method introduced by Liu & Kiureghian (1986), and the Optimal Linear Estimation method developed by Li & Kiureghian (1993) also can be classified in this category. The other members of this group are integration point method which is presented in Brenner & Bucher (1995).

- Average Discretisation,

  In these methods, the random variable related to a given χ_i is calculated as the weighted integrals of $H(.)$ over a domain Ω_e

  $$\chi_i = \int_{\Omega_e} H(x)\omega(x)d\Omega. \tag{6.3}$$

  For instance, Spatial average method proposed by Vanmarcke & Grigoriu (1983) evaluate the random variable related to a given element of the finite element/finite difference deterministic mesh as the average of random fields over that element. The weighted integral method developed by Deodatis (1990) can also be classified in this group. Besides, one can mention the Local Average Subdivision method Fenton & Vanmarcke (1990) as a commonly used method in geotechnical engineering.

- Series Expansion methods

  In the series expansion discretisation methods, the random field is approximated by an expansion that involves deterministic and stochastic functions. The value of the random field is calculated on the basis of the coordinates of the point in deterministic functions. In these techniques, the field is represented as a series involving random variables and deterministic spatial functions. As examples of this group of methods, one can mention the Expansion Optimal Linear estimation method. A comparative review on the above mentioned methods was provided in Li & Kiureghian (1993), Al-Bittar & Soubra (2013) employed this method (a.k.a.

EOLE) in a geotechnical application. As commonly used series expansion method, one can mention Orthogonal Series Expansion method Ellingwood (1994) and the Karhunen-Loève expansion method. The Karhunen-Loève is utilised in the present study to discretize the random field and it is briefly described in the following.

6.3 Karhunen-Loéve expansion

We consider $H(x,\psi)$ as random process, when H denotes the expected value of the random field. The random field can be calculated by the Karhunen-Loéve expansion as follows

$$\hat{H}(x,\psi) = \mu_H + \sum_{i=1}^{\infty} \sqrt{\lambda_i}\phi_i(x)\xi_i(\psi), \tag{6.4}$$

where λ_i and ϕ_i are the eigenvalues and eigenfunctions of the auto-covariance function, respectively. $\xi_i(\psi)$ is a vector of standard uncorrelated random variables. μ_H is the mean function of the field. It should be noticed here that $\xi_i(\psi) : \Psi \to \mathbb{R}$ are the stochastic variables that represent the random nature of the uncertain parameter. For practical purposes, the expansion in Eq. 6.4 can be truncated to a given number of terms, M as follows

$$\hat{H}(x,\psi) \approx \mu_H(x) + \sum_{i=1}^{M} \sqrt{\lambda_i}\phi_i(x)\xi_i(\psi), \tag{6.5}$$

where M is the size of the series expansion. However, the eigenvalues and eigenfunctions λ_i and ϕ_i are the deterministic functions of the Karhunen-Loève expansion. They can be evaluated as the solution of the following Fredholm integral equation:

$$\int_{\Omega} C_H[H(x_1), H(x_2)]\phi_i(x_2)dx_2 = \lambda_i\phi_i(x_1). \tag{6.6}$$

For an one-dimensional Gaussian random field generated in the interval $[-a, a]$, the exponential covariance function is defined as below,

$$C_H[H(x_1), H(x_2)] = \sigma exp(-\frac{x_1 - x_2}{l_x}), \tag{6.7}$$

where, σ is the standard deviation of the random field, l_x shows the vertical autocorrelation length. Ghanem & Spanos (1991) presented the detailed analytical solution of the integral

in Eq. 6.6 for an exponential auto-covariance function. In this approach,

$$\lambda_i = \frac{2(\frac{1}{l_x})}{\omega_i^2 + \frac{1}{l_x}}, \tag{6.8}$$

and,

$$\begin{cases} \phi_i(x) = \frac{cos(\omega_i x)}{\sqrt{a + \frac{sin(2\omega_i a)}{2\omega_i}}} & \text{for } i \text{ odd}, \\ \phi_i(x) = \frac{sin(\omega_i x)}{\sqrt{a - \frac{sin(2\omega_i a)}{2\omega_i}}} & \text{for } i \text{ even}. \end{cases} \tag{6.9}$$

Huang et al. (2001) studied the convergence of this approach for different covariance functions using polynomials (Betz et al., 2014). The choice of the number M of terms depends on the required accuracy of the considered problem. Sudret & Der Kiureghian (2000) proposed the following error estimate ($err(x)$) after truncating the expansion to M terms,

$$err(x) = \sigma_H^2 - \sum_{i=1}^{M} \lambda_i \phi_i^2(x), \tag{6.10}$$

where σ_H is the standard deviation of the random field. Finally, notice that in most geotechnical problems, the random fields are assumed to follow a log-normal PDF. This assumption can be adjusted by the fact that a soil parameter cannot take a negative value. Thereupon, for an exponential random field, $\log(H)$ is a normal random field with mean value μ_{logH} and standard deviation σ_H given as follows:

$$\mu_{\log H} = \log(\frac{\mu_H^2}{\sqrt{\sigma^2 + \mu^2}}) \tag{6.11}$$

$$\sigma_{\log_H} = \sqrt{\log(1 + COV^2)} \tag{6.12}$$

$$\hat{H}(x, \psi) \approx exp[\mu_{\ln E} + \sum_{i=1}^{M} \sqrt{\lambda_i} \phi_i(x) \xi_i(\psi)] \tag{6.13}$$

6.4 Deterministic model of a rock salt cavern

Within this chapter, a gas cavern with the capacity of 368,000 m^3 is simulated by an axisymmetrical numerical model, its casing shoe is assumed to be located in the depth of 400 m. The shape of the cavern after excavation is idealised as a cylinder with the height of 150 m and 60 m diameter. The floor and roof of the cavern are considered as

semi-spheres with 30 m radius. Fig. 6.3a shows the geometry and boundary conditions of this cavity in detail. The considered mesh discretisation is also shown in Fig. 6.3b. The uniform load at the top of the model substitutes the overburden weight. In order to model the solution mining procedure, the entire excavation phase is simplified by reducing the internal pressure of the cavern to the minimum gas pressure (First discharge phase) in a time interval of 300 days. In this study, the minimum inner pressure of the cavity is assumed to be equal to 4 MPa. In our simulation, the temperature of intact rock salt is assumed to be equal to 50 °C. The thermal boundary condition of the wall of the cavity is decreased during the discharge phase to 30 °C (for more details about the variation of thermal condition see Khaledi, Mahmoudi, Datcheva & Schanz (2016*a*)).

In this study, the creep behaviour of the rock salt is modelled on the basis of the BGRa constitutive model (see Sec. 2). The mechanical stability of storage cavities is the most important issue which should be assured in an accurate geotechnical design. Therefore, the dilatant zones which can be initiated by a specific stress state in rock salt should be avoided. The dilatancy boundary, which is defined by the beginning of the irreversible volumetric expansion, can be considered as a criterion which divides the stress space into compression and dilatancy regions. As mentioned in chapter 2 dilatancy boundary, known as compression/dilation (C/D) boundary can be identified on the basis of experimental data (for more details about different C/D boundaries, the reader is referred to Mahmoudi et al. (2015*a*)). In the present chapter, Desai C/D boundary Desai & Zhang (1987) is used as no dilation criterion. In order to determine whether a region in the simulated rock salt cavity encountered dilatancy or not. In this regard, the quantity of DF defined in 6.3 is employed.

$$DF = \sqrt{\frac{J_2}{J_2^{dil}(I_1)}}. \tag{6.14}$$

where $J_2^{dil}(I_1)$ denotes the second stress invariant of C/D boundary corresponding with the value of first invariant (I_1) in each observation point. When $DF < 1$, the stresses are inside the compressibility domain and opening of micro-cracks does not occur and subsequently, damage does not progress. In contrary, when $DF \geq 1$, the cavern may experience long-time failure due to the damage progress.

In the next step, the finite element numerical simulation of the typical cavern is conducted. Although in real cases the designer must assure that no-dilatant region around the entire cavern will take place, here, the considered observation points are limited. The level of one-third of cavern's height from its bottom is generally treated as a benchmark region

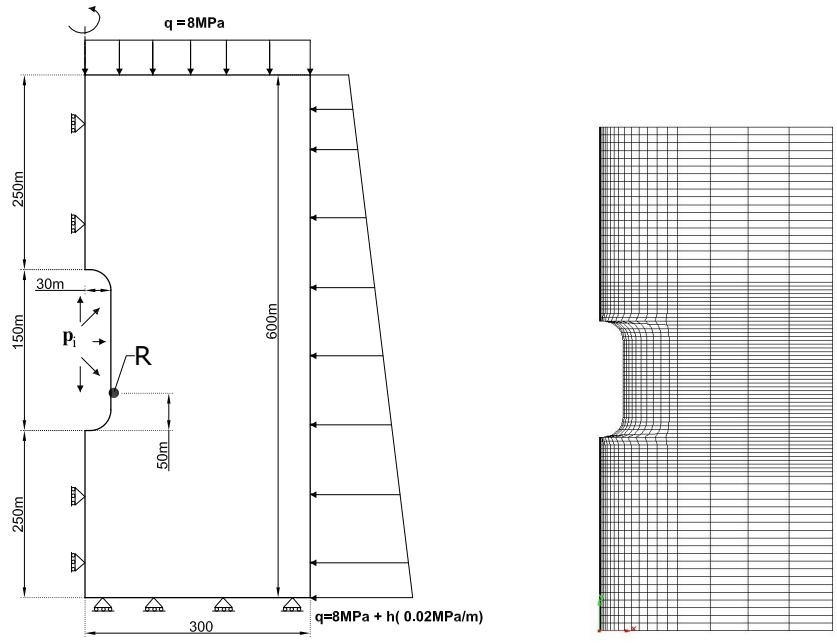

(a) (b)

Figure 6.3: (a) Representative geometry and boundary conditions of the salt cavern model and (b) Finite element mesh discretisation

in measurements and numerical simulations as well. Hence, in this study the DF factor is evaluated in the region of R, illustrated in Fig. 6.3a.

It should be stated that the method of the Karhunen-Loève can cope with domains of arbitrary geometric mesh, different from the FEM mesh. However, the size of a given element in the deterministic mesh depends on the auto-correlation distances of the rock properties. Kiureghian & Ke (1988) suggested that the length of the largest element of the deterministic mesh should not be less than half of the auto-correlation distance in that direction. In order to respect this criterion, the geometrical model is vertically divided to 65layers, with a specific random value assigned to each layer (with 10meter thickness).

6.5 Probabilistic results

Before generating the random field, the most important input parameter which makes the largest contribution to the variation of model response is identified by conducting a global sensitivity analysis. The variance-based technique for evaluating the sensitivity indices of input parameters is proposed by Sobol' (1993). In this thesis, Sobol's method (as a Monte Carlo based implementation) is utilised to evaluate the sensitivity measures of different

constitutive parameters (see Sec. 4.6). It should be mentioned that the sensitivity analysis is conducted on a random variable homogeneous model. Tab. 6.1 represents the considered range of variation for each input variable. All the input variables follow a lognormal probability distribution function. Fig. 6.4 depicts the evaluated total-effect sensitivity index (S_{Ti}) for each constitutive parameter. The most influential input parameter on the stress-state of the cavern's wall against dilation is u. Hence, all parameters but u are fixed to their mean values, and the variable of u is discretised as a random field. The mean value and coefficient of variation of parameter u are respectively $\mu = 4$ and $COV = 10\%$, and follows a lognormal probability density function. Fig. 6.5 shows a typical random field realisations of the variable u for two different auto-correlation distances. For larger values of auto-correlation distances, the model tends to a homogeneous field, while less auto-correlation lengths limit the correlations in a given simulation to smaller zones. In general, for a specific auto-correlation length, layers which are very close together tend to have similar u values and express a higher correlation.

As mentioned earlier, the size of the Karhunen-Loève expansion M will effect on the accuracy of the approximated random field $\hat{H}$. Fig. 6.6a depicts the estimated error of random field approximation versus the assumed M value for different auto-correlation lengths. The error estimation converges to less than 5%, if $M \geq 200$. In this study, M is assumed to be equal to 200 terms to ensure the accuracy level of random field approximation.

The crude Monte Carlo simulation is a well-established methodology to evaluate the probability of failure which has been used for many decades. As conducting a Monte Carlo simulation requires thousands of model evaluation and each run of the numerical model in this study takes more than two hours, employing Monte Carlo seems not feasible. In order to address this drawback, the subset simulation technique, introduced previously in **Chapter 5** is employed.

The probability analysis here is conducted for the region R in Fig. 6.3a and the failure probability for different auto-correlation lengths (l_y) is computed against $DF = 1$. Fig. 6.6b illustrates the obtained results. In addition to different spatial variability scenarios, we also conduct a homogeneous simulation, where the constitutive parameters are assumed to be random variables. As Fig. 6.6b illustrates, with decreasing the auto-correlation length in random field discretisation, the probability of encountering a dilatant region at the considered observation point increases. Although in real cases, a local dilatant zone may not mainly endanger the stability of the entire structure, but in our case, we considered the no-dilatant region as the failure criterion, which is conservative.

Table 6.1: Parameters' value of BGRa constitutive model

Elastic Parameters		Creep Parameters			Thermal Properties
E [GPa]	ν [-]	A [s^{-1}]	u [-]	Q [kJ/mol]	α_t [1/ °C]
[19 - 3]	[0.25 - 0.35]	[0.1e-5 - 0.5e-5]	[3 - 5]	[40000 - 70000]	[3e-5 - 5.5e-5]

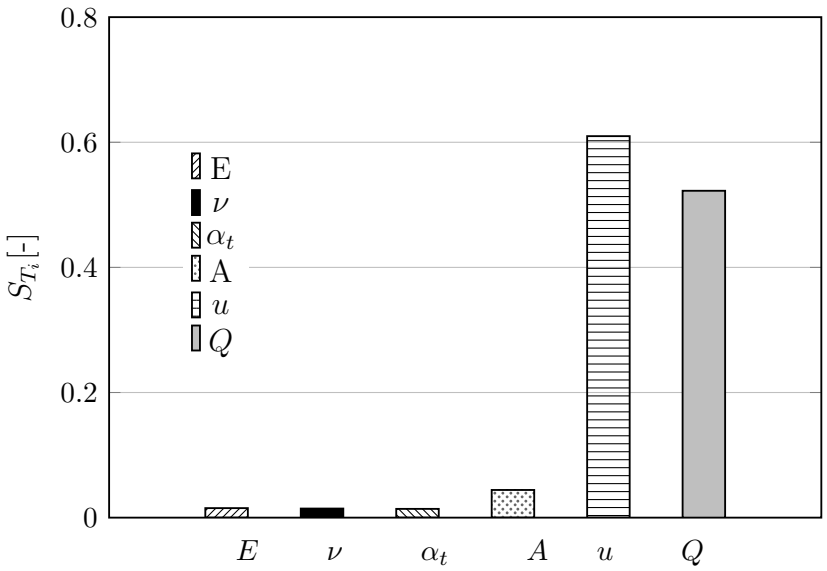

Figure 6.4: Estimation of total effect sensitivity index S_{Ti}, regarding FS

6.6 Conclusion

The inherent randomness of natural materials like rocks and soils causes a wide extent of spatial distribution in their physical properties. Thereupon, the spatial variability and consequently the induced uncertainty, have to be considered in the complex geotechnical problems. In this thesis, the random field method is applied in a probabilistic analysis of a gas storage cavern in the rock salt. A random field discretisation of constitutive parameters of the BGRa creep law using Karhunen-Loéve is conducted. The failure probability of a rock salt cavity against the no-dilatant criterion is calculated for different spatial variability scenarios to present the effect of the auto-correlation lengths on the safety measures of the system against dilation. The obtained failure probabilities are compared with the corresponding results considering homogeneous rock in a random variable analysis. The comparison represents the necessity of considering spatial variability in the material properties.

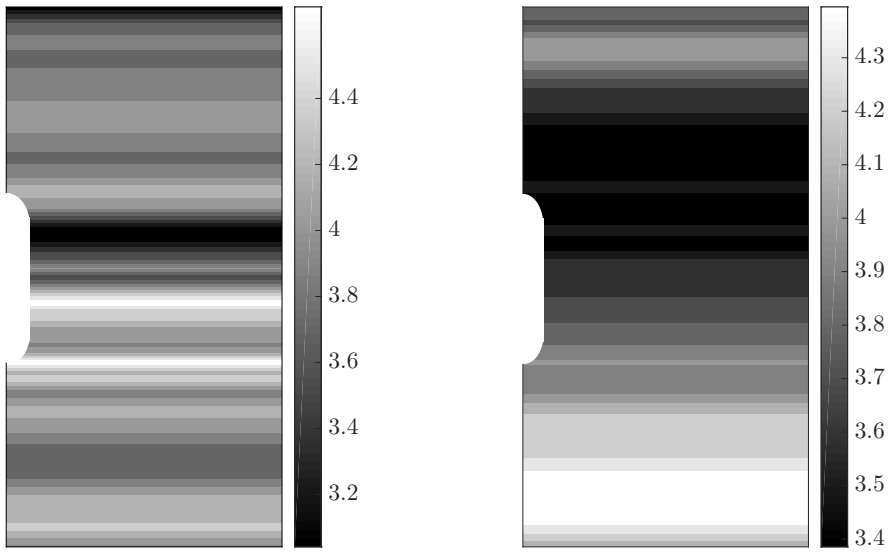

(a) (b)

Figure 6.5: Random field realisations of the parameter u for auto-correlation distance (a) l_y=30 m (b) l_y=650 m

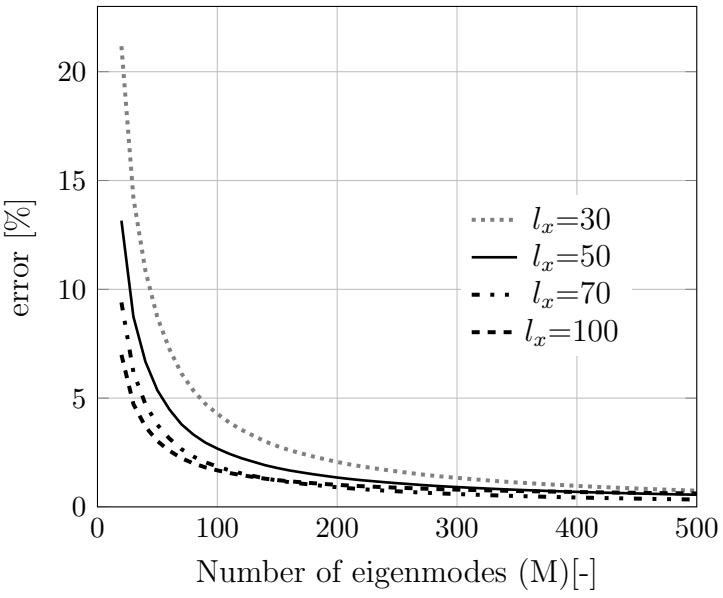

(a)

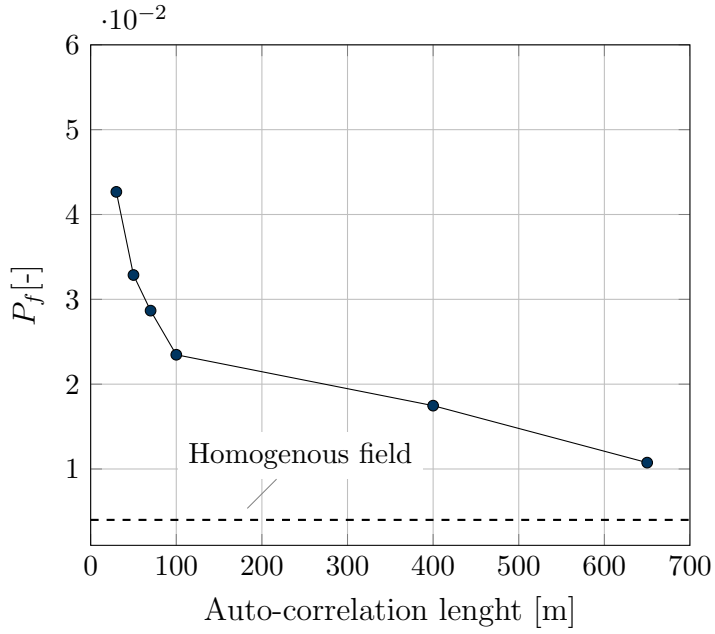

(b)

Figure 6.6: a) Error estimation vs. number of eigenmodes for different values of auto-correlation lengths, b) Probability of failure against dilatancy for different auto-correlation lengths

7 Conclusions and Future Work

Nowadays, the energy community undergoes a major transmission time from fossil/nuclear fuels to renewable energy sources. Thereupon, due to the fluctuating nature of the produced electrical energy, it should be stored in rock salt caverns for short and long terms to balance out the energy generation and consumption, within CAES or hydrogen storage projects. Due to the daily or weekly charge and withdrawal cycles of pressurised gas, the surrounding rock salt undergoes cyclic loading. The present thesis proposed an iterative study that consists of experimental investigation, constitutive, and numerical modelling to provide a precise analysis of the complicated stress strain behaviour of rock salt under this loading condition. In particular, this dissertation intends to study the rock salt behaviour under such loading conditions through a numerical study. Furthermore, it considers the effects of the corresponding uncertainty in the modelling procedure as well.

Analogous to most geotechnical engineering concepts, a numerical analysis is conducted to evaluate the behaviour of rock salt cavities. In this regard, the excavation and different operation scenarios are simulated using the finite element analysis approach. A study has been carried out to find the impact of different depths of location on the behaviour of the cavity. The obtained results may provide the designer a pre-assumption for the proper depth based on the intended function for the cavern. Furthermore, the finite element analysis revealed that the excavation procedure significantly changes the stress state of the rock salt and it has to be modelled to achieve a realistic response prediction. A comparative study concluded that a detailed excavation procedure including leaching debrining and first filling can be substituted with a simplified scenario, without a remarkable impact on the final stress state of the cavity's boundary at the end of the excavation phase.

Three different constitutive models have been employed to simulate the rock salt behaviour, each of them has different features to approximate the response of the rock salt. However, the realistic and comprehensive prediction of the rock salt cavity behaviour, obtained from a deterministic simulation, depends on the accuracy level of the conducted numerical analysis. The geotechnical design procedure of a rock salt cavity like each computational simulation is associated with a level of inevitable uncertainties involved in the

input parameters. Therefore, the probabilistic approaches are utilised in order to achieve a reliable design. To accomplish this, two different types of randomness, namely, random variable and random field are considered as the source of uncertainties in the modelling. In the first one, the entire host rock is assumed as a homogeneous medium, while the latter one considers the probable heterogeneity using the random field theory. Three global sensitivity methods have been presented to identify the most effective input variables on the output uncertainty level. The corresponding uncertainty in the input variables has been introduced assuming different probabilistic scenarios. The failure probability of a typical rock salt cavity considering stability and serviceability criteria was evaluated using crude Monte Carlo simulation and subset simulation methods. In the following, the reliability-based design has been introduced to determine the safe value of the input design variables. As it has been mentioned previously, the analysed case studies are synthetic and the assumptions about their design and material parameters are made to be close to the realistic cases. Nevertheless, the proposed deterministic and non-deterministic methodologies can be applied analogously to realistic problems.

In the following, the utilised statistical tools are concluded as well as some suggestions for future studies:

7.1 Sensitivity analysis

Different sensitivity analysis methods in this thesis are employed for investigating the impacts of the geomaterials constitutive properties uncertainty on an underground structure response. Utilising the approach of sensitivity analysis, the designer may perform both quantitative and qualitative investigations on the parameters which have the greatest effects on the system output variation as well as its reliability. The various aspects of different methods are described and compared to each other. Furthermore, a primitive criterion was proposed to choose the most proper sensitivity analysis method based on the model features like complexity, the number of input parameters, and the required calculation effort.

7.2 Probabilistic analysis

In the following, the mechanical stability of a typical rock salt cavern in an underground renewable energy storage facility has been investigated in the framework of a probabilistic study. To describe the long-term behaviour of rock salt under cyclic and static loading, an

elasto-viscoplastic creep constitutive law has been introduced. Furthermore, the stability and serviceability of the rock salt cavern are investigated. In this context, the constitutive parameters have been represented as random variables with predefined PDF, mean, and standard deviation. The relevant uncertainties of the governing parameters have been proposed within three probabilistic scenarios. In order to compute the failure probability of the system, the classical Monte Carlo-based method as well as the subset simulation approach, with a considerably less computational burden are employed. A comparative analysis has justified the accuracy of the subset simulation method. Moreover, the minimal allowable internal pressure in a typical salt cavity, as a governing design parameter, has been evaluated to avoid any dilatant area around the cavern's wall.

7.3 Random field discretisation

The existing spatial scatter in host rocks is commonly disregarded in the geotechnical engineering investigations. However, based on the unavoidable observations and gathered data sets from different storage fields, this thesis studied the effects of consideration of this aspect of uncertainty as well. Spatial variations in the geomaterials can be represented in the design procedure using the random field concept. As a vigorous statistical tool, it draws inferences from in-situ investigations and tests to describe the spatial variability of the site and incorporates it to the reliability design concept. The main focus of this chapter is on the random field discretisation in a probabilistic analysis of a rock salt gas storage cavity. The Karhunen-Loève expansion has been introduced to generate the random field and the subset simulation methodology was utilised to facilitate the execution of the Monte Carlo method. Based on the obtained results, taking into account the heterogeneity of the rock medium leads to a remarkable difference in the reliability level of the system.

7.4 Future works

This thesis could be developed further based on the findings of this study. Further research is suggested as follows:

- Consideration of realistic geometry with non-smooth wall to enable the designer to observe the creation of any dilatant region around the convex and concave zones.
- In case of availability of real field data, the numerical simulation could be validated. Furthermore, the constitutive model's parameters could be calibrated using

further experimental measurements based on the iterative framework proposed in **Chapter 1**.

- This study mainly focused on the behaviour prediction of a single cavern, while the salt cavities are commonly excavated in a storage site including a group of them. Such a storage field should be constructed in a way to assure non-unwanted effects on the integrity and function of each individual cavity. Therefore, modelling of a group of caverns to investigate their probable interactions could be also done in the future.
- This thesis shown the results of a probabilistic analysis considering no-dilatancy and limited volume convergence criteria, while it may be extended to investigate the structure behaviour against the other criteria as no-damage as well as no-tension and limited subsidence.
- Due to the practical issues, performing measurement procedures for determining the exact geometry in the cavities are mostly limited in number. Therefore, the geometrical alterations of the cavern's shape within the operation phase can also be regarded as a source of uncertainty. One may extend this study to include the variability in the geometry of the cavern in the probabilistic analysis.
- Although the spatial variation of the rock salt properties in the vertical direction is more obvious, consideration of horizontal heterogeneity could also be interesting. It may reflect different reliability measures for the system.

Bibliography

AGEB (2016), Auswertungstabellen zur Energiebilanz Deutschland (1990 bis 2015), Technical report, Arbeitsgemeinschaft Energiebilanzen e.V.

Ahmed, A. & Soubra, A.-H. (2012*a*), 'Extension of subset simulation approach for uncertainty propagation and global sensitivity analysis', *Georisk: Assessment and Management of Risk for Engineered Systems and Geohazards* **6**, 162–176.

Ahmed, A. & Soubra, A.-H. (2012*b*), 'Extension of subset simulation approach for uncertainty propagation and global sensitivity analysis', *Georisk: Assessment and Management of Risk for Engineered Systems and Geohazards* **6**(3), 162 – 176.

Al-Bittar, T. & Soubra, A.-H. (2013), 'Bearing capacity of strip footings on spatially random soils using sparse polynomial chaos expansion', *International Journal for Numerical and Analytical Methods in Geomechanics* **37**(13), 2039–2060.

Alkan, H., Cin, Y. & Pusch, G. (2007), 'Rock salt dilatancy boundary from combined acoustic emission and triaxial compression tests', *International Journal of Rock Mechanincs and Mining Sciences* **44**, 108–119.

Allen, R. D., Doherty, T. J. & Thorns, R. (1982), Geotechnical factors and guidelines for storage of compressed air in solution mined salt cavities, Technical Report PNL-4242, UC-94e, Pacific Northwest Laboratory. Prepared for the U.S. Department of Energy under Contract DE-AC06-76RLO 1830.

Ang, A. H.-S. & Tang, W. H. (2007), *Probability Concepts in Engineering: Emphasis on Applications to Civil and Environmental Engineering*, John Wiley & Sons Inc.

Au, S. & Beck, J. (1999), 'A new adaptive importance sampling scheme for reliability calculations', *Structural Safety* **21**(2), 135 – 158.

Au, S. & Beck, J. (2003*a*), 'Important sampling in high dimensions', *Structural Safety* **25**(2), 139 – 163.

Au, S.-K. & Beck, J. L. (2001), 'Estimation of small failure probabilities in high dimensions by subset simulation', *Probabilistic Engineering Mechanics* **16**, 263–277.

Au, S. K. & Beck, J. L. (2003*b*), 'Subset simulation and its application to seismic risk based on dynamic analysis', *Journal of Engineering Mechanics* **129**(8), 901–917.

Au, S.-K. & Wang, Y. (2014), *Engineering risk assessment with subset simulation*, John Wiley & Sons Ltd.

Baecher, G. B. & Christian, J. T. (2005), *Reliability and statistics in geotechnical engineering*, John Wiley & Sons.

Bardow, A. (2008), 'Optimal experimental design of ill-posed problems: The meter approach', *Computers & Chemical Engineering* **32**, 115–124.

Bauer, S. J., Broome, S. T., Bronowski, D. R., Rinehart, A. & Ingraham, M. (2011), Experimental deformation of salt in cyclic loadinginsights from acoustic emission measurements., Technical report, Sandia National Laboratories (SNL-NM), Albuquerque, NM (United States).

Bay, C. A. (1963), Use of salt solution cavities for underground storage, *in* 'Symp. On Salt, Northern Ohio Geol Soc.', pp. 564–578.

Bérest, P. (2011), Thermomechanical aspects of high frequency cycling in salt storage caverns, *in* 'International Gas Union Research Conference, Oct 2011, Seoul, South Korea'.

Bérest, P. & Brouard, B. (2003), 'Safety of salt caverns used for underground storage', *Oil & Gas Science and Technology* **58**, 361–384.

Bérest, P., Brouard, B., Feuga, B. & Karimi-Jafari, M. (2008), 'The 1873 collapse of the saint-maximilien panel at the varangeville salt mine', *International Journal of Rock Mechanics and Mining Sciences* **45**(7), 1025 – 1043.

Berést, P., Brouard, B., Hertz, E., Lheur, C., Hévin, G., d. Laguérie, P. & Hardy, J. (2013), Cavern abandonment: three in situ tests, *in* 'SMRI conference, Avignon, France', pp. 1–13.

Bérest, P., Brouard, B., Karimi-Jafari, M. & Sambeek, L. V. (2007), 'Transient behavior of salt caverns, interpretation of mechanical integrity tests', *International Journal of Rock Mechanics and Mining Sciences* **44**(5), 767 – 786.

Berést, P., Djizanne, H., Brouard, B. & Hévin, G. (2013), Effects of a rapid depressurization in a salt cavern, *in* X.-T. Feng, J. A. Hudson & F. Tan, eds, 'Rock Characterisation, Modelling and Engineering Design Methods', CRC Press, pp. 653–658.

Betz, W., Papaioannou, I. & Straub, D. (2014), 'Numerical methods for the discretization of random fields by means of the karhunen-loève expansion', *Computer Methods in Applied Mechanics and Engineering* **271**, 109 – 129.

Bolzon, G. & Buljak, V. (2011), 'An effective computational tool for parametric studies and identification problems in materials mechanics', *Comput Mech* **48**, 657–687.

Bornemann, O., J., B., R., F., J., H., W., J., S., K., G., M. & M., S. (2008), *Results of the geological surface and underground exploration of the salt formation*, Description of the Gorleben site, Bundesanstalt für Geowissenschaften und Rohstoffe.

Boucly, P. (1982), 'Expérience in situ et modélisation du comportement des cavités salines utilisées pour le stockage de gaz', *Revue française de Géotechnique* (18), 49–57.

Bräuer, V., Eickemeier, R., Eisenburger, D., Grissemann, C., Hesser, J., Heusermann, A., Kaiser, D. & Nipp, H. K. (2011), *Geotechnical Exploration of the Gorleben Salt Dome*, Description of the Gorleben site, Bundesanstalt für Geowissenschaften und Rohstoffe.

Breitung, K. (1984), 'Asymptotic approximations for multinormal integrals', *Journal of Engineering Mechanics* **110**(3), 357–366.

Breitung, K. & Hohenbichler, M. (1989), 'Asymptotic approximations for multivariate integrals with an application to multinormal probabilities', *Journal of Multivariate Analysis* **30**(1), 80 – 97.

Brenner, C. E. & Bucher, C. (1995), 'A contribution to the sfe-based reliability assessment of nonlinear structures under dynamic loading', *Probabilistic Engineering Mechanics* **10**(4), 265 – 273.

Brouard, B., Berést, P. & K. Jafari, M. (2007), Onset of tensile effective stresses in gas storage caverns, *in* 'SMRI conference, Halifax, Canada', pp. 1–16.

Bucher, C. G. (1988), 'Adaptive sampling, an iterative fast monte carlo procedure', *Structural Safety* **5**(2), 119–126.

Buljak, V. (2010), 'Proper orthogonal decomposition and radial basis functions algorithm for diagnostic procedure based on inverse analysis', *FME Transactions* **38**, 129–136.

Buljak, V. (2012), *Inverse Analysis with Model Reduction: Proper Orthogonal Decomposition in Structural Mechanics*, Springer Verlag.

Cacuci, D. G. (2003), *Sensitivity and Uncertainty Analysis, Volume 1: Theory*, CRC Press.

Campolongo, F., Cariboni, J. & Saltelli, A. (2007), 'An effective screening design for sensitivity analysis of large models', *Environmental Modelling & Software* **22**(10), 1509 – 1518. Modelling, computer-assisted simulations, and mapping of dangerous phenomena for hazard assessment.

Chan, K., Saltelli, A. & Tarantola, S. (1997), Sensitivity analysis of model output: variance-based methods make the difference, *in* 'Proceedings of the 29th conference on Winter simulation', IEEE Computer Society, pp. 261–268.

Ching, J., Au, S. & Beck, J. (2005), 'Reliability estimation for dynamical systems subject to stochastic excitation using subset simulation with splitting', *Computer Methods in Applied Mechanics and Engineering* **194**(12), 1557 – 1579. Special Issue on Computational Methods in Stochastic Mechanics and Reliability Analysis.

Cristescu, N. (1993), 'A general constitutive equation for transient and stationary creep of rock salt', *International Journal of Rock Mechanics and Mining Sciences* **30**(2), 125–139.

Cristescu, N. & Gioda, G. (1994), *Visco-Plastic Behaviour of Geomaterials*, CISM International Centre for Mechanical Sciences, Springer Vienna.

Cristescu, N. & Hunsche, U. (1998), *Time Effects in Rock Mechanics*, John Wiley & Sons Ltd.

Crotogino, F., Mohmeyer, C. & Scharf, R. (2001), More than 20 years of successful operation, *in* 'SMRI conference, Orlando, USA', pp. 1–7.

Cukier, R. I., Fortuin, C. M., Schuler, K. E., Petschek, A. G. & Schaibly, J. H. (1973), 'Study of the sensitivity of coupled reaction systems to uncertainties in rate coefficients, i theory', *Journal of Chemical Physics* **59**(8), 3873–3878.

Cukier, R. I., Schaibly, J. H. & Shuler, K. E. (1975), 'Study of the sensitivity of coupled reaction systems to uncertainties in rate coefficients. iii. analysis of the approximations', *The Journal of Chemical Physics* **63**(3), 1140–1149.

Cukier, R., Levine, H. & Shuler, K. (1978), 'Nonlinear sensitivity analysis of multiparameter model systems', *Journal of Computational Physics* **26**(1), 1–42.

Deodatis, G. (1990), 'Bounds on response variability of stochastic finite element systems', *Journal of Engineering Mechanics, ASCE* **116**(3), 565 – 585.

Desai, C. & Zhang, D. (1987), 'Viscoplastic model for geologic material with generalized flow rule', *International Journal for Numerical and Analytical Methods in Geomechanics* **11**, 603–627.

DeVries, K., Mellegard, K. & Callahan, G. (2003), Cavern design using a salt damage criterion: Proof of concept final report, *in* 'SMRI conference, Houston, USA', pp. 1–17.

Ditlevsen, O. D. & Madsen, H. O. (1996), *Structural Reliability Methods*, John Wiley & Sons Inc.

Djizanne, H., Berést, P. & Brouard, B. (2012), Tensile effective stresses in hydrocarbon storage caverns, *in* 'SMRI conference, Bremen, Germany', pp. 1–18.

Düsterloh, U., Lerche, S. & Lux, K.-H. (2013), Damage and healing properties of rock salt: long-term cyclic loading tests and numerical back analysis, *in* 'Clean Energy Systems in the Subsurface: Production, Storage and Conversion', Springer, pp. 341–362.

EIA (2015), Natural gas annual respondent query system (eia-191 data through 2015), Technical report, U.S. energy Information Administration.

Einstein, H. H. & Baecher, G. B. (1983), 'Probabilistic and statistical methods in engineering geology', *Rock Mechanics and Rock Engineering* **16**(1), 39–72.

Ellingwood, J. Z. B. (1994), 'Orthogonal series expansions of random fields in reliability analysis', *Journal of Engineering Mechanics* **120**(12), 2660–2677.

Fenton, G. A. & Vanmarcke, E. H. (1990), 'Simulation of random fields via local average subdivision', *Journal of Engineering Mechanics* **116**(8).

Fiessler, B., Neumann, H. & Rackwitz, R. (1979), 'Quadratic limit states in structural reliability', *Journal of the Engineering Mechanics Division* **105**.

Fishman, G. (1996), *Monte Carlo: Concepts, Algorithms, and Applications*, Springer-Verlag New York.

Forrester, A. I. J., Sobester, A. & Keane, A. (2008), *Engineering Design via Surrogate Modelling: A Practical Guide*, John Wiley & Sons Ltd.

Fuenkajorn, K. & Phueakphum, D. (2010), 'Effects of cyclic loading on mechanical properties of maha sarakham salt', *Engineering Geology* **112**(1), 43–52.

Ghanem, R. G. & Spanos, P. D. (1991), *Stochastic finite elements : a spectral approach*, Dover publications 2003, Mineola, New York.

Gillhaus, A. (2007), Natural gas storage in salt caverns - present status, developments and future trends in europe, *in* 'SMRI conference, Basel, Switzerland', pp. 1–18.

Griffiths, D., Paiboon, J., Huang, J. & Fenton, G. A. (2012), 'Homogenization of geomaterials containing voids by random fields and finite elements', *International Journal of Solids and Structures* **49**(14), 2006 – 2014.

Griffiths, D. V. & Fenton, G. A., eds (2007), *Probabilistic Methods in Geotechnical Engineering*, Springer.

Günther, R. (2009), Phänomenologisches Stoffmodell für DUKTILE Salzgesteine zur Beschreibung primären, sekundären und tertiären kiechens, PhD thesis, Fakultät für Geowissenschaften, Geotechnik und Bergbau der Technischen Universität Bergakademie Freiberg.

Günther, R. & Salzer, K. (2007), A model for rock salt, describing transient, stationary, and accelerated creep and dilatancy., *in* 'In 6th Conference on The Mechanical Behavior of Salt- SALTMECH6, Hannover, Germany, 22-25 May', pp. 109–117.

Guo, Y., Yang, C. & Mao, H. (2012), 'Mechanical properties of jintan rock salt under-complex stress paths', *International Journal of Rock Mechanics and Mining Sciences* **56**, 54–61.

Haldar, A. & Mahadevan, S. (2000), *Probability, Reliability, and Statistical Methods in Engineering Design*, John Wiley & Sons Ltd.

Hamby, D. M. (1994), 'A review of techniques for parameter sensitivity analysis of environmental models', *Environmental Monitoring and Assessment* **32**(2), 135–154.

Hamby, D. & Tarantola, S. (1999), Exploring sensitivity analysis techniques for the assessment of an environmental transfer model, in safety and reliability, *in* G. Schüller & P. Kafka, eds, 'ESREL'99, The Tenth European Conference on Safety and Reliability'.

Hamm, N., Hall, J. & Anderson, M. (2006), 'Variance-based sensitivity analysis of the probability of hydrologically induced slope instability', *Computers & geosciences* **32**(6), 803–817.

Hammersley, J. M. (1960), 'Monte carlo methods for solving multivariable problems', *Annals of the New York Academy of Sciences* **86**(3), 844–874.

Hammersley, J. M. & Handscomb, D. C. (1964), *Monte Carlo Methods*, Methuen & Co Ltd.

Hampel, A. & Schulze, O. (2007), The composite dilatancy model: A constitutive model for the mechanical behavior of rock salt, *in* '6th Conference on The Mechanical Behavior of Salt- SALTMECH6, Hannover, Germany, 22-25 May', pp. 99–107.

Hansen, F. & Carter, N. (1983), 'Review creep of rock salt', *Tectonophysics journal* **92**, 275–333.

Hansen, F. D., Mellegard, K. D. & Senseny, P. E. (1984), Elasticity and strength of ten natural rock salts, *in* H. R. J. Hardy & M. Langer, eds, 'The Mechanical Behavior of Salt,Proc. of the First Conferenc', pp. 53–70.

Hardy, R. L. (1971), 'Multiquadric equations of topography and other irregular surfaces', *Journal of Geophysical Research* **76**(8), 1905–1915.

Hartford, D. N. D. & Baecher, G. B. (2004), *Risk and uncertainty in dam safety*, Thomas Telford Publishing.

Hasofer, A. M. & Lind, N. C. (1974), 'Exact and invariant second-moment code format', *Journal of the Engineering Mechanics Division* **100**, 111–121.

Hastings, W. K. (1970), 'Monte carlo sampling methods using markov chains and their applications', *Biometrika* **57**, 97–109.

Helton, J. C. (1993), 'Uncertainty and sensitivity analysis techniques for use in performance assessment for radioactive waste disposal', *Reliability Engineering & System Safety* **42**(2), 327 – 367.

Helton, J., Garner, J., McCurley, R. & Rudeen, D. (1991), Sensitivity analysis techniques and results for performance assessment at the waste isolation pilot plant, Technical Report SAND-90-7103ON: DE91012331, Sandia National Labs., Albuquerque, NM (USA).

Helton, J., Iman, R., Johnson, J. & Leigh, C. (1986), *Uncertainty and sensitivity analysis of a dry containment test problem for the MAEROS aerosol model*, Taylor & Francis Group.

Heusermann, S., Eickemier, R., Hanisch, J. & Sprado, K. (2002), Gebirgsspannungsuntersuchungen in den Schächten 1 und 2, Technical report, Bundesamt für Strahlenschutz.

Heusermann, S., Rolfs, O. & Schmidt, U. (2003), 'Nonlinear finite element analysis of solution mined storage caverns in rock salt using the lubby2 constitutive model', *Computers and structures journal* **81**, 629–638.

Hölter, R., Mahmoudi, E. & Schanz, T. (2015), 'Optimal sensor location for parameter identification in soft clay', *AIP Conference Proceedings* **1684**.

Hölter, R., Zhao, C., Mahmoudi, E., Lavasan, A. A. & Schanz, T. (2017), Optimal measurement setup for parameter identification in 3d-tunnelling cases, *in* 'ECCOMAS Thematic Conference EURO:TUN 2017', pp. 1–9.

Homma, T. & Saltelli, A. (1996), 'Importance measure in global sensitivity analysis of nonlinear models', *Reliability Engineering & System Safety* **52**(12), 1–17.

Hou, Z. (2003), 'Mechanical and hydraulic behavior of rock salt in the excavation disturbed zone around underground facilities', *International Journal of Rock Mechanics and Mining Sciences* **40**, 725–738.

Hou, Z., Gou, Y., Xie, L. & Zhang, R. (2010), Natural gas storage cavern design under special consideration of the thin bedded salt layer in jintan and the intermediate layers of mudstone, *in* M. Hou, H. Xie & J. Yoon, eds, 'Underground storage of CO2 and energy', CRC Press, pp. 211–216.

Hsu, W.-C. & Ching, J. (2010), 'Evaluating small failure probabilities of multiple limit states by parallel subset simulation', *Probabilistic Engineering Mechanics* **25**(3), 291 – 304.

Huang, S. P., Quek, S. T. & Phoon, K. K. (2001), 'Convergence study of the truncated karhunen-loève expansion for simulation of stochastic processes', *International Journal for Numerical Methods in Engineering* **52**(9), 1029–1043.
URL: *http://dx.doi.org/10.1002/nme.255*

Hunsche, U. & Hampel, A. (1999), 'Rock salt- the mechanical properties of the host rock material for radio active waste repository', *Engineering Geology* **52**, 271–291.

Hunsche, U., Schulze, O., Walter, F. & Plischke, I. (2003), Projekt Gorleben - Thermomechanisches Verhalten von Salzgestein, 9G2138110000, Final report, Bundesanstalt für Geowissenschaftenund Rohstoffe (BGR), Hannover.

Hureau, G. (2016), Natural gas annual respondent query system (eia-191 data through 2015). European Gas Transmission Conference, Berlin.

Iman, R. L. & Hora, S. C. (1990), 'A robust measure of uncertainty importance for use in fault tree system analysis', *Risk Analysis* **10**(3), 401–406.

Ishigami, T. & Homma, T. (1990), An importance quantification technique in uncertainty analysis for computer models, *in* 'Uncertainty Modeling and Analysis, 1990. Proceedings., First International Symposium on', IEEE, pp. 398–403.

Jafari, M., Berést, P. & Brouard, B. (2008), Subsidence, sinkholes and craters above salt caverns, *in* 'SMRI conference, Porto, Portugal', pp. 1–10.

Jafari, M., Gatelier, N., Brouard, B. & Berést, P. (2011), Multi cycle gas storage in salt caverns, *in* 'SMRI conference, York, UK', pp. 1–18.

Jafari, M., Reveillere, A. & Frassy, C. (2014), Cavern integrity and performance management at geomethane underground storage, *in* 'SMRI conference, Groningen, The Netherlands', pp. 1–16.

Joshi, M., Seidel-Morgenstern, A. & Kremling, A. (2006), 'Exploiting the bootstrap method for quantifying parameter confidence intervals in dynamical systems', *Metabolic Engineering* **8**, 447–455.

Juang, C. H. & Wang, L. (2013), 'Reliability-based robust geotechnical design of spread foundations using multi-objective genetic algorithm', *Journal of Computers and Geotechnics* **48**, 96–106.

Katafygiotis, L. & Cheung, S. (2007), 'Application of spherical subset simulation method and auxiliary domain method on a benchmark reliability study', *Structural Safety* **29**(3), 194 – 207. A Benchmark Study on Reliability in High Dimensions.

Kennedy, M. C. & O'Hagan, A. (2001), 'Bayesian calibration of computer models', *Journal of the Royal Statistical Society: Series B (Statistical Methodology)* **63**(3), 425–464.

Khaledi, K., Mahmoudi, E., Datcheva, M., König, D. & Schanz, T. (2016), 'Sensitivity analysis and parameter identification of a time dependent constitutive model for rock salt', *Journal of Computational and Applied Mathematics* **293**, 128–138.

Khaledi, K., Mahmoudi, E., Datcheva, M. & Schanz, T. (2016*a*), 'Analysis of compressed air storage caverns in rock salt considering thermo-mechanical cyclic loading', *Environmental Earth Sciences* **75**(15), 1–17.

Khaledi, K., Mahmoudi, E., Datcheva, M. & Schanz, T. (2016*b*), 'Stability and serviceability of underground energy storage caverns in rock salt subjected to mechanical cyclic loading', *International Journal of Rock Mechanics and Mining Sciences* **86**, 115 – 131.

Khaledi, K., Mahmoudi, E., König, D. & Schanz, T. (2016), Effect of temperature and pressure on mechanical behavior of rock salt in underground storage caverns, *in* F. Wuttke, S. Bauer & M. Sanchez, eds, 'Energy Geotechnics', Taylor & Francis Group, pp. 293–298.

Khaledi, K., Miro, S., König, M. & Schanz, T. (2014), 'Robust and reliable metamodels for mechanized tunnel simulations', *Computer and Geotechnics* **61**, 1–12.

Kiureghian, A. D. & Ke, J.-B. (1988), 'The stochastic finite element method in structural reliability', *Probabilistic Engineering Mechanics* **3**(2), 83 – 91.

Knabe, T., Schweiger, H. F. & Schanz, T. (2012), 'Calibration of constitutive parameters by inverse analysis for a geotechnical boundary problem', *Canadian Geotechnical Journal* **49**(2), 170–183.

Koda, M., Mcrae, G. J. & Seinfeld, J. H. (1979), 'Automatic sensitivity analysis of kinetic mechanisms', *International Journal of Chemical Kinetics* **11**(4), 427–444.

Kottegoda, N. T. & Rosso, R. (2008), *Applied Statistics for Civil and Environmental Engineers*, 2 edn, Wiley-Blackwell.

Köylüoglu, H. U. & Nielsen, S. R. (1994), 'New approximations for sorm integrals', *Structural Safety* **13**(4), 235 – 246.

Lahmer, T. (2011), 'Experimental design for nonlinear ill-posed problems applied to gravity dams', *Journal of Inverse Problems* **27**(12), 1–20.

Lancaster, P. & Salkauskas, K. (1981), 'Surfaces generated by moving least squares methods', *Math Comput* **37**(155), 141–158.

Leighty, W. (2008), 'Running the world on renewables: Hydrogen transmission pipelines and firming geologic storage', *International Journal of Energy Research* **32**(5), 408–426.

Li, C. C. & Kiureghian, A. D. (1993), 'Optimal discretization of random fields', *Journal of Engineering Mechanics* **119**(6), 1136–1154.

Li, H.-S., Ma, Y.-Z. & Cao, Z. (2015), 'A generalized subset simulation approach for estimating small failure probabilities of multiple stochastic responses', *Computers & Structures* **153**, 239 – 251.

Liang, W., Zhang, C., Gao, H., Yang, X., Xu, S. & Zhao, Y. (2012), 'Experiments on mechanical properties of salt rocks under cyclic loading', *Journal of Rock Mechanics and Geotechnical Engineering* **4**(1), 54 – 61.

Liu, J., Xie, H., Hou, Z., Yang, C. & Chen, L. (2014), 'Damage evolution of rock salt under cyclic loading in unixial tests', *Acta Geotechnica* **9**(1), 153–160.

Liu, P.-L. & Kiureghian, A. D. (1986), 'Multivariate distribution models with prescribed marginals and covariances', *Probabilistic Engineering Mechanics* **1**(2), 105 – 112.

Long, N.-T. (2014), Coupled thermo-Hydro-Mechanical Analysis: Experiment and Back Analysis, PhD thesis, Faculty of Civil and Environmental Engineering, Ruhr-Universität Bochum.

Lord, A. S., Kobos, P. H., Klise, G. T. & Borns, D. J. (2011), A life cycle cost analysis framework for geologic storage of hydrogen: A user's tool, Technical report, Sandia National Laboratories, SAND2011-6221.

Lux, K.-H. (2013), Recent developments in geotechnical design of natural gas storage cavities regarding physical modelling as well as numerical simulation, *in* M. Z. Hou, H. Xie & P. Were, eds, 'Clean Energy Systems in the Subsurface: Production, Storage and Conversion', Springer Berlin Heidelberg, pp. 451–485.

Lux, K. H., Düsterloh, U. & Hou, Z. (2002), 'Erhoehung der Wirtschaftlichkeit von Speicherkavernen durch Anwendung eines neuen Entwurfsund Nachweiskonzeptes', *Erdöl Erdgas Kohle* **118**(6), 294–300.

Ma, L.-j., Liu, X.-y., Wang, M.-y., Xu, H.-f., Hua, R.-p., Fan, P.-x., Jiang, S.-r., Wang, G.-a. & Yi, Q.-k. (2013), 'Experimental investigation of the mechanical properties of rock salt under triaxial cyclic loading', *International Journal of Rock Mechanics and Mining Sciences* **62**, 34–41.

Ma, L., Liu, X.-y., Fang, Q., Xu, H.-f., Xia, H.-m., Li, E.-b., Yang, S.-g. & Li, W.-p. (2012), 'A new elasto-viscoplastic damage model combined with the generalized hoek–brown failure criterion for bedded rock salt and its application', *Rock Mechanics and Rock Engineering* **46**(1), 53–66.

Mahmoudi, E., Khaledi, K., König, D. & Schanz, T. (2015*a*), Numerical simulation of deep and shallow energy storage systems in rock salt, *in* T. Schanz & A. Hettler, eds, 'Aktuelle Forschung in der Bodenmechanik 2015', pp. 69–83.

Mahmoudi, E., Khaledi, K., König, D. & Schanz, T. (2015*b*), Sensitivity analyses on the influence of constitutive parameters on the numerical simulation of the behavior of a cavern in rock salt, *in* 'Geomechanics from Micro to Macro', pp. 933–938.

Mahmoudi, E., Khaledi, K., König, D. & Schanz, T. (2016), Probabilistic analysis of a rock salt cavern with application to energy storage systems, using subset simulation methodology, *in* F. Wuttke, S. Bauer & M. Sanchez, eds, 'Energy Geotechnics', Taylor & Francis Group, pp. 609–615.

Mahmoudi, E., Khaledi, K., Miro, S., König, D. & Schanz, T. (2017), 'Probabilistic analysis of a rock salt cavern with application to energy storage systems', *Rock Mechanics and Rock Engineering* **50**(1), 139–157.

Mahmoudi, E., Khaledi, K., von Blumenthal, A., König, D. & Schanz, T. (2016), 'Concept for an integral approach to explore the behavior of rock salt caverns under thermo-mechanical cyclic loading in energy storage systems', *Environmental Earth Sciences* **75**, 1069.

Mara, T. A. (2009), 'Extension of the rbd-fast method to the computation of global sensitivity indices', *Reliability Engineering & System Safety* **94**(8), 1274 – 1281.

Marzban, S. & Lahmer, T. (2016), 'Conceptual implementation of the variance-based sensitivity analysis for the calculation of the first-order effects', *Journal of Statistical Theory and Practice* **10**(4), 589–611.

McKay, M. D. (1997), 'Nonparametric variance-based methods of assessing uncertainty importance', *Reliability Engineering & System Safety* **57**(3), 267 – 279.

Meier, J., Rudolph, S. & Schanz, T. (2009), 'Effective algorithm for parameter back calculation–geotechnical applications', *Bautechnik* **86**(1), 86–97.

Metropolis, N., Rosenbluth, A. W., Rosenbluth, M. N., Teller, A. H. & Teller, E. (1953), 'Equation of state calculations by fast computing machines', *The Journal of Chemical Physics* **21**, 1087–1092.

Minkley, M. & Muehlbauer, J. (2007), Constitutive models to describe the mechanical behavior of salt rocks and the imbedded weakness planes, *in* '6th Conference on The Mechanical Behavior of Salt- SALTMECH6, Hannover, Germany', pp. 119–127.

Miro, S., Hartmann, D. & Schanz, T. (2014), 'Global sensitivity analysis for subsoil parameter estimation in mechanized tunneling', *Computers and Geotechnics* **56**, 80–88.

Miro, S., König, M., Hartmann, D. & Schanz, T. (2015), 'A probabilistic analysis of subsoil parameters uncertainty impacts on tunnel-induced ground movements with a back-analysis study', *Computers and Geotechnics* **68**, 38–53.

Moghadam, S. N., Nazokkar, K., Chalaturnyk, R. J. & Mirzabozorg, H. (2015), 'Parametric assessment of salt cavern performance using a creep model describing dilatancy and failure', *International Journal of Rock Mechanics and Mining Sciences* **79**, 250 – 267.

Mollon, G., Dias, D. & Soubra, A.-H. (2013), 'Range of the safe retaining pressures of a pressurized tunnel face by a probabilistic approach', *Journal of Geotechnical and Geoenvironmental Engineering* **139**, 1954–1967.

Morris, M. D. (1991), *Technometrics, Factorial Sampling Plans for Preliminary Computational Experiments*, Taylor & Francis, Ltd.

Müller-Hoeppe, N., Polster, M., Müller, C. & Linkamp, M. (2012), Performance of tight historic drift seals from the viewpoint of current knowledge on EDZ, *in* B. P., G. M., H.-H. F. & T. M., eds, 'Mechanical Behaviour of Salt VII', Taylor & Francis Group, CRC press, London, pp. 461–468.

Nazary, S., Mirzabozorg, H. & Noorzad, A. (2013), 'Modeling time-dependent behavior of gas caverns in rock salt considering creep, dilatancy and failure', *Tunneling and Underground Space Technology* **33**, 171–185.

Nguyen, M. D., Braham, S. & Durup, J. G. (1993), Surface subsidance over deep solution mined storage cavern field, *in* 'International conference on case histories in geotechnical engineering'.

Nguyen-Tuan, L., Lahmer, T., Datcheva, M. & Schanz, T. (2017), 'Global and local sensitivity analyses for coupled thermo-hydro-mechanical problems', *International Journal for Numerical and Analytical Methods in Geomechanics* **41**(5), 707–720.

Nieland, J. & Ratingen, J. (2006), Geomechanical evaluation of two gulf coast natural gas storage caverns, *in* 'Solution mining research institute, SMRI', pp. 1–28.

Olivella, S. & Gens, A. (2002), 'A constitutive model for crushed salt', *International Journal for Numerical and Analytical Methods in Geomechanics* **26**, 719–746.

Olivella, S., Gens, A., Carrera, J. & Alonso, E. (1996), 'Numerical formulation for a simulator(Code–Bright) for the coupled analysis of saline media', *Engineering Computations* **13**, 87–112.

Perzyna, P. (1966), 'Fundamental problems in viscoplasticity', *Advances in Applied Mechanics* **9**, 243–377.

Phoon, K. K. (2008), *Reliability-Based Design in Geotechnical Engineering: Computations and Applications*, CRC Press.

Phoon, K.-K. & Ching, J. (2014), *Risk and Reliability in Geotechnical Engineering*, CRC Press.

Phoon, K.-K. & Kulhawy, F. H. (1999), 'Characterization of geotechnical variability', *Canadian Geotechnical Journal* **36**(4), 612–624.

Plischke, E. (2010), 'An effective algorithm for computing global sensitivity indices (easi)', *Reliability Engineering & System Safety* **95**(4), 354 – 360.

Pollak, R. (1994), History of first u.s. compressed-air energy storage (caes) plant (110mw, 26h), volume 2: construction, final report, Electric Power Research institute.

Powell, M. J. D. (1987), Radial basis functions for multivariable interpolation: A review, in algorithms for approximation, *in* J. C. Mason & M. G. Cox, eds, 'Algorithms for approximation', Clarendon Press, New York, chapter 3, pp. 143–167.

Pudewills, A. (2007), Modeling of hydro-mechanical behavior of rock salt in the near field of repository excavation, *in* '6th Conference on The Mechanical Behavior of Salt-SALTMECH6, Hannover , Germany, 22-25 May', pp. 195–200.

Rackwitz, R. & Fiessler, B. (1978), 'Structural reliability under combined random load sequences', *Computers & Structures* **9**(5), 489–494.

Ratigan, J. & Yogt, T. (1993), 'Lpg storage at mont belvieu, texas: A case history', *SPE Advanced Technology Series* **1**, 204–211.

Ratigan, W. R. & Hannum, W. D. (1980), 'Mechanical behavior of new mexico rock salt in triaxial compression up to 200 c', *Journal of Geophysical Research* **85**, 891–900.

Roberts, L. A., Buchholz, S. A., Mellegard, K. D. & Düsterloh, U. (2015), 'Cyclic loading effects on the creep and dilation of salt rock', *Rock Mechanics and Rock Engineering* **48**(6), 2581–2590.

Roberts, L. A., McCullough, E., Buchholz, S. & DeVries, K. (2015), Introducing a probabilistic-based method for analyzing dilation in salt caverns, *in* L. A. Roberts, K. Mellegard & F. Hansen, eds, 'Mechanical Behavior of Salt VIII', pp. 193–198.

Rocquigny, E., Devictor, N. & Tarantola, S., eds (2008), *Uncertainty in Industrial Practice: A Guide to Quantitative Uncertainty Management*, John Wiley & Sons Inc.

Rosenbluth, E. (1975), 'Point estimates for probability moments', *National Academy of Science* **72**(10), 3812–3814.

Rubinstein, R. Y. (2008), *Simulation and the Monte Carlo Method*, John Wiley & Sons Ltd.

Saltelli, A. (2002), 'Making best use of model evaluations to compute sensitivity indices', *Computer Physics Communications* **145**(2), 280 – 297.

Saltelli, A., Andres, T. & Homma, T. (1993), 'Sensitivity analysis of model output', *Computational Statistics & Data Analysis* **15**(2), 211 – 238.

Saltelli, A., Andres, T. & Ratto, M. (2008), *Global Sensitivity Analysis. The Primer*, John Wiley & Sons Ltd.

Saltelli, A. & Homma, T. (1992), 'Sensitivity analysis for model output: Performance of black box techniques on three international benchmark exercises', *Computational Statistics & Data Analysis* **13**(1), 73 – 94.

Saltelli, A. & Sobol', I. M. (1995), 'About the use of rank transformation in sensitivity analysis of model output', *Reliability Engineering & System Safety* **50**(3), 225 – 239.

Saltelli, A., Tarantola, S. & Campolongo, F. (2000), 'Sensitivity analysis as an ingredient of modeling', *Statistical Science* **15**(4), 377–395.

Saltelli, A., Tarantola, S., Campolongo, F. & Ratto, M. (2004), *Sensitivity analysis in practice: a guide to assessing scientific models*, John Wiley & Sons.

Saltelli, A., Tarantola, S. & Chan, K. P. S. (1999), 'A quantitative model-independent method for global sensitivity analysis of model output', *Technometrics* **41**(1), 39–56.

Sane, S., Desai, C., Jenson, J., Contractor, D., Carlson, A. & Clark, P. (2008), 'Disturbed state constitutive modeling of two pleistocene tills', *Quaternary Science Reviews* **27**, 267–283.

Santoso, A., Phoon, K. & Quek, S. (2011), 'Modified metropolis−hastings algorithm with reduced chain correlation for efficient subset simulation', *Probabilistic Engineering Mechanics* **26**, 331–341.

Satterthwaite, F. E. (1959), 'Random balance experimentation', *Technometrics* **1**(2), 111–137.

Schanz, T., Zimmerer, M. M., Datcheva, M. & Meier, J. (2006), 'Identification of constitutive parameters for numerical models via inverse approach', *Felsbau* **24**(2), 11–21.

Schenkendorf, R., Kremling, A. & Mangold, M. (2009), 'Optimal experimental design and model selection by a sigma point approach', *IET Systems Biology* **3**, 10–23.

Schuëller, G. & Pradlwarter, H. (2007), 'Benchmark study on reliability estimation in higher dimensions of structural systems - an overview', *Structural Safety* **29**(3), 167 – 182. A Benchmark Study on Reliability in High Dimensions.

Schuëller, G. & Stix, R. (1987), 'A critical appraisal of methods to determine failure probabilities', *Structural Safety* **4**(4), 293–309.

Schulze, O., Popp, T. & Kern, H. (2001), 'Development of damage and permeability in deforming rock salt', *Engineering Geology* **61**, 163–180.

Schweiger, H. & Peschl, G. (2005), 'Reliability analysis in geotechnics with the random set finite element method', *Computers and Geotechnics* **32**(6), 422 – 435.

Shinozuka, M. (1983), 'Basic analysis of structural safety', *Journal of Structural Engineering* **109**(3).

Sobol', I. M. (1990), 'On sensitivity estimation for nonlinear mathematical models', *Matematicheskoe Modelirovanie* **2**(1), 112–118.

Sobol', I. M. (1993), 'Sensitivity estimates for nonlinear mathematical models', *Mathematical Modelling and Computational Experiment* **1**, 407–414. English translation of russian original paper Sobol' (1990).

Spreckels, H. & Crotogino, F. (2002), Salt caverns for peak shaving - reservoirs for seasonal balance? new market requirements and appropriate storage solutions, *in* 'SMRI Fall meeting, Bad Ischl, Austria', pp. 1–13.

Sudret, B. & Der Kiureghian, A. (2000), Stochastic finite element methods and reliability, a state of the art., Technical Report UCB/SEMM- 2000/08, Dept. of Civil and Environmental Engineering, Univ. of California, Berkeley, Berkeley, Calif.

Tang, W. H., Yucemen, M. S. & Ang, A. H. S. (1976), 'Probability based short-term design of slope', *Canadian Geotechnical Journal* **13**, 201–215.

Tarantola, S., Gatelli, D. & Mara, T. (2006), 'Random balance designs for the estimation of first order global sensitivity indices', *Reliability Engineering & System Safety* **91**(6), 717 – 727.

Tarantola, S. & Koda, M. (2010), 'Improving random balance designs for the estimation of first order sensitivity indices', *Procedia - Social and Behavioral Sciences* **2**(6), 7753 – 7754.

Thomas, R. & Gehle, R. (2000), A brief history of salt cavern use, *in* 'Proceeding of 8^{th} world salt symposium', pp. 207–2014.

Tissot, J.-Y. & Prieur, C. (2012), 'Bias correction for the estimation of sensitivity indices based on random balance designs', *Reliability Engineering & System Safety* **107**, 205–213. Special Issue: SAMO 2010.

Ucinski, D. (2005), *Optimal Measurement Methods for Distributed Parameter System Identification*, CRC Press.

Urai, J. & Spiers, C. (2007), The effects of grain boundary water on deformation mechanisms and rheology of rock salt during long-term deformation, *in* '6th Conference on The Mechanical Behavior of Salt- SALTMECH6, Hannover, Germany, 22-25 May', pp. 149–158.

Valdebenito, M., Pradlwarter, H. & Schuëller, G. (2010), 'The role of the design point for calculating failure probabilities in view of dimensionality and structural nonlinearities', *Structural Safety* **32**(2), 101 – 111.

Van Sambeek, L. L., Ratigan, J. L. & Hansen, F. D. (1993), 'Dilatancy of rock salt in laboratory tests', *International Journal of Rock mechanics and mining Sciences* **30**(7), 735–738.

Vanmarcke, E. & Grigoriu, M. (1983), 'Stochastic finite element analysis of simple beams', *Journal of Engineering Mechanics, ASCE* **109**(5), 1203–1214.

von Blumenthal, A., Mahmoudi, E., Khaledi, K., König, D. & Schanz, T. (2016), 'Innovative concept for analysing a rock salt cavern under cyclic thermo-mechanical loading', *Energy Procedia* **97**, 478 – 485.

Wainwright, H. M., Finsterle, F., Jung, Y., Zhou, Q. & Birkholzer, J. T. (2014), 'Making sense of global sensitivity analyses', *Computers & Geosiences* **65**, 84–94.

Wang, L., Bérest, P. & Brouard, B. (2015), 'Mechanical behavior of salt caverns: Closed-form solutions vs numerical computations', *Rock Mechanics and Rock Engineering* **48**(6), 2369–2382.

Wang, L. & Grandhi, R. (1996), 'Safety index calculation using intervening variables for structural reliability analysis', *Computers & Structures* **59**(6), 1139 – 1148.

Wang, T., Yan, X., Yang, H., Yang, X., Jiang, T. & Zhao, S. (2013), 'A new shape design method of salt cavern used as underground gas storage', *Applied Energy Journal* **104**, 50–61.

Wang, T., Yang, C., Ma, H., Li, Y., Shi, X., Li, J. & Daemen, J. (2016), 'Safety evaluation of salt cavern gas storage close to an old cavern', *International Journal of Rock Mechanics and Mining Sciences* **83**, 95–106.

Wang, Y. (2011), 'Reliability-based design of spread soundations by monte carlo simulations', *Géotechnique* **61**, 677–685.

Wu, J. (2012), 'Construction and consideration of america's underground gas storage', *Journal of Petroleum Science Research* **1**(3), 51 – 56.

Xing, W., Zhao, J., Hou, Z., Were, P., Li, M. & Wang, G. (2015), 'Horizontal natural gas caverns in thin-bedded rock salt formations', *Environmental Earth Sciences* **73**(11), 6973–6985.

Yang, J. (2011), 'Convergence and uncertainty analyses in monte-carlo based sensitivity analysis', *Environmental Modelling & Software* **26**(4), 444–457.

Zhao, Y. G. & Ono, T. (1999), 'A general procedure for first/second-order reliability method (FORM/SORM)', *Structural Safety* **21**(2), 95 – 112.

Schriftenreihe des Lehrstuhls für Grundbau, Boden- und Felsmechanik der Ruhr-Universität Bochum

Herausgeber: H.L. Jessberger

1	(1979)	**Hans Ludwig Jessberger** Grundbau und Bodenmechanik an der Ruhr-Universität Bochum
2	(1978)	**Joachim Klein** Nichtlineares Kriechen von künstlich gefrorenem Emschermergel
3	(1979)	**Heinz-Joachim Gödecke** Die Dynamische Intensivverdichtung wenig wasserdurchlässiger Böden
4	(1979)	**Poul V. Lade** Three Dimensional Stress-Strain Behaviour and Modeling of Soils
5	(1979)	**Roland Pusch** Creep of soils
6	(1979)	**Norbert Diekmann** Zeitabhängiges, nichtlineares Spannungs-Verformungsverhalten von gefrorenem Schluff unter triaxialer Belastung
7	(1979)	**Rudolf Dörr** Zeitabhängiges Setzungsverhalten von Gründungen in Schnee, Firn und Eis der Antarktis am Beispiel der deutschen Georg-von-Neumayer- und Filchner-Station
8	(1984)	**Ulrich Güttler** Beurteilung des Steifigkeits- und Nachverdichtungsverhaltens von ungebundenen Mineralstoffen
9	(1986)	**Peter Jordan** Einfluss der Belastungsfrequenz und der partiellen Entwässerungs-möglichkeiten auf die Verflüssigung von Feinsand
10	(1986)	**Eugen Makowski** Modellierung der künstlichen Bodenvereisung im grundwasserdurchströmten Untergrund mit der Methode der finiten Elemente
11	(1986)	**Reinhard A. Beine** Verdichtungswirkung der Fallmasse auf Lastausbreitung in nichtbindigem Boden bei der Dynamischen Intensivverdichtung
12	(1986)	**Wolfgang Ebel** Einfluss des Spannungspfades auf das Spannungs-Verformungsverhalten von gefrorenem Schluff im Hinblick auf die Berechnung von Gefrierschächten
13	(1987)	**Uwe Stoffers** Berechnungen und Zentrifugen-Modellversuche zur Verformungsabhängigkeit der Ausbaubeanspruchung von Tunnelausbauten in Lockergestein
14	(1988)	**Gerhard Thiel** Steifigkeit und Dämpfung von wassergesättigtem Feinsand unter Erdbebenbelastung

15 (1991) **Mahmud Thaher**
Tragverhalten von Pfahl-Platten-Gründungen im bindigen Baugrund, Berechnungsmodelle und Zentrifugen-Modellversuche

16 (1992) **Rainer Scherbeck**
Geotechnisches Verhalten mineralischer Deponieabdichtungsschichten bei ungleichförmiger Verformungswirkung

17 (1992) **Martin M. Bizialiele**
Torsional Cyclic Loading Response of a Single Pile in Sand

18 (1993) **Michael Kotthaus**
Zum Tragverhalten von horizontal belasteten Pfahlreihen aus langen Pfählen in Sand

19 (1993) **Ulrich Mann**
Stofftransport durch mineralische Deponieabdichtungen: Versuchsmethodik und Berechnungsverfahren

20 (1992) **Festschrift anlässlich des 60. Geburtstages von Prof. Dr.-Ing. H. L. Jessberger**
20 Jahre Grundbau und Bodenmechanik an der Ruhr-Universität Bochum

21 (1993) **Stephan Demmert**
Analyse des Emissionsverhaltens einer Kombinationsabdichtung im Rahmen der Risikobetrachtung von Abfalldeponien

22 (1994) **Diethard König**
Beanspruchung von Tunnel- und Schachtausbauten in kohäsionslosem Lockergestein unter Berücksichtigung der Verformung im Boden

23 (1995) **Thomas Neteler**
Bewertungsmodell für die nutzungsbezogene Auswahl von Verfahren zur Altlastensanierung

24 (1995) **Ralph Kockel**
Scherfestigkeit von Mischabfall im Hinblick auf die Standsicherheit von Deponien

25 (1996) **Jan Laue**
Zur Setzung von Flachfundamenten auf Sand unter wiederholten Lastereignissen

26 (1996) **Gunnar Heibrock**
Zur Rissbildung durch Austrocknung in mineralischen Abdichtungsschichten an der Basis von Deponien

27 (1996) **Thomas Siemer**
Zentrifugen-Modellversuche zur dynamischen Wechselwirkung zwischen Bauwerken und Baugrund infolge stoßartiger Belastung

28 (1996) **Viswanadham V. S. Bhamidipati**
Geosynthetic Reinforced Mineral Sealing Layers of Landfills

29 (1997) **Frank Trappmann**
Abschätzung von technischem Risiko und Energiebedarf bei Sanierungsmaßnahmen für Altlasten

30 (1997) **André Schürmann**
Zum Erddruck auf unverankerte flexible Verbauwände

31 (1997) **Jessberger, H. L. (Herausgeber)**
Environment Geotechnics, Report of ISSMGE Technical Committee TC 5 on Environmental Geotechnics

Herausgeber: Th. Triantafyllidis

32 (2000) **Triantafyllidis, Th. (Herausgeber)**
Boden unter fast zyklischer Belastung: Erfahrung und Forschungsergebnisse (Workshop)

33 (2002) **Christof Gehle**
Bruch- und Scherverhalten von Gesteinstrennflächen mit dazwischenliegenden Materialbrücken

34 (2003) **Andrzej Niemunis**
Extended hypoplastic models for soils

35 (2004) **Christiane Hof**
Über das Verpressankertragverhalten unter kalklösendem Kohlensäureangriff

36 (2004) **René Schäfer**
Einfluss der Herstellungsmethode auf das Verformungsverhalten von Schlitzwänden in weichen bindigen Böden

37 (2005) **Henning Wolf**
Zur Scherfugenbänderung granularer Materialien unter Extensionsbeanspruchung

38 (2005) **Torsten Wichtmann**
Explicit accumulation model for non-cohesive soils under cyclic loading

39 (2008) **Christoph M. Loreck**
Die Entwicklung des Frischbetondruckes bei der Herstellung von Schlitzwänden

40 (2008) **Igor Arsic**
Über die Bettung von Rohrleitungen in Flüssigböden

41 (2009) **Anna Arwanitaki**
Über das Kontaktverhalten zwischen einer Zweiphasenschlitzwand und nichtbindigen Böden

Herausgeber: T. Schanz

42 (2009) **Yvonne Lins**
Hydro-Mechanical Properties of Partially Saturated Sand

43 (2010) **Tom Schanz (Herausgeber)**
Geotechnische Herausforderungen beim Umbau des Emscher-Systems
Beiträge zum RuhrGeo Tag 2010

44 (2010) **Jamal Alabdullah**
Testing Unsaturated Soil for Plane Strain Conditions: A New Double-Wall Biaxial Device

45 (2011) **Lars Röchter**
Systeme paralleler Scherbänder unter Extension im ebenen Verformungszustand

46 (2011) **Yasir Al-Badran**
Volumetric Yielding Behavior of Unsaturated Fine-Grained Soils

47 (2011) **Usque ad finem**
Selected research papers

48 (2012) **Muhammad Ibrar Khan**
Hydraulic Conductivity of Moderate and Highly Dense Expansive Clays

49 (2014) **Long Nguyen-Tuan**
Coupled Thermo-Hydro-Mechanical Analysis: Experimental and Back Analysis

50 (2014) **Tom Schanz (Herausgeber)**
Ende des Steinkohlenbergbaus im Ruhrrevier: Realität und Perspektiven für die Geotechnik
Beiträge zum RuhrGeo Tag 2014

51 (2014) **Usque ad finem**
Selected research papers

52 (2014) **Houman Soleimani Fard**
Study on the Hydro-Mechanical Behavior of Fiber Reinforced Fine Grained Soils,
with Application to the Preservation of Historical Monuments

53 (2014) **Wiebke Baille**
Hydro-Mechanical Behaviour of Clays - Significance of Mineralogy

54 (2014) **Qasim Abdulkarem Jassim Al-Obaidi**
Hydro-Mechanical Behavior of Collapsible Soils

55 (2015) **Veselin Zarev**
Model Identification for the Adaption of Numerical Simulation Models -
Application to Mechanized Shield Tunneling

56 (2015) **Meisam Goudarzy**
Micro and Macro Mechanical Assessment of Small and Intermediate Strain
Properties of Granular Material

57 (2016) **Oliver Detert**
Analyse einer selbstregulierenden interaktiven Membrangründung für Schüttkörper
auf geringtragfähigen Böden

58 (2016) **Yang Yang**
Analyses of Heat Transfer and Temperature-induced Behaviour in Geotechnics

59 (2016) **Alborz Pourzargar**
Application of suction stress concept to partially saturated compacted soils

60 (2017) **Hanna Haase**
Multiscale Analysis of Clay-Polymer Composites for Geoenvironmental Applications

61 (2017) **Kavan Khaledi**
Constitutive modeling of rock salt with application to energy storage caverns

62 (2017) **Nina Silvia Müthing**
On the consolidation behaviour of fine-grained soils under cyclic loading

63 (2017) **Elham Mahmoudi**
Probabilistic analysis of a rock salt cavern with application to energy storage systems